University of Bremen
Department 2 Biology and Chemistry

Bacterial colonization of gel particles in the sea ice of Fram Strait

Master Thesis

Study Program Marine Biology

Submitted by Ulrike Dietrich

Bremen, March 2015

First supervisor: Prof. Dr. Anya Waite, Alfred Wegener Institute

Second supervisor: PD Dr. Bernhard Fuchs, Max Planck Institute for Marine Microbiology

Third supervisor: Dr. Ilka Peeken, Alfred Wegener Institute

Alfred Wegener Institute
Helmholtz-Centre for Polar
and Marine Research

Max Planck Institute
for Marine Microbiology

Declaration

I hereby confirm that I have independently composed this Master thesis and that no other than the indicated aid and sources have been used. This work has not been presented to any other examination board.

Bremen, 23rd of March 2015

Ulrike Dietrich

Abstract

The Fram Strait is characterized by seasonal ice cover, influenced by cold Arctic waters flowing southward on the western margin and warm Atlantic waters flowing northward on the eastern margin. A key component of sea ice ecology is the organic particles and their bacterial communities, about which little is known. We investigated the within-ice distribution of transparent exopolymeric particles (TEP, primarily polysaccharide) and Coomassie stainable particles (CSP, primarily protein) as well as parameters affecting their respective abundance within sea ice. We then explored differences in the bacterial community composition associated with TEP and CSP, compared to free-living bacteria in early summer sea ice of Fram Strait.

Photometric and microscopic analysis of gel particles indicated highest TEP and CSP values in landfast ice and lowest values in small ice floes floating on cold Arctic and warm Atlantic waters, respectively (only significant for CSP). TEP were generally found in the bottom half of sea ice, dominating in terms of particle number and area, whereas CSP were evenly distributed, dominating in the top half of sea ice in terms of particle area. TEP values were significantly correlated with indices of recent productivity such as chlorophyll *a*, POC and PON concentrations. CSP values were less obviously dependent on the productivity of the system. Instead, CSP seemed driven more by low temperature and low light, possibly conditions negatively affecting the survival of sea ice microorganisms generally.

Fluorescence in-situ hybridization and particle-specific staining methods were combined to investigate the bacterial community directly living attached to either TEP or CSP. The composition of particle-associated bacteria was different from that of free-living bacteria, but was dominated by the same bacterial groups, *Bacteroidetes* and ɣ-proteobacteria. *Polaribacter* spp. was the only genus significantly reduced on particles. We found minor preferences of some bacterial groups for either TEP or CSP, none of which was significant.

Abstract

Distribution patterns and drivers of TEP and CSP suggest different roles of these particles in sea ice. Since no complete shifts in bacterial community composition were observed, we conclude that sea ice selects for bacteria able to acclimate rapidly to changing conditions.

Contents

Contents

List of Figures

List of Tables

I Introduction

1.1 Study Area

1.1.1 Arctic Sea Ice

The Arctic Ocean is a closed basin surrounded by land with only one deep passage through which water can be exchanged with the rest of the world's oceans (Thomas & Dieckmann, 2003). Shelf seas in the Arctic take up about one-third of the ocean area with a depth below 100 m, the mean depth is 1800 m (Wadhams, 2000). At the time of its maximum extent in February and March ($15x10^6$ km^2), sea ice covers the entire Arctic Ocean. It extends from the North Pole to about latitude 44° in the Sea of Japan (Wadhams, 2000). By September it usually reaches its minimum. More than half of the Arctic sea ice used to be multi-year ice (Gloersen et al. 1992). A substantial reduction in Arctic sea ice extent has been observed for the last two decades, with the 2012 minimum ice extent ($3.61x10^6$ km^2) 16% below the previous low of 2007 and corresponding to the largest recorded decrease in minimum sea ice extent (http://nsidc.org/cryosphere/sotc/sea_ice.html). Hence, the ratio of multi-year to first-year sea ice has decreased tremendously. In the Arctic, sea ice is subjected to considerable input of terrestrially sourced particles and organic matter, due to river run-off with high sediment loads, and/or suspension freezing of bottom sediments.

1.1.2 Fram Strait

The Fram Strait represents a unique deep water connection between the Arctic Ocean and the rest of the world's oceans. The Strait forms a seaway from the North Atlantic to the Arctic Ocean approximately 500 km wide, separating the northeast of Greenland from the Svalbard archipelago in the east (Fig. 1). Its bathymetry controls the exchange of water masses between

the Arctic basin and the North Atlantic. The Fram Strait is the outlet of ice transported from the building zones of ice on the Siberian shelves across the North pole into the North Atlantic by the so called "Transpolar Drift" (Polyak et al., 2010).The Fram Strait is characterized by its transport of fresh water and sea ice southwards, and transport of warm saline waters northwards, thus, influencing the thermohaline circulation at a global scale (Schmitz, 1995; Gerdes & Schauer, 1997).

Two main currents control the water mass exchange. At the western margin it is characterized by cold Arctic surface waters which flow southward in the East Greenland Current, while on the eastern margin, Atlantic Waters flow northward in the West Spitsbergen Current. These major currents are separated by a transition zone (Beszczynska-Möller et al., 2012). Results of recent modelling studies emphasize the importance of the Fram Strait for both heat inflow to, and freshwater export from, the Arctic Ocean (Zhang & Zhang, 2001; Meredith et al. 2001).
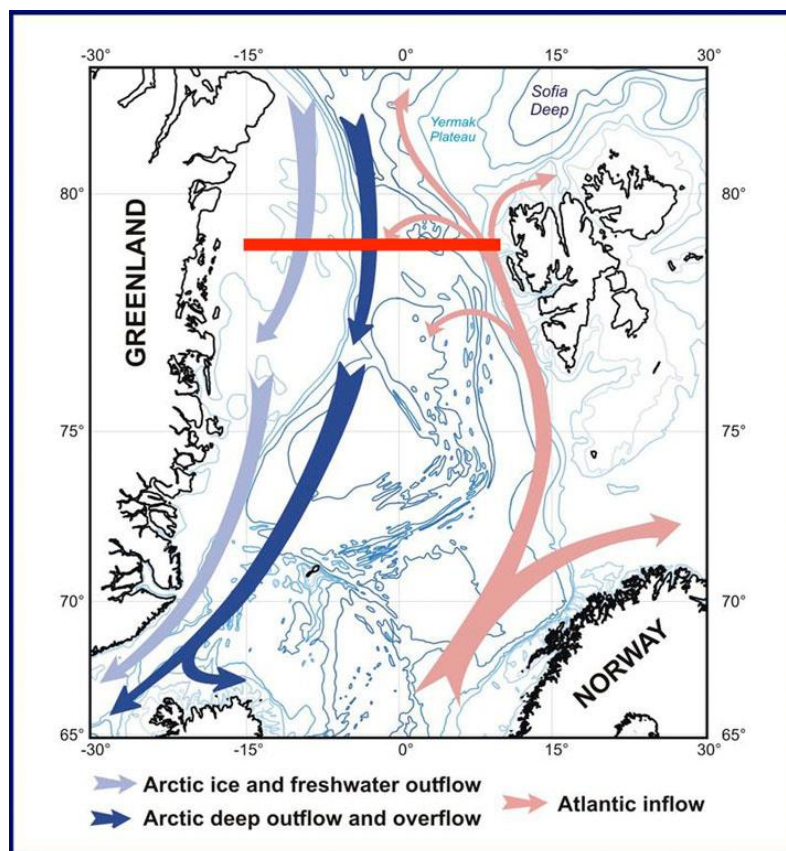
Figure 1. Currents in the Fram Strait (www.whoi.edu).

1.2 Sea Ice

Sea ice covers a vast area of $15 \times 10^6 \, km^2$ in the Arctic and $18 \times 10^6 \, km^2$ in the Antarctic (http://nsidc.org/cryosphere/seaice/characteristics/difference.html) at its maximum extent, thus being an important component of the cryosphere and the global climate system (Maykut, 1986). Since sea ice contains much of the productivity of polar regions, it influences global energy budgets and strongly influences the atmospheric-oceanic interaction in polar regions (Legendre et al., 1992). Sea ice forms in the winter months and breaks up and melts during the polar summer. The formation of sea ice begins when the surface waters reach temperatures of about -1.8 °C, the freezing point of seawater at a salinity of 35‰ (Staley & Gosink, 1999).

The coldest and most variable temperatures are reached at the ice-air interface (Fig. 2), ranging from 0 to -35 °C during winter (Maykut, 1986). Thus, sea ice provides the coldest habitat on earth for marine life. Temperatures at the ice-water interface remain stable at about -2 °C (Staley & Gosink, 1999).

Sea ice is temporally and spatially highly variable with large gradients in light, temperature, nutrient availability and salinity (Eicken, 1992). Sea ice is therefore a surprisingly complex environment for microbial life. The sea ice crystal matrix is permeated by a highly connected network of pores and brine channels, typically ranging from 1 to 20% volume as a result of temperature, salt content and ionic composition (Weeks & Ackley, 1986). As the ice cools, the volume fraction of liquid decreases and the salinity of the brine increases. Brine salinity may reach concentrations greater than 200‰. Brine inclusions range from several micro-meters to centimeters in size and become increasingly disconnected at lower temperatures (Eicken et al.,2000).

1.2.1 Sea Ice Microorganisms

Most of the sea ice microorganisms (SIMCOs) have been observed to reside within the brine ice channels (Junge et al., 2001), in the lower 10 to 20 cm of the sea ice column at the ice-water interface (Staley & Gosink, 1999; Krembs & Engel, 2001; Palmisano & Garrison, 1993; Horner et al., 1992). There, nutrients are available from the water column and light is available from the surface (Staley & Gosink, 1999). Flushing by under-ice water replaces nutrient-

depleted interstitial waters and removes accumulated waste products (Thomas & Dieckmann, 2003; Kattner et al., 2004).

The SIMCO comprises viruses, bacteria, algae, fungi, and protozoans and meiofauna (Horner et al., 1992). The community is dominated by diatoms, such as the pennate diatom *Nitzschia spp.*, which serves as the major primary producer within Arctic sea ice (Krembs et al., 2001). Concentrations of bacteria are enriched relative to those found in surface seawater, therefore, they are considered to be important members of the SIMCO (Helmke & Weyland, 1995). Bacterial heterotrophy includes direct consumption of dissolved substrates, and the decomposition and uptake of dissolved and particular matter produced by the SIMCO via exoenzymes (Thomas & Dieckmann, 2003). Bacterial secondary production rates are high, generally ranging between 10 to 15% of primary production (Kottmeier et al., 1987). In thick or heavily snow covered sea ice, bacterial secondary production may even exceed primary production as the light supply to the bottom is restricted (Grossman, 1994).

Thomas and Dieckmann (2003) described the three main mechanisms by which microorganisms from the water column and the sea floor might become incorporated into sea ice. One is the enclosure of water, which can occur as ice consolidates. The second are active concentration mechanisms. They are best known for initial stages of ice formation by scavenging. Adherence of cells to ice crystals moving through the water column is one mode of scavenging (Gleitz & Thomas, 1993). Another scavenging mode occurs at the ocean's surface as frazil ice collects to form a grease ice layer. This layer acts as a filter collecting particles and cells from water that was pumped through by wave action. Lifting of benthic material attached to anchor ice occurs only in the shallowest, coldest regions of polar seas and is thus almost exclusive to the Arctic (Thomas & Dieckmann, 2003). The third mechanism is active colonization. High concentrations of algal cells, their waste and breakdown products, could be attractants to decomposers (bacteria) from the water column. However, due to their small size, most marine bacteria are not concentrated by ice scavenging mechanisms (Gradinger & Ikävalko, 1998), except for large cells (1 μm^3) and those attached to larger particles and cells.

1.2.2 DOM

High concentrations of dissolved organic matter (DOM), both dissolved organic carbon (DOC) and dissolved organic nitrogen (DON), are associated with the dense SIMCO at the ice-water interface (Thomas et al., 1998; Herborg et al., 2001; Papadimitriou et al., 2007, 2009). Sea ice DOM is present at concentrations several fold higher than in surface seawater (Underwood et al., 2010). The major producers of this DOM are the algae that grow on the ice surfaces (e.g. *Melosira arctica*) and within the brine channels (e.g. *Nitzschia spp.*) (Krembs & Engel, 2001; Meiners et al., 2003, 2008). Furthermore, sea ice DOM is highly bioavailable (Amon et al., 2001) resulting in increased microbial growth and activity in sea ice compared to the surface seawater. Extensive microbial communities from Antarctic sea ice have been reported to significantly contribute to the polar ocean carbon budget (Thomas & Dieckmann, 2002).
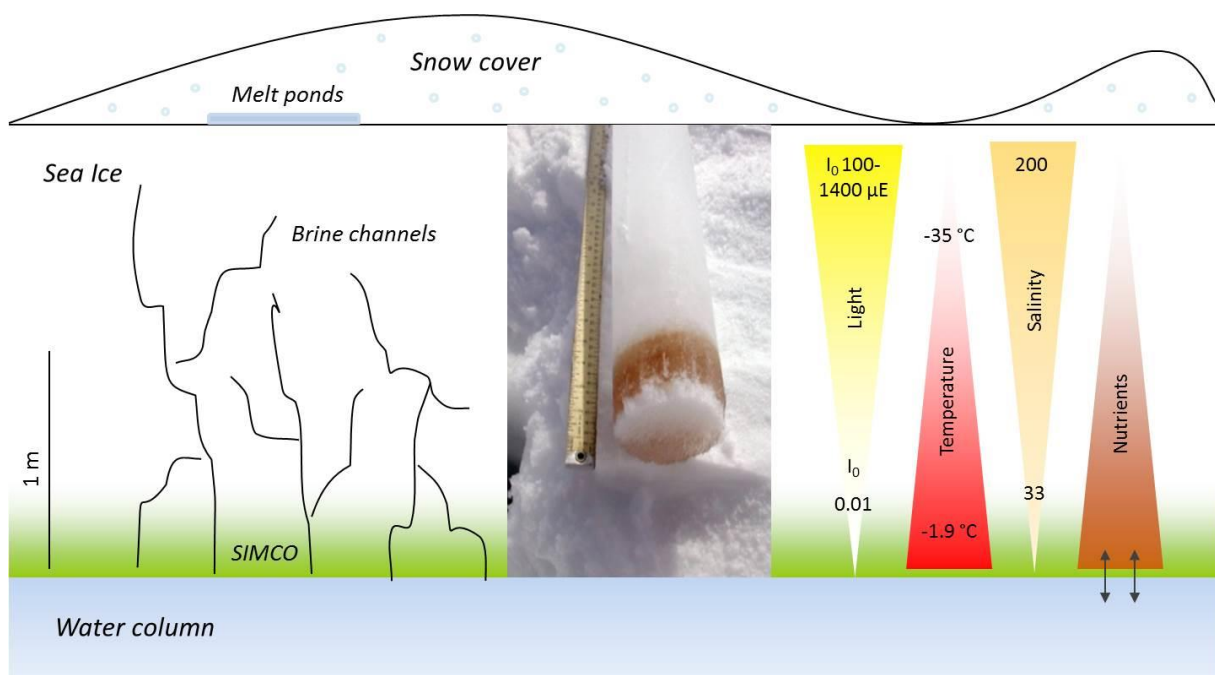
Figure 2. A shematic view of the sea ice habitat (modified after Krell & Krembs).

1.3 Extracellular polymeric substances

A significant proportion of organic matter in sea ice can be present in form of extracellular polymeric substances (EPS), predominantly composed of polysaccharides with carbon

backbones of high molecular weight (1-3x10^5 daltons) (Krembs et al., 2008). Although variable in composition and shape (Santchi et al., 1998), they typically carry carboxylic acid groups in the form of uronic acids (Meiners et al., 2003; Krembs et al., 2011). EPS further consist of highly branched heteropolysaccharides that can contain fructose, rhamnose, mannose, D-glucose, xylose, D-glucuronic acid, galactose and half-ester sulphate (Percival et al., 1980), and sometimes significant amounts of protein (Mancuso Nichols et al., 2005).

EPS co-occur inseparably with microbial assemblages in both, terrestrial and aquatic environments, underscoring their wide ranging importance and diverse functions in microbial ecology (Passow, 2000). Within sea ice, dissolved EPS (dEPS) concentrations have a heterogeneous distribution, whereas particulate EPS (pEPS) are mainly found in biomass-rich horizons in the ice (Krembs et al., 2002, 2011; Meiners et al., 2003). EPS are released by bacteria and algae in form of mucous slime or gels (Krembs & Engel, 2001; Mancuso Nichols et al., 2005; Krembs & Deming et al., 2008; Collins et al., 2010).

EPS can contribute substantially to a wide range of categories of organic material in the ocean (Fig. 3), from the dissolved fraction to colloidal and particulate classes (Passow, 2000), thus closing the gap between dissolved and particulate matter realms (Verdugo et al., 2004).
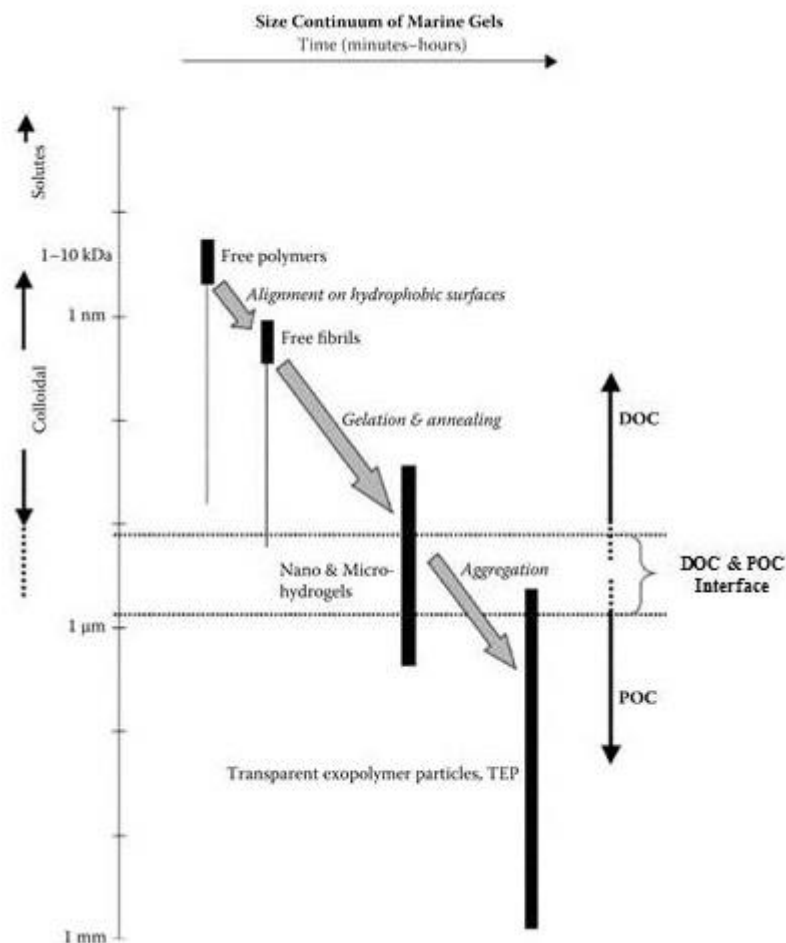
Figure 3. Size continuum of EPS depicting size distribution and processes affecting formation (Verdugo et al., 2004, as cited in Engel 2009, modified).

1.3.1 Particulate EPS

Particulate EPS (pEPS) are often named gel particles as their solid three-dimensional network of organic compounds and inorganic cations is penetrated by seawater, resulting in a semisolid or jelly-like structure (Engel, 2009; Underwood et al., 2010). Gel particles are generated abiotically from interactions of dissolved and colloidal organic matter by spontaneous assembly (Chin et al., 1998), bubble adsorption (Mopper et al., 1995; Mari, 1999), or laminar and turbulent shear (Engel & Passow, 2001). Therefore, gel particles can be easily produced artificially as shown by Engel and Passow (2001). Whereas the origin of precursor material is biotic, the aggregation is abiotic, changing the traditional view of bacteria as the primary transformer of DOM to POM (Chateauvert et al., 2012).

pEPS can be found as thick gels surrounding microbial cells (Myklestad, 1995; Underwood et al., 1995; Waite et al., 1995), as free colloidal organic matter (Decho, 1990; Passow, 2000), or as part of large particles and aggregates (Alldredge et al., 1993; Passow et al., 2001). Among their many roles, pEPS can aid in locomotion (Wetherbee et al., 1998), adhesion to surfaces (Cooksey & Wigglesworth-Cooksey, 1995), and sequestering of nutrients and organic compounds from solution (Decho, 1990). pEPS can further provide a protective buffer zone around a cell against unfavorable shifts in the environment, e.g. changing ionic, osmotic, desiccation, or pH conditions (Decho & Lopez, 1993). Furthermore, they might also serve as an important carbon and nitrogen sources for bacteria (Mock & Thomas 2005).

pEPS in sea ice are often not discrete particles, but rather cell-associated (Riedel et al., 2006). They are usually densely colonized by bacteria and are likely to increase sea ice bacterial diversity by providing microhabitats for distinct bacterial groups (Mock & Thomas, 2005). Collins et al. (2007) and Krembs et al. (2002) found pEPS in very high concentrations in sea ice brines during winter, with pEPS concentrations increasing significantly with decreasing temperatures. This may lend support to the assumption that pEPS may serve as a cryoprotectant to enhance the survival of SIMCO. Coatings of pEPS might buffer against osmotic shock (hypersalinity) and cryoprotecting SIMCO against external ice-crystal formation by depressing the ice nucleation temperature of water, due to their high polyhydroxyl content (Krembs et al., 2002; Krembs & Deming, 2008; Mancuso Nichols et al., 2005). The study by Krembs et al. (2011) clearly indicates that pEPS, if present in sufficient quantity and quality, alter the microstructure and desalination of growing ice. Therefore, it can be stated that pEPS improve sea ice habitability, survivability and increase the potential for increased primary production (Krembs et al., 2011).

Marine gels, such as transparent exopolymeric particles (TEP; Alldredge et al., 1993) and Coomassie stainable particles (CSP; Long & Azam, 1996), are made of large organic polymers and are considered stable macrogels (Verdugo, 2012).

TEP are visualized by staining with Alcian Blue (AB; Alldredge et al., 1993; Mopper et al., 1995), a cationic copper phthalocyanine dye that reacts with the carboxyl (COO^-) and sulfate half ester (OSO_3^-) functional groups of acidic polysaccharides and glycosaminoglycans (Decho,

1990). CSP are protein-containing particles that are stainable with Coomassie Brilliant Blue G (CBBG) (Long & Azam, 1996). CBBG is an unspecific protein-binding dye that binds to alkaline residues of amino acids (Long & Azam, 1996).

TEP and CSP characteristics overlap in many respects, and so far it is not known to what extent CSP and TEP represent different chemical subunits (proteins and polysaccharides) of the same gel particle (Engel, 2009). If they do not represent distinct classes, the overall contribution of pEPS to particulate organic carbon (POC) is prone to overestimation.

The discovery of new classes of particles represents an important advance toward understanding the nutritional quality of pEPS and cycling of carbon through aquatic ecosystems. Because of their potential ecological importance, pEPS, especially TEP received much recent research attention.

1.3.1.1 TEP

TEP are carbon-rich particles that seem to be ubiquitous in marine and freshwater ecosystems (Chateauvert et al., 2012). The high fraction of sulfate half-ester groups explains their strong tendency to form metal ion bridges and hydrogen bonds, which makes TEP highly sticky (probability that two particles remain attached after collision) (Passow, 2002a; Krembs et al., 2008). TEP are discrete particles rather than dissolved substances or cell coatings (Alldredge et al., 1993).

Their role differs from non-particulate EPS, as independent particles, TEP may impact aggregation processes (Logan et al., 1995). Since particle-free TEP are positively buoyant (Azetsu-Scott & Passow, 2004), they need to associate with other particles or cells to form aggregates that actually sink.

According to many studies (Passow & Alldredge, 1994; Mari & Kiørboe, 1996; Carrias et al., 2002; Lemarchand et al., 2006) the vast majority of TEP are colonized by bacteria, representing 1 to 20% of the total bacterial count. Carrias et al. (2002) and Lemarchand et al. (2006) indicated that TEP are particularly important for bacterial growth in lakes with low nutrient loading.

1.3.1.1.1 TEP Producers

It is well established that the majority of TEP present in sea ice is produced by algae (Krembs & Engel, 2001; Meiners et al., 2003, 2008; Krembs et al., 2001). Although cultured bacteria are known to generate large amounts of TEP (Mancuso Nichols et al., 2005; Grossart, 1999), in-situ their production often appears to be insignificant (Schuster & Herndl, 1995; Krembs et al., 2001). Phytoplankton exudates closely resemble polysaccharides found for TEP (Mopper et al. 1995; Aluwihare & Repeta, 1999). Furthermore, in most studies, concentrations of TEP are significantly correlated with chlorophyll *a* (Passow, 2002b; Riedel et al., 2006; Krembs & Engel, 2001; Meiners et al., 2003; Arnous et al., 2010), confirming the significance of phytoplankton for the formation of TEP. Studies by Krembs & Engel (2001) and Meiners et al. (2003) have found pennate diatoms of the genus *Nitzschia* to be the most important producers of TEP within sea ice.

Sea ice algae are of particular importance, they are an early source of carbon for water column grazers (Michel et al., 2002) and can contribute 25% or more to the total primary production in the Arctic (Legendre et al., 1992; Gosselin et al., 1997). Depending on their nutrient status, they release 3 to 40% of photosynthetic carbohydrates via exudation (Baines & Pace, 1991), 75% of which as polysaccharides (Myklestad et al., 1989).

1.3.1.1.2 Role of TEP in Carbon Cycle

Marine phytoplankton have a unique role in the global carbon cycle as they remove dissolved inorganic carbon from the upper ocean via photosynthesis and redirect it to the deep ocean through sedimentation. This process is referred to as the biological pump, and is mainly driven by the coagulation of single phytoplankton cells into rapidly settling aggregates (Shanks & Trent, 1980; Waite et al., 1997).

The presence of glue-like TEP enhances the formation of these aggregates (Alldredge et al., 1993; Logan et al., 1995; Engel, 2000). Because TEP can be an essential component of marine and lake snow (Alldredge et al., 1993), they may play an important role in the downward flux of organic matter (Passow et al., 2001).

Since DOM does not sink it is generally assumed that it does not participate in the biological pumping of carbon to the deep ocean. However, TEP coagulation is likely to be a

pathway for the sedimentation of originally dissolved organic carbon (Engel & Passow, 2001). Moreover, since TEP are carbon-rich particles, the biogeochemistry of aggregates should differ from organisms by an enrichment of carbon relative to the expected C:N:P ratio of 106:16:1 (Redfield et al., 1963). Therefore, the sedimentation of TEP may even lead to a selective export of carbon from surface waters (Engel & Passow, 2001).

TEP can represent a significant source of carbon, contributing 14 to 32% of POC values in Arctic and Antarctic sea ice of varying age (Meiners et al., 2003, 2004). Krembs et al. (2002) converted TEP from weight units (Xanthan Gum equivalents) to carbon units. Given the ice thickness near Barrow (Alaska), they estimated the areal TEP-carbon content in March and May. Their estimates are similar to average DOC concentrations, and are equivalent in magnitude to the average POC content measured in March (Eicken et al., 1999). Thus, TEP may contribute significantly to polar ocean carbon cycles, not only within the ice but after springtime release into the water column and subsequent export to deeper regions (Krembs et al., 2001). Large TEP pulse from Arctic sea ice (transition from winter to spring) observed by Wurl et al. (2011) was suggested to be the result of discharge from the ice with draining brines. The short life span of the TEP pulse, with a substantial decline after only 8 days, implies rapid removal from the surface and/or recycling.

1.3.1.2 CSP

CSPs are protein containing particles that seem to be similar to TEP in size range and shape (Long & Azam, 1996), but their origin and formation seems to be quite different from those of TEP. CSP appeared to be less closely related to the productivity of the ecosystem, supporting the assumption that their origin is multiple (Long & Azam, 1996). Furthermore, Lemarchand et al. (2006) did not find a relation of CSP abundance and chlorophyll *a* in lakes. Various mechanisms of cell lysis and death, or the adsorption of protein onto nonproteinaceous particles could produce CSP (Long & Azam, 1996). Another study by Bhaskar et al. (2005) found bacteria to be able to cause CSP formation. However, there is evidence that CSP are abundant in seawater (Long & Azam, 1996; Cisternas-Novoa et al., 2014), fresh water (Berman & Viner-Mozzini, 2001; Lemarchand et al., 2006) and phytoplankton cultures (Prieto et al.,

2002; Cisterna-Novoa et al., 2014). Depending on the study area, CSP are more or less abundant than TEP, or similar. Field observations of aggregation during phytoplankton blooms by Prieto et al. (2002) revealed CSP to have no contribution to macroaggregate production. But, like TEP, CSP are frequently colonized by bacteria (Lemarchand et al., 2006), and since proteins are a valuable nitrogen and carbon source for them, CSP might be more labile than TEP (Cisternas-Novoa et al., 2014). Moreover, CSP production and utilization may influence flux and cycling of nitrogen in pelagic systems. Until recently, there was no method to determine CSP concentrations photometrically, thus, information on CSP origin, formation, function and dynamics are scarce (Lemarchand et al., 2006; Cisternas-Novoa et al., 2014).

1.4 Sea ice bacteria

Most sea ice bacteria are psychrophilic and therefore differ in abundance, size, activity and taxonomy from bacteria living in the underlying seawater (Helmke & Weyland, 1995; Bowman, 1997). Abundance of sea ice heterotrophic bacteria varies widely, with highest numbers usually being found in association with high algal biomass. Junge et al. (2002) found bacterial numbers to range from 5.4×10^4 mL^{-1} in clear ice to 2.4×10^6 mL^{-1} in algal band ice samples in Arctic sea ice during summer.

1.4.1 Community Composition

Most studies concerning the bacterial community within sea ice have been conducted during spring and summer. Results from culture-independent methods (cloning, sequencing of 16S rRNA genes, fluorescence in-situ hybridization (FISH)) overlap extraordinary well with culture-based results, confirming the prevalence of the α- and γ-subclass of *Proteobacteria* and *Bacteroidetes* in spring and summer sea ice at both poles (Brinkmeyer et al., 2003; Brown & Bowman, 2001; Thomas & Dieckmann, 2003; Collins et al., 2010; Han et al., 2014).

Differences in bacterial communities at the poles were mainly found at the species level, which implies the occurrence of similar selection mechanisms in these two geographically separated environments (Brinkmeyer et al., 2003).

In the Arctic, approximately 50, 30 and 25% were identified as belonging to the γ-proteobacteria, α-proteobacteria and *Bacteroidetes* group, respectively. Brinkmeyer et al. (2003) further detected β-Proteobacteria, making up 6% of the total, whereas abundances of Gram-positive bacteria, *Planctomycetes* and *Archaea* were shown to be below the detection limit of FISH. *Archaea* have only been detected in winter sea ice, making up 3.4% of the total (Junge et al., 2004).

The highest diversity of phylotypes was found within the γ-proteobacteria, dominated by the genera *Colwellia, Glaciecola* and *Marinobacter* (Brinkmeyer et al., 2003; Groudieva et al., 2004). Identified phylotypes within the α-proteobacteria were affiliated to the Roseobacter clade, with *Octadecabacter spp*. being the most abundant isolate. *Salegentibacter spp*. and *Psychroserpens spp*. were abundant phylotypes within the *Bacteroidetes* group.

In contrast, the bacterial community of Arctic winter sea ice is dominated by SAR11 (α-proteobacteria) and strongly overlaps with under-ice water. *Polaribacter* is the only genus that was detected to reside within sea ice throughout the year (Collins et al., 2007).

It seems that, in all studies investigating the bacterial community composition of Arctic sea ice, the whole bacterial community was analyzed, without differentiation between the liquid and pEPS attached fraction.

1.4.2 Attachment to Particles

Sea ice is a porous habitat with many attachment sites (ice crystals, pEPS, algal cells) that may select for specific types of bacteria. Many of the species isolated from sea ice, especially among the *Bacteroidetes,* are known for their attached life style (Bernardet et al., 1996) and for their extracellular enzymes that degrade a wide variety of polymeric substances (Reichenbach & Dworkin, 1992). In Antarctic sea ice, more than 30% of the bacteria in melted sea ice were observed to be attached to algae and detritus (Sullivan & Palmisano, 1984). Junge

et al. (2004) found an even higher attachment rate of over 50% in an unmelted Arctic sea ice sample.

Association with particles is common among sea ice bacteria, as it is an important mechanism for survival and growth, even though underlying mechanisms remain poorly known (Junge et al., 2004). Generally, attached bacteria are larger than free-living bacteria and have higher specific uptake rates for some substrates (Unanue et al., 1992).

Meiners et al. (2008) described pEPS as microbial hotspots with bacteria possessing high enzymatic activities. Thanks to their physiological adaptation at the enzyme level, psychrophilic sea ice bacteria stay highly active at low temperatures (Feller & Gerday, 2003). Junge et al. (2004) showed that, within slices of intact sea ice, the percentage of active bacteria attached to particles increased with decreasing temperature. Additionally, all bacterial cells that stay metabolically active down to -20 °C were attached to particles. This suggests that bacteria living attached to pEPS are of major importance in biogeochemical processes and the food web, not only in the sunlit, but also during the coldest season.

Although sea ice is known to harbor high concentrations of pEPS and their potential role for the SIMCO has been discussed, it is not studied yet in which ways they influence the bacterial sea ice community composition.

Furthermore, there are no studies of the bacterial sea ice community directly living attached to either TEP or CSP. Since the composition of the particles differs we would also expect a different bacterial community.

There is only one study by Lemarchand et al. (2006) where they investigated the bacterial community attached to TEP and CSP in lake water samples by combining FISH with the gel particle specific stains mentioned above. They found all TEP and more than 90% of CSP to be colonized by bacteria. Numbers of bacterial cells for all tested bacterial groups were significantly higher for TEP than CSP, indicating that particles containing acidic sugars are favored attachment sites for bacteria. In contrast, Berman and Viner-Mozzini (2001) found CSP to be more colonized, arguing that proteinaceous particles provide a more nutritious substrate, resulting in a more rapid turnover of CSP in lakes.

1.5 Hypothesis and Aims

By analyzing ice cores from different sea ice types for their number, area and concentration of TEP and CSP, we aimed to investigate the distribution of TEP and CSP, and to identify which particle class might dominate in Arctic early summer sea ice. By correlating TEP and CSP values with abiotic and biotic factors recorded at the same stations, we aimed to identify parameters likely to affect the abundance of TEP and CSP.

By analyzing melted sea ice samples and samples from an experiment to study the effect of pEPS on the composition of the bacterial sea ice community, we aimed to identify bacterial groups that are favored by the presence of pEPS, and to compare the bacterial community composition living free or attached to either TEP or CSP in Arctic early summer sea ice. We further aimed to identify which particle class might be favored by bacteria.

With respect to present knowledge, we hypothesize that (**a**) highest TEP and CSP values occur at the ice-water interface, (**b**) TEP values mainly correlate with sea ice algal abundance (chlorophyll *a*), whereas (**c**) CSP correlates with abiotic parameters that in turn affect survivability of SIMCO, (**d**) the presence of pEPS will favor bacteria known for their attached life-style, like *Bacteroidetes*, (**e**) the bacterial community composition/relative abundance differs between the free-living and pEPS attached fraction and (**f**) between pEPS of different chemical composition (TEP and CSP).

II Material and Methods

2.1 Sampling and Processing

Sea ice samples were collected with a Mark II 9 cm inner diameter ice corer (Kovacs Enterprise, Roseburg, OR, USA) during the R. V. *Polarstern* summer cruise PS 85 / ARKXXIII/1 (June 2014) in the Fram Strait. A total of ten stations were approached either by helicopter or rubber boat. Positions of all stations are shown in Fig. 4. On the Transect from the West to the East of Fram Strait sea ice exposed to different conditions was sampled. Sea ice stations 1 and 2 were located close to Greenland and were identified as landfast ice (Table 1). In the middle and in the North we found large single ice floes of different size and thickness. The smallest and thinnest floes were observed in the East floating on warmer Atlantic water.
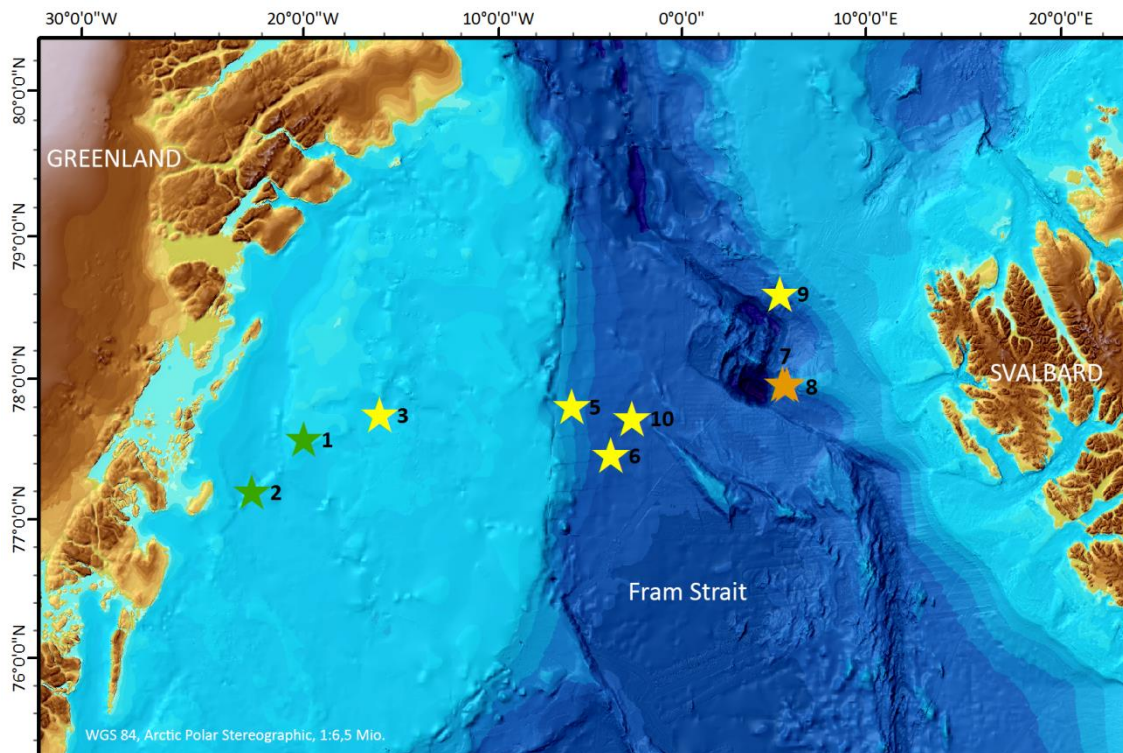
Figure 4. Sampling stations in Fram Strait. Green stars mark locations of landfast ice, yellow stars of large ice floes and orange stars of small ice floes. Map was generated by Lars Radig with IBCAO v3 (http://www.gebco.net).

Table 1: Summary of station metadata

Station	Position Longitude N	Latitude	Ice type	Ice thickness cm	Snow coverage cm
1	78 15.915	14 42.859W	Landfast	135	9
2	77 45.609	16 3.58W	Landfast	190	4
3	78 49.0	8 46.167W	Large floe	164	3
5	78 52.091	4 29.551W	Large floe	272	27.5
6	78 30.403	2 47.951W	Large floe	177	24
9	79 45.284	4 18.279E	Large floe	173	9
10	78 48.175	2 00.996W	Large floe	213	20
7	79 3.044	4 9.188E	Very s. floe	69	4
8	79 2.428	4 18.576E	Small floe	89	5

Separate cores from each sampling site were used to measure salinity and temperature profiles, biological variables, and bacteriology (see below). Transmission of light through the ice was measured as described by Chresten Lund-Hansen et al. (2015).

2.1.1 Salinity – Temperature Core Measurements

In-situ temperature of the cores was determined directly after sampling by drilling small holes every 5 cm and subsequent measurement with an Testo 720 temperature sensor (accuracy: 0.1 °C; Lenzkirchen, Germany). Ice cores were cut into 10 cm sections and melted in plastic boxes at room temperature. After melting the salinity was determined using a WTW Probe (WTW 206; Weilheim, Germany).

2.1.2 Biological Core Measurements

Biological cores were immediately cut into 10 cm sections, transferred in plastic boxes and stored in a cooling box. Sections were transferred in filtered seawater (pore size, 0.2 µm; for each centimeter of ice 200 mL of filtered seawater were added) and melted at 4 °C. After melting, the entire volume of the ice and filtered seawater was determined to calculate the exact dilution factor for each section. Therefore all concentrations given in this study are concentration per liter of ice. For the analysis of transparent exopolymeric particles (TEP) and Coomassie stainable particles (CSP) within the ice, subsamples of the upper and the lower halves of the original ice core were pooled into a "Top" and a "Bottom", respectively.

Subsamples of the Top and Bottom were stained for microscopic and colorimetric analysis of TEP and CSP. 30 - 150 mL of melted sea ice were filtered onto 0.4 µm polycarbonate filter (PC-filter) at low and constant vacuum (< 150 mmHg). TEP were stained with an aqueous solution of Alcian Blue (AB), CSP with Coomassie Brilliant Blue G (CBBG) directly on the filter and rinsed with ultrapure water. Fresh filters were checked for an evaluable number of particles. Blank filters were prepared from 0.4 µm PC-filters moistened with MilliQ water and processed like the samples. For microscopic and colorimetric analysis filters were mounted on CytoClear slides (Poretics Corp., Livermore, US) and put in plastic cups, respectively and stored at -20 °C. For each sample two filters for microscopic and three filters for colorimetric analysis were prepared.

In addition, fractionated chlorophyll *a* (< 10 μm and > 10 μm, filtered onto glass fiber- (GF/F)-filters; Whatman, and 10 μm polycarbonate- (PC)-filters), particulate organic carbon (POC) and particulate organic nitrogen (PON) concentrations (filtered onto precombusted GF/F-filters) were measured by other scientists.

Chlorophyll *a* was determined with a Turner-Design fluorometer after Evans and O'Reily (1987).

POC and PON were analyzed in the stable isotope laboratory of the Museum für Naturkunde, Berlin. Stable isotope analysis and concentration measurements of nitrogen and carbon were performed simultaneously with a THERMO/Finnigan MAT V isotope ratio mass spectrometer, coupled to a THERMO Flash EA 1112 elemental analyzer via a THERMO/Finnigan Conflo III- interface. Stable isotope ratios were expressed in the conventional delta notation (δ^{13}C / δ^{15}N) relative to atmospheric nitrogen (Mariotti, 1983) and VPDB (Vienna PeeDee Belemnite standard). Standard deviation for repeated measurements of lab standard material (peptone) is generally better than 0.15 per mill (‰) for nitrogen and carbon, respectively. Standard deviations of concentration measurements of replicates of our lab standard are < 3% of the concentration analyzed.

2.1.3 Bacteriological Core Measurements

Careful attention was paid to maintain sterile conditions during sampling and subsequent processing of the bacteriological cores. Special emphasis was put on the lower 5 cm of ice cores to study the bacterial community that lives attached to TEP and CSP. The layer at the ice-water interface is considered to harbor the highest concentration of ice algae and extracellular particles due to its exchange of nutrients with the water below. The lower 5 cm section of bacteriological cores were cut and stored in sterile sampling bags in a cooling box. On board, single sections were crushed mechanically and melted in filtered (0.2 μm pore size) autoclaved under-ice water (ratio seawater to sea ice 1:1) to reduce the mechanical and osmotic stress on bacterial cells during melting.

The under-ice seawater also contains dissolved particle precursors. However, since the concentration of exopolymeric particles is one order of magnitude lower than in sea ice their contribution was neglected. To minimize bacterial growth during melting, the melting-process

was speed up by continuous agitation on a shaking platform. The ice had melted at room temperature within 2 to 3 h (sample temperature stayed below 0 °C). After melting, samples were directly transferred to a temperature controlled room at 0 °C.

Two molecular approaches were conducted. The first approach was to separately analyze attached-living bacteria and the free-living bacterial community using denaturing gradient gel electrophoresis (DGGE) and subsequent sequencing of the 16S rRNA gene. Therefore, melted sea ice was filtered through different pore sizes. First, melted sea ice was filtered onto 2.0 µm PC-filter to exclude most of the free-living bacterial cells as long rods can measure up to 0.65 µm x 4.0 µm (Helmke & Weyland, 1995). Air dried filters were stored in Eppendorf cups at -80 °C. To compare the mainly attached-living with the free-living bacterial community using DGGE, the filtrate was further filtered onto 0.2 µm PC-filters.

The second approach was to combine catalyzed reporter deposition fluorescence in-situ hybridization (CARD-FISH) with the respective stain for TEP and CSP. Thus, one can estimate the relative abundance of bacterial groups that life free or attached to either TEP or CSP. Prior to filtration onto 0.2 µm PC-filters supported with 0.45 µm cellulose-nitrate filters, melted sea ice was fixed with formaldehyde solution (final concentration, 2 to 4% [vol/vol]) for 24 hours at 4 °C. Air dried filters were stored in petri dishes at -20 °C.

2.2 Experiments

To study how TEP and CSP influence the bacterial sea ice community, three experiments with melted sea ice of different stations (Table 2) were set up in the dark at 0 °C. Due to their high stickiness, TEP are usually attached to particles such as algae and debris (Verdugo et al., 2004). Algae and debris surfaces harbor bacteria, too, but our aim was solely to study the bacteria living directly attached to either TEP or CSP. Therefore, we produced exopolymeric particles artificially from dissolved precursors (< 0.2 µm) using bubble coagulation (Mari, 1999; Engel, 2009). This has the advantage that algae, debris and bacteria can be removed by filtration prior to the production of particulate extracellular polymeric substances (pEPS). Artificially generated pEPS were then inoculated with a natural bacterial community of sea ice.

Table 2: Sources of water and natural bacterial sea ice community for experiments

Experiment	Melted ice from station	Inoculum from station	Ice type
1	1	2	Landfast
2	5	6	Large ice floe
3	9	9	Large ice floe

In detail: Melted lower 5 cm sections of three sea ice cores of the same station were pooled and filtered through 0.2 µm PC-filters. The filtrate contains dissolved precursors for exopolymeric particles but should be free of bacterial cells and particles. The filtrate was decanted into two Schott flasks (Fig. 5). To prevent sedimentation, the flasks were put on a shaking platform during the whole experiment.

Flask 1 ("precursor") only contained dissolved precursors. Flask 2 ("bubbled") was bubbled with air throughout the whole experiment using a glass frit to produce exopolymeric particles from dissolved precursors within 24 h. Flask 2 should contain pEPS as well as dissolved precursors.

After one day, two ice cores (of another station) were melted and used as a natural bacterial inoculum (10 mL Inoculum per 100 mL sample volume) for the two Schott flasks. A third Schott flask ("control") was filled with the unfiltered sea ice water and served as a control to identify changes in the stock solution. The flasks were incubated over a period of four days.

Subsamples to determine the concentration of TEP and CSP photometrically as well as samples for DGGE and FISH (both filtered onto 0.2 µm PC-filters) were taken after 0, 2 and 4 days (exception for experiment 1: no FISH samples on day 0) and stored at their respective storing temperature until analysis.
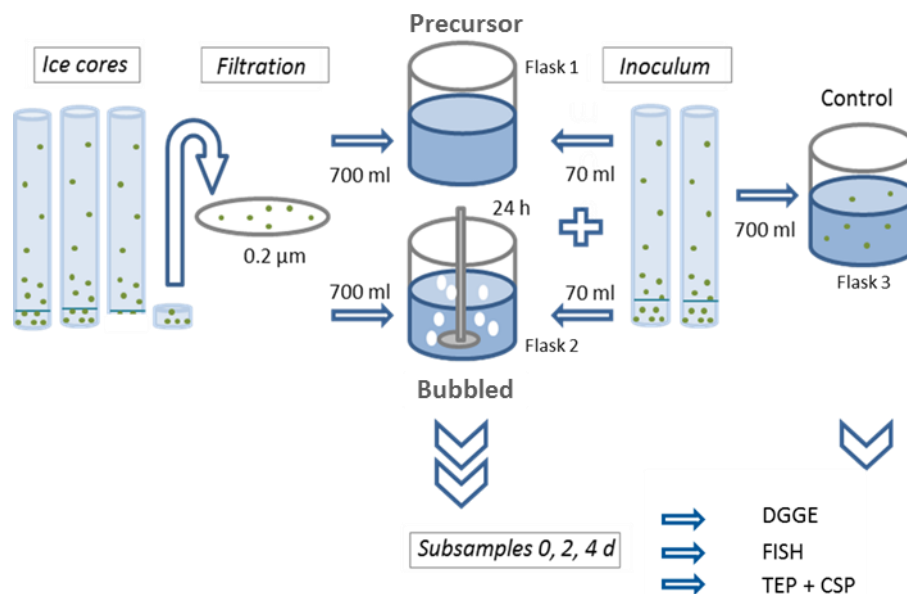
Figure 5. Experimental set-up.

2.3 DNA Extraction

Total community nucleic acids from filtered bacterioplankton of melted sea-ice and experiment samples were extracted using the NucleSpin Soil kit (Macherey-Nagel, Düren, Germany), where the sample material is resuspended in lysis buffer and mechanically disrupted using ceramic beads. Extracts were stored at -20 °C.

2.4 PCR Amplification and DGGE

2.4.1 PCR Amplification of 16S rDNA

A part of the 16S ribosomal RNA gene of bacteria was amplified using bacteria-specific primers (Table 3). GM5 (corresponding to positions 341–358 of the *Escherichia coli* 16S rRNA) with an attached GC-clamp (5'-CGC CCG CCG CGC CCC GCG CCC GGC CCG CCG CCC CCG CCC CAC GGG CGG TGT GTR C-3') and 907R (corresponding to positions 907–927 of the *E. coli* 16S rRNA; Thermo Scientific, Waltham, USA) were used for amplification in 50 µL reaction mixtures as listed in Table 4.

Table 3: Bacteria-specific primers used for PCR amplification; Wobble M = A/C

Primer	Sequence	Reference
GM5F	5`-CCT ACG GGA GGC AGC AG-3`	Muyzer et al., 1993
907R	5`-CCG TCA ATT CMT TTG AGT TT-3`	Muyzer et al., 1993

Table 4: PCR mixture for amplification of DNA extracts for DGGE

Component	Volume in μL
Primer GM5-GC [10 pmol]	1
Primer 907R [10 pmol]	1
5Prime Mastermix	20
PCR H_2O	26
Template	2

The template DNA was denatured in a thermal cycler (Eppendorf, Hamburg, Germany) for 4 min at 95 °C followed by a touchdown-PCR (see Table 5) to increase the specificity of amplification and to avoid the formation of spurious by-products (Muyzer et al., 1997). The success of the amplification reaction was controlled by an agarose gel electrophorese. Therefore, 0.5 g agarose were heated in 60 mL 1xTAE buffer (Sigma Aldrich, St. Louis, USA), then GelRed (Biotium, Hayward, USA) was added to stain the DNA within the gel. 3 μL PCR products mixed with 2 μL loading buffer were loaded. A 1kb ladder was used as a reference. Gels were run for 30 min at 100 V.

Table 5: PCR conditions for amplification of DNA extracts for DGGE

Phase	Temperature in °C	Duration in min
Initial denaturation	95	4
Denaturation	95	1
Annealing	65	1
Elongation	72	3
Cycles	Annealing temperature decreases by 1 °C per cycle until 55 °C are reached, followed by 24 cycles at 55 °C.	
Final elongation	72	5

2.4.2 DGGE

PCR-products were analyzed by DGGE, based on the protocol of Muyzer et al. (1997) using a gradient-chamber.

2.4.2.1 Production of DGGE Gels

For the production of a DGGE gel two stock solutions with a formamide (Applichem, Darmstadt, Germany) gradient of 0% and 80% were prepared (Table 6). Both solutions have an acrylamide (Bio-Rad, Hercules, USA) concentration of 6%. PCR products were separated on 20 to 70% denaturant (7 M urea and 40% deionized formamide) DGGE gels. From the stock solutions the two initial gradients were prepared (Table 7). Ammoniumpersulfate (APS; Bio-Rad) solution and TEMED (Bio-Rad) were added just before the gradient mixer (SG Series Gradient Makers; Hoefer Pharmacia Biotech, Holliston, USA) was loaded to initialize the polymerization of acrylamide. After pouring the gradient gel it was covered with a layer of 0% stock solution. After complete polymerization, the gel was transferred in the DGGE chamber filled with 1xTAE buffer (40 mM Tris-acetate and 1 mM Na-EDTA, pH 8.0) heated up to 60 °C. Before loading 20 to 40 µL of the PCR products, gel pockets were thoroughly washed. Gels were run at 60 °C and constant voltage of 100 V for 18 h.

Gels were stained in 1xTAE containing SYBR Gold (diluted 1:10000; Molecular Probes; Waltham, USA) for 20 min in the dark. Stained gels were immediately photographed under UV transillumination (Gel iX20 imager; Intas Science Imaging, Göttingen, Germany). Digitized DGGE profiles were straightened and aligned with the Bionumerics Gelcompare software (Applied Maths, Sant-Martens-Latern, Belgium).

Table 6: Stock solutions for DGGE gels

Component	0% Gradient	80% Gradient
Acrylamid/Bis (37.5:1, 40%)	15 mL	15 mL
50xTAE buffer	2 mL	2 mL
Formamide, deionized	-	32 mL
Urea	-	33.6 g
Final volume with MilliQ	100 mL	100 mL

Table 7: Instructions for the preparation of initial gradients

Component	70%	20%
0% Stock solution	1.4 mL	8.25 mL
80% Stock solution	9.6 mL	2.75 mL
TEMED	7 µL	7 µL
APS 10%	40 µL	40 µL

2.4.2.2 Excision of Bands and Reamplification

All visible unique bands were picked for sequencing, and bands recurring several times on the same gel were picked at least twice. Bands were excised with a flamed scalpel under UV-light (Transilluminator UVT-28 BE; Herolab, Wiesloch, Germany) and resuspended in 100 µL PCR H$_2$O (Sigma Aldrich). To elute the DNA from the gel, samples were shaken (Vortex-Genie 2; Scientific Industries, New York, USA) for 2 h at 4 °C before refrigeration at –20 °C overnight.

Then, the eluted DNA was reamplified using same primers but without the GC-clamp (Table 4) under the conditions stated in Table 8. Successful amplification was checked as described above. PCR products were purified with Agencourt AMPure (Beckman Coulter, Pasadena, USA) following producers instructions and checked again on an agarose gel.

Table 8: PCR conditions for reamplification of excised DGGE bands

Phase	Temperature in °C	Duration in min
Initial denaturation	95	4
Denaturation	95	1
Annealing	55	1
Elongation	72	3
Cycles	28	
Final elongation	72	7

2.5 Sequencing of DGGE Bands

Sequencing was carried out using the BigDye Terminator v3.1 sequencing kit (Applied Biosystems, Waltham, USA). The primer GM5 was used in the sequencing PCR (Table 9). The conditions for the amplification are listed in Table 10. PCR products were checked as described above, purified with Agencourt ClenSEQ (Beckman Coulter, Pasadena, USA) following

producers instructions and checked again before sequencing was carried out on an ABI 3700 sequencing system (Applied Biosystems, Californien, USA).

Table 9: PCR mixture for sequencing PCR

Component	Volume in µL
Primer GM5 [1 pmol]	1
5x Sequence buffer	1.5
Pre Mix Big Dye RR100	0.3
PCR H_2O	4.2-5.2 (depending on amount of template)
Template	2-3

Table 10: Conditions for sequencing PCR

Phase	Temperature in °C	Duration in sec
Initial denaturation	96	60
Denaturation	96	10
Annealing	50	5
Elongation	60	240
Cycles	24	

2.5.1 Sequence Processing and Analysis

With the program Codon Code Aligner (CodonCode Corporation, Centerville, USA) chromatograms of the sequences were visualized. The primer was removed manually based on quality data calculated by the program and bad quality ends were cropped. Sequences with an overall average quality below 90 were discarded. To taxonomically classify the bacterial community present in the samples, single sequences were submitted to the SINA alignment service of the high quality ribosomal RNA database silva (SINA Alignment Service, Pruesse et al., 2012; silva, http://www.arb-silva.de/). Strains showing highest overlap with the submitted sequences were identified.

2.6 Fluorescence In-Situ Hybridization (CARD-FISH)

CARD-FISH analysis was used to examine community structure and relative abundances of bacterial groups in samples collected from the experiments after one, two and for days of incubation at 0 °C. Samples were fixed with buffered paraformaldehyde solution (final concentration, 2 - 4% [w/v]). Within 24 h of fixation, samples were filtered in duplicates (10 and 20 mL) at a low vacuum pressure (< 150 mmHg) onto 0.2 µm PC-filters (Whatman; diameter 50 mm), and then rinsed with sterile filtered and autoclaved under-ice water and distilled water. Air dried filters were stored at -20 °C in the dark until further processing.

CARD-FISH analysis was conducted according to the method of Pernthaler and colleagues (2004) using horseradish-peroxidase (HRP)-labeled oligonucleotide probes (Thermo Fisher Scientific) Probes ranged in specificity from domain to species level, with GLAC227, MB-ICO22a, SF825, POL740 being characteristic for sea ice communities (Brinkmeyer et al., 2003; Gerdes et al., 2005). Probes used are listed in Table 11.

Experiments showed that it is possible to combine TEP and CSP staining techniques with FISH. Counts of positive cells before and after staining filters with AB or CBBG did not differ (Lemarchand et al., 2006), therefore, combined protocols were used to observe particles and their attached bacterial cells at the same time.

First, filters were embedded in low gelling point agarose (0,1%) to prevent substantial cell loss during permeabilisation with lysozyme solution (10 mg mL^{-1} in 0.05 M EDTA, pH 8.0; 0.1 M Tris-HCl, pH 8.0) for 60 min at 37 °C. After washing with MilliQ water endogenous peroxidases were inactivated by incubation in 0.01 M HCl for 20 min at room temperature, followed by washing in MilliQ water and 96% ethanol.

Prior to hybridization, the filters were cut into small sections. These sections were hybridized in a humidity chamber for 2 h at 46 °C. The hybridization buffer consisted of 0.9 M NaCl; 20 mM Trsi HCl, pH 8.0; 0.02% sodium dodecyl sulfate (SDS); 1% Blocking Reagent (Roche, Basel); 10% dextran sulfate and a variable concentration of formamide depending on probe (see Table 11) The hybridization buffer was mixed in a ratio of 150:1 with probe working solution (50 ng DNA µL^{-1}). Filters were then incubated in a prewarmed washing buffer composed of 5 mM EDTA, pH 8.0; 20 mM Tris HCl, pH 8.0; 0,01% SDS and a variable

concentration of NaCl, at 48 °C for 10 min. Followed by an incubation in 1xPBS for 15 min at room temperature for catalyzed reporter detection.

The amplification buffer (1xPBS; 0.1% Blocking Reagent; 2 M NaCl; 10% dextran sulfate) was first mixed in a ratio of 100:1 with H_2O_2 solution (0.15% in PBS), then $Alex_{488}$-labeled tyramide was added in a ratio of 1000:1. Filter pieces were covered with the amplification mix, put in a humidity chamber and incubated at 46 °C for 30 min in the dark. After incubation, the samples were transferred to 1xPBS for 10 min, washed in excess MilliQ water and then dehydrated in ethanol and air-dried in the dark.

Sections were counterstained with 4',6-diamidino-2-phenylindole (DAPI; 1 µg mL^{-1}) for 5 min, afterwards washed in MilliQ water, 96% ethanol to remove unspecific staining and air-dried in the dark before staining with either AB or CBBG.

TEP and CSP were visualized on separate filter sections. Slight modifications of the instructions by Engel (2009) were used to obtain quantitative microscopic analysis of TEP and CSP, respectively. TEP were stained on filter sections with AB working solution. Filter sections were fully covered with the dye (500 mL) for about 30 s. CSP were stained for 90 s with CBBG working solution. All filter sections were then rinsed with MilliQ water, air-dried in the dark, mounted onto Cytoclear slides in a mixture of four parts Citifluor and one part Vecta Shield, and stored at -20 °C in the dark.

Image acquisition was done within a week after staining by using an Eclipse 50i epifluorescent microscope (Nikon Instruments, Tokyo, Japan) equipped with a camera (Axiovision, Zeiss, Germany).

To analyze the free-living bacterial fraction fields without any cell accumulations were enumerated by switching between green-light excitation to visualize probe labelled bacteria and UV light to visualize DAPI stained bacteria. At least 500 DAPI stained cells per probe and sample were counted. For analyzing the bacterial community on either TEP or CSP, first blue stained particles were identified under visible light. Then DAPI stained and probe labelled cells were directly counted under the microscope. A first picture was taken under visible light, a second under UV light, and a third under green-light excitation. Approximately 20 TEP and CSP particles per probe and sample were evaluated.

Table 11: HRP-labeled probes used in this study

Probe	Target organisms	Sequence (5' -> 3')	FA[1] [%]	Reference
EUB338-I	*Bacteria*	GCTGCCTCCCGTAGGAGT	35	Amann et al. 1990
NON338	control	ACTCCTACGGGAGGCAGC	35	Wallner et al. 1993
BET42a	β-subgroup of Proteobacteria	GCCTTCCCACTTCGTTT	35	Manz et al. 1992
comp Gam42a	Competitor for BET42a, targets 23S rRNA	GCCTTCCCACATCGTTT	35	Manz et al. 1992
GAM42a	γ-subgroup of Proteobacteria	GCCTTCCCACATCGTTT	35	Manz et al. 1992
comp Bet42a	Competitor for GAM42a, targets 23S rRNA	GCCTTCCCACTTCGTTT	35	Manz et al. 1992
Alt1413	*Alteromonas / Colwellia*	TTTGCATCCCACTCCCAT	40	Eilers et al. 2000
PSA184	*Pseudoalteromonas/ Colwellia*	CCCCTTTGGTCCGTAGAC	30	Eilers et al. 2000
GLAC227	*Glaciecola*	AATCTCGCTTAGGCCACT	30	unpublished Kassabgy, Fuchs
MB-IC022a	*Marinobacter* sp. strain IC022 group	GTTTCCGCCCGACTTGCA	25	Brinkmeyer et al. 2003
comp MB-IC022a	Competitor for MB-IC022	GTTTCCGCTCGACTTGCA	25	Brinkmeyer et al. 2003
SF825	*Shewanella frigidimarina*	AAGTCACCAAACTCCGAG	10	Brinkmeyer et al. 2003
CF319a	*Bacteroidetes*	TGGTCCGTGTCTCAGTAC	35	Manz et al., 1996
POL740	Polaribacter	CCCTCAGCGTCAGTACATACGT	35	Malmstrom et al. 2007
ROS537	*Roseobacter* clade	CAACGCTAACCCCCTCC	35	Eilers et al. 2001
PLA46	*Planctomycetes*	GACTTGCATGCCTAATCC	30	Neef et al. 1998

2.7 Extracellular Polymeric Substances

As part of this study, both TEP and CSP were assessed in terms of abundance, area, concentration, carbon content and size frequency distribution within ice cores and in terms of concentration over the course of the experiment. In order to quantify these naturally transparent gel particles, two dyes were used to differentiate between TEP and CSP. Both particle categories were analyzed microscopically and photometrically following the instructions by Engel (2009) and Cisternas-Novoa et al. (2014).

2.7.1 Alcian Blue Solution

Aqueous AB solution was used to stain TEP. AB is a cationic dye that binds electrostatically to negatively charged residues of acidic mucopolysaccharides, in particular to carboxyl and sulfate groups (Decho, 1990).

Prior to the expedition, AB stock solution (97 mL MilliQ water, 3 mL acetic acid, 1 g Alcian Blue (8GX, Sigma)) was diluted in MilliQ water in a ratio of 1:50 (vol:vol), yielding a working solution of 0.02% AB solution at pH 2.5. The working solution was stored at 4 °C in the dark. Directly

before usage, AB working solution was filtered through 0.2 µm syringe filters (Minisart; Sartorius, Göttingen, Germany) to remove dye particles that may have formed spontaneously in the solution.

2.7.2 Coomassie Brilliant Blue G

Aqueous CBBG was used to stain CSP. CBBG is an unspecific protein-binding dye that binds to alkaline residues of amino acids (Long & Azam, 1996). Stock solution was prepared on board by adding 1 g Coomassie Brilliant Blue G (Serva, Heidelberg, Germany) to 100 mL MilliQ water. CBBG working solution was prepared freshly prior to staining by diluting the stock solution with 0.2 µm filtered (Minisart, Sartorius) seawater in a ratio of 1:25, giving a 0.04% CBBG solution.

2.7.3 TEP and CSP Filtration

Melted sea ice was filtered onto 0.4 µm PC-filters (25 mm diameter; Whatman, Maidstone, USA) at low and constant vacuum (< 150 mmHg). For microscopic analysis 30 to 60 mL were filtered, whereas for photometric analysis 25 mL (experiment) and 150 mL (stations) were filtered.

Immediately after the filters fell dry, vacuum was released and 750 µL AB working solution for staining TEP or CBBG working solution for staining CSP was added and allowed to react with the material on the filter for approximately 4 and 30 s, respectively. Then the vacuum pressure was reestablished to remove excess stain and the filters were rinsed with MilliQ water.

Between filtration of samples, filter holders and funnels were rinsed with MilliQ water. Filters for microscopic analysis were prepared in duplicates, filters for photometric analysis in triplicate. Blank filters were prepared for every station and sampling event of the experiment from MilliQ water.

For microscopic analysis filters were mounted sample side up onto CytoClear slides with a drop of immersion oil underneath and on top. CytoClear slides are glass slides that are glazed on one side that removes the interference with the filter pores under bright field and

epifluorescence microscopes. Thus, particles can be viewed directly on the filter. Before storing the slides a cover slip was put on top. For photometric analysis filters were folded twice and stored in Eppendorf cups at -20 °C.

2.7.4 Microscopic Analysis of TEP and CSP

The microscopic analysis gives an estimate of the abundance and size frequency distribution of a certain class of gel particles. Filters were transferred to a compound light microscope (Axioskop 2 plus; Zeiss, Oberkochen, Germany) equipped with a digital camera (AxioCam HRc, Zeiss) and a PC. Using the software AxioVision (version 4.6, Zeiss), filters were screened at 100x magnification and 30 pictures per filter were randomly taken in a cross section (15 pictures on the vertical axis, 15 pictures on the horizontal axis). In addition, five pictures were taken randomly to have spare photos in case that phytoplankton cells disturb the analysis.

Then, the image analysis software WCIF ImageJ (Version 1.44, Public Domain, developed at the US National Institutes of Health, courtesy of Wayne Rasband, National Institute of Mental Health, Bethesda, Maryland) was used to semi-automatically analyze particle number and area.

First, all pictures of each filter were stacked and split into their color channels red, green and blue. All but the red channel was discarded, since here the contrast between particle and background is highest. After manually choosing a threshold range that tries to encompass all stained gels but no other particles, the minimum area size to be analyzed was set to 0.2 μm^2.

Finally, ImageJ calculated area and size for each individual particle. The number of counted particles on approximately 30 pictures was extrapolated to full filter size and per volume of sample using the formula:

$$N\ (L^{-1}) = \ - \frac{A_{p \times n}}{b\ \times M \times V}$$

where A_p is the total filter area (mm^2) stained with AB or CBBG solution, n the number of exopolymeric particles counted, b the number of fields examined, M the area size of one field of view (mm^2), and V the volume (L) of sample. Total area per filter and volume was calculated accordingly.

2.7.5 Colorimetric Method for Analyzing TEP and CSP

2.7.5.1 Colorimetric Method for Analyzing TEP

The principle of TEP colorimetry is to photometrically determine the amount of AB dye bound to transparent exopolymeric particles in a sample. Comparing the absorption values to those of a standard reference yields estimates of TEP concentration. Gum Xanthan (G-1253; Sigma) was used as a standard. Therefore, AB stained filters were transferred into acid-resistant tubes, 6 mL of 80 % H_2SO_4 was added and tubes were tightly sealed. The tubes were agitated to ensure that the whole filter is covered by the acid. During incubation for 2 h, particulate organic matter (POM) is decomposed while AB is released from its binding sites. About 2 times during incubation tubes were agitated gently. Afterwards, the absorbance of the amount of AB was measured with a photometer (Spectronic Genesys 5; Milton Roy, Philadelphia, USA) at 787 nm in a 1 cm cell against sulfuric acid (80% H_2SO_4). TEP concentrations are given in micrograms of Gum Xanthan equivalents per liter (µg Xeq. L^{-1}) and calculated using:

$$TEP \text{ (µg Xeq. L}^{-1}) = \frac{(E_{787} - C_{787})}{V} \times F(x)$$

where E_{787} is the absorption of the sample at 787 nm, C_{787} the absorption of the blank at 787 nm, V is the volume in L and F is the calibration factor determined for the standard polysaccharide Gum Xanthan.

2.7.5.1.1 Calibration of AB Solution

For the calibration of the AB working solution the exact concentration of stain needs to be determined using the standard polysaccharide Gum Xanthan. Gum Xanthan is a heteropolysaccharide that contains D-glucuronic acid and is produced by the bacterium *Xanthomonas campestris.* The amount of AB absorbed is directly related to the weight of the standard. The calibration factor is the slope of the linear relationship between the weight of the standard polysaccharide and the amount of stain absorbed. Using the calibration factor, the equivalent mass of Gum Xanthan is calculated from the sample absorption.

The standard was prepared by adding 15 mg Gum Xanthan to 200 mL MilliQ water. The solution was allowed to swell for 15 min. To obtain a size distribution of the polysaccharide similar to what is expected for TEP, the solution was treated with a tissue grinder.

A 5-point calibration was carried out with volumes 0.5, 1, 2, 3, and 4 mL of standard solution. Triplicate filters of each volume were stained and analyzed according to TEP filtration and the colorimetric method, respectively, as explained above. Three blank filters were prepared to determine AB adsorption to the filter.

For determination of Gum Xanthan weight retained on the filter, a second series of the aforementioned volumes was filtered onto preweighed 0.4 μm PC-filters. Five replicate filters were prepared for each volume of standard solution. After filtration, filters were dried at 60 °C for 12 hours, cooled to room temperature and stored in a dessicator.

Prior to weighing, filters were allowed to equilibrate with temperature and moisture in the room. The weight of each filter was determined three times before and after filtration using a Mettler Toledo UMX-2 microbalance (1 μg accuracy; Mettler Corp., Germany). Electrostatic charges of dry Nuclepore filters were neutralized by an ionization system before weighing (Haug PRX U Small SET; Haug Corp., Germany). Filters were kept in combusted glass petridishes during all times to avoid contamination (Engel, 2009). To retrieve the weight (W_i) of Gum Xanthan on the filters for the respective volumes, the average weight of empty filters (W_{fe}) is subtracted from the average weight of filters containing Gum Xanthan (W_{fi}). To account for weight fluctuations due to moisture change, the average weight of blank filters (W_{bl1} - W_{bl2}) is also subtracted:

$$W_i = \left(W_{fi} - W_{fe}\right) - (W_{bl1} - W_{bl2})$$

The calibration factor F(x) of the standard is calculated from the slope of the regression of weight (μg) against the corresponding absorbance (ABS):

$$f(x) = \frac{\Delta W}{\Delta ABS}$$

2.7.5.1.2 TEP-Carbon Determination

TEP-C_{color} was estimated using the following relationship:

$$TEP - C_{color} = 0.75 \times TEP_{color}$$

where the carbon content of TEP is given in μg and TEP_{color} in μg Xeq. (Engel & Passow, 2001). As species-specific differences were statistically significant, this relationship assumes that the polysaccharide composition of TEP is similar to that released by the mix of diatoms used during the study (Engel & Passow, 2001).

2.7.5.2 Colorimetric method for analyzing CSP

This method is analogous to the colorimetric method for TEP determination in many ways and follows the description by Cisternas-Novoa et al. (2014) with minor modifications. The amount of CBBG dye bound to CSP is determined. By comparing absorption values to those of a standard reference, estimates of CSP concentration are yielded. Therefore, CBBG stained filters were transferred into acid-resistant tubes. To elute CBBG dye, 6 mL of extraction solution (3% SDS in 50% isopropyl alcohol) was added. The tubes were sonicated in a water bath (35 kHz) for 2 h at 37 °C. Afterwards, the absorbance of the amount of CBBG was measured with a photometer (Spectronic Genesys 5; Milton Roy, Philadelphia, USA) at 615 nm in a 1 cm cell against the extraction solution. CSP concentrations are given in micrograms of Bovine serum albumin (BSA) equivalents per liter (μg BSAeq. L^{-1}) and calculated using:

$$CSP \text{ (μg BSAeq. } L^{-1}) = \frac{(E_{615} - C_{615})}{V} \times F(x)$$

where E_{615} is the absorption of the sample at 615 nm, C_{615} the absorption of the blank at 615 nm, V is the volume in L and F is the calibration factor determined for the standard protein BSA.

2.7.5.2.1 Calibration of CBBG Solution

For the calibration of the CBBG working solution the exact concentration of stain needs to be determined using the standard protein BSA. BSA is a serum albumin protein derived from cows. The amount of CBBG absorbed is directly related to the weight of the standard. The calibration factor is the slope of the linear relationship between the weight of the standard protein and the amount of stain absorbed. Using the calibration factor, the equivalent mass of BSA is calculated from the sample absorption.

The stock solution of the standard was prepared by adding 1 mg BSA (Sigma) per mL MilliQ water. The solution was homogenized by stirring for 30 min. To form gel aggregate particles, the BSA solution was first put in a heating bath at 85 °C for 2 h, immediately cooled in a water bath at 25 °C and refrigerated overnight at 4 °C. Second, the solution was treated with a tissue grinder to break apart excessively large aggregates. A set of five calibration standards of increasing concentration (16, 32, 80, 200, and 400 µg mL^{-1}) was prepared by diluting the BSA stock with MilliQ water.

The calibration of the CBBG solution is similar to the calibration of the AB solution with slight modifications. A 5-point calibration was carried out with the aforementioned concentrations of BSA solution. Triplicate filters of each volume were stained and analyzed according to CSP filtration and the colorimetric method, respectively, as explained above. Three blank filters were prepared to determine CBBG adsorption to the filter.

For determination of BSA weight retained on the filter, a second series of the same concentrations was filtered onto preweighed 0.4 µm PC-filters. Five replicate filters were prepared for each volume of standard solution. After filtration, filters were treated and weighed in the same manner as mentioned above. To calculate the weight of BSA (W_i) on the filters for the respective volumes and the calibration factor F(x) of the standard, same equations were used as for Gum Xanthan.

2.8 Statistical Analyses

Statistical analyses were performed using SigmaPlot (Systat Software Inc., San Jose, USA). Potential relationships between TEP, CSP and bacterial measurements with sea ice parameters were tested using multiple linear regression. The equality of the variances and the normality of the residuals were tested by a Brown-Forsythe test and a Shapiro-Wilk test, respectively.

Differences in sea ice parameters between bottom and top ice core sections as well as between different ice types were tested using one-way analysis of variance (ANOVA). When the assumptions of ANOVA were not satisfied, a Kruskal Wallis ANOVA on ranks was performed.

For statistical analysis the three experiments were handled as individual replicates although they were performed with melted ice of different ice types (Table 2), since overall the ice type did not have a significant effect on the bacterial community composition living either free or particle attached. Paired t-tests were used to test for differences in the relative abundance of single probes (**i**) in the free living bacterial fraction during the course of the experiment, (**ii**) of attached bacteria between particle types and the free living fraction, and (**iii**) of the overall particle-attached and free living bacterial fraction.

III Results

3.1 Stations

3.1.1 Environmental and Physical Sea Ice Parameters

On the transect from the Greenland side of Fram Strait to Svalbard during Polarstern cruise PS 85 in June 2014 (Fig. 4), sea ice was sampled at in total 10 stations (Table 12). Sampled sea ice differed greatly in its size, thickness and snow cover. Ice thickness ranged from 69 (station 7) to 272 cm (station 5). Snow coverage was lowest at station 3 (3 cm) and highest at station 5 (27.5 cm).

For comparison of different ice types, station 7 and 8 were grouped as small ice floes. Both were floating on warm Atlantic waters and were thinner than one meter. They can be considered to be rapidly melting ice floes since their under-ice water temperatures were above 0 °C. Small ice floes are thinner than either large ice floes and landfast ice (one-way ANOVA; $p < 0.001$ and 0.008 respectively), warmer than the other ice types ($p < 0.001$) and clearer than the other ice types, with higher light transmission through the ice ($p < 0.001$ and 0.011, respectively). Salinity was lowest in large ice floes (median 3.6) significantly different from landfast ice ($p = 0.038$). Except for small ice floes, under-ice water temperature was below 0 °C. Ice core temperatures were highest for large ice floes and lowest for landfast ice (median -0.71 and -0.99 °C, respectively). Except for station 2 and 3, the bottom half of ice cores were colder than the top.

Table 12: Environmental and physical parameters (average ± SD) within sea ice core sections of the sampling sites

	Position		Ice	Ice thickness	Snow coverage	Trans-mission	UIW temp.	Core	Ice core temperature	Salinity
Station	Longitude N	Latitude	type	cm	cm	%	°C	section	°C	
1	78 15.915	14 42.859W	Landfast	135	9	2,8		Bottom	-1,56 ± 0,23	4,53 ± 2,14
								Top	-0,99 ± 0,59	5,02 ± 0,62
2	77 45.609	16 3.58W	Landfast	190	4	2,6	-1,65	Bottom	-0,56 ± 0,30	4,42 ± 1,23
								Top	-0,84 ± 0,34	5,57 ± 1,28
3	78 49.0	8 46.167W	Large floe	164	3	2,7	-1,36	Bottom	-0,36 ± 0,24	3,54 ± 1,41
								Top	-1,06 ± 0,36	4,30 ± 0,81
5	78 52.091	4 29.551W	Large floe	272	27,5	0,8	-1,64	Bottom		
								Top		
6	78 30.403	2 47.951W	Large floe	177	24	1,8	-1,42	Bottom	-0,21 ± 0,26	3,91 ± 0,69
								Top	-0,14 ± 0,13	4,65 ± 0,76
9	79 45.284	4 18.279E	Large floe	173	9	3,7	-1,68	Bottom	-1,32 ± 0,25	3,60 ± 0,44
								Top	-1,07 ± 0,59	3,76 ± 1,17
10	78 48.175	2 00.996W	Large floe	213	20	1,9	-1,06	Bottom	-0,85 ± 0,16	3,42 ± 0,34
								Top	-0,66 ± 0,22	1,76 ± 1,42
7	79 3.044	4 9.188E	Very s. floe	69	4	10,2	1,30	Bottom	-0,80 ± 0,10	4,23 ± 0,51
								Top	-0,41 ± 0,22	5,05 ± 1,04
8	79 2.428	4 18.576E	Small floe	89	5	5,9	1,00	Bottom	-1,06 ± 0,15	5,02 ± 0,55
								Top	-0,65 ± 0,23	4,13 ± 1,48

3.1.2 Biotic and Abiotic Sea Ice Parameters

Total bacterial counts of bottom 5 cm sections ranged from 0.2×10^8 cells L^{-1} (very small ice floe) to 8.6×10^8 cells L^{-1} (landfast; Table 13). Lowest numbers were found for small ice floes significantly different from large ice floes and landfast ice ($p < 0.001$) as shown in Fig. 6.

Chlorophyll *a*, particulate organic carbon (POC) and particulate organic nitrogen (PON) concentrations were lowest in small ice floes. Chlorophyll *a* measurements show highest values in large ice floes, whereas, POC and PON were highest in landfast ice. POC:PON ratios were statistically similar between different sea ice types, ranging from 7.6 for landfast ice to 8.0 for large ice floes. In large ice floes and landfast ice, chlorophyll *a* concentrations were higher in bottom than top sections, with significantly higher values only for chlorophyll *a* smaller than 10 µm (median 0.33 and 0.05 µg L^{-1}, respectively, $p = 0,047$). In small ice floes, higher concentrations of chlorophyll *a* were generally found in the top half of ice cores (one exception for chlorophyll *a* bigger than 10 µm at station 8). PON and POC concentrations over

all stations were similar for the top and bottom half of ice cores. If differentiated by sea ice type, POC and PON dominated in the bottom section of landfast ice and in the top section of small ice floes, except for POC at station 8. In large ice floes, POC and PON were equally distributed within the ice.

Bottom section of station 2 yielded much higher concentrations for chlorophyll *a*, POC and PON than all other stations. Since high concentrations were present in several 10 cm subsections of the bottom half of ice core, data were not excluded from further analysis.

Table 13: Concentrations (average ± SD) of biotic parameters and particulate organic nitrogen (PON) and carbon (POC) within sea ice core sections of the sampling sites. Chlorophyll *a* (Chl*a*)

Station	Bacterial cell number 10^8 L^{-1}	Core section	Total *Chla* µg L^{-1}	< 10 µm *Chla* µg L^{-1}	> 10 µm *Chla* µg L^{-1}	PON µg N L^{-1}	POC µg C L^{-1}
1	1,5 ± 0,6	Bottom	0,316 ± 0,541	0,259 ± 0,477	0,052 ± 0,057	88 ± 33	556 ± 232
		Top	0,060 ± 0,058	0,050 ± 0,057	0,010 ± 0,003	80 ± 32	545 ± 221
2	8,6 ± 2,9	Bottom	1,575 ± 0,730	0,893 ± 0,752	0,682 ± 0,244	157 ± 38	1500 ± 646
		Top	0,084 ± 0,023	0,052 ± 0,021	0,032 ± 0,016	89 ± 14	720 ± 236
3	3,1 ± 1,0	Bottom	0,953 ± 1,024	0,390 ± 0,455	0,564 ± 0,573	80 ± 34	523 ± 269
		Top	0,106 ± 0,069	0,055 ± 0,031	0,051 ± 0,045	65 ± 6	538 ± 36
5	1,5 ± 0,6						
6	3,6 ± 1,0	Bottom	0,929 ± 0,705	0,397 ± 0,407	0,532 ± 0,302	71 ± 12	605 ± 65
		Top	0,058 ± 0,034	0,036 ± 0,024	0,022 ± 0,016	82 ± 38	703 ± 222
9	3,1 ± 0,9	Bottom	0,986 ± 0,961	0,289 ± 0,385	0,697 ± 0,677	77 ± 59	651 ± 553
		Top	0,045 ± 0,023	0,030 ± 0,015	0,015 ± 0,009	74 ± 22	467 ± 152
10		Bottom	0,906 ± 0,778	0,367 ± 0,267	0,539 ± 0,553	69 ± 62	556 ± 449
		Top	0,059 ± 0,017	0,041 ± 0,016	0,018 ± 0,006	63 ± 18	618 ± 182
7	0,2 ± 0,2	Bottom	0,068 ± 0,035	0,044 ± 0,014	0,023 ± 0,032	56 ± 5	436 ± 30
		Top	0,077 ± 0,048	0,046 ± 0,016	0,030 ± 0,029	85 ± 39	635 ± 325
8	0,4 ± 0,3	Bottom	0,207 ± 0,125	0,088 ± 0,065	0,119 ± 0,084	63 ± 9	473 ± 66
		Top	0,216 ± 0,203	0,134 ± 0,177	0,082 ± 0,108	62 ± 20	435 ± 159
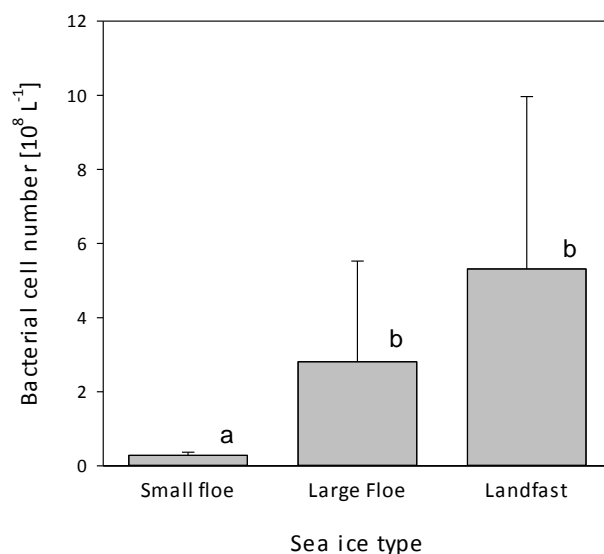
Figure 6. Bacterial counts in different sea ice types. Average of stations (small floe and landfast n = 2, large floe n = 4) with standard error. Bars topped with different letters are statistically different.

3.1.3 TEP and CSP Number, Area and Concentration in Sea Ice

Over all, transparent exopolymeric particle (TEP) and Coomassie stainable particle (CSP) values including particle number, area and photometric measurements were lowest for small ice floes and highest for landfast ice. TEP area only showed the highest values in large ice floes (Table 14). CSP number and area were significantly lower in small ice floes compared to large ice floes and landfast ice (Fig. 7).

Over all stations, TEP microscopy yielded higher values for bottom sections, whereas values obtained photometrically did not show a difference between bottom and top sea ice sections. No difference in CSP values between bottom and top were detected, except for CSP area; here, values are higher for the top section of sea ice cores.

If differentiated by sea ice type, all TEP measurements show the same pattern. Top half sections of small ice floes harbor higher values of TEP, whereas bottom sections show higher values for large ice floes and landfast ice. CSP measurements yielded less consistent results. Although values are highest in top sections of small ice floes, too, CSP values are higher in bottom or top sections of large ice floes and landfast ice depending on station and method.

Carbon content of TEP follows the pattern of TEP photometry. TEP-carbon contribution to POC ranges from 10 to 24% (median 20%), with no apparent pattern. 64% of TEP-C variability can be explained by POC concentrations (Fig. 8).

Differentiated by top and bottom half of sea ice, analysis of particle area and number of particulate extracellular polymeric substances (pEPS) yielded higher values for TEP in the bottom half section. In the top half of ice cores particle number is greater for TEP, whereas particle area is greater for CSP. Thus, TEP seems to dominate in the bottom half of arctic sea ice sampled during early summer. In contrast, CSP seems to dominate in terms of particle area and TEP dominates in terms of number in the upper half of sampled sea ice.

Table 14: Total number, area and concentration (average ± SD) of TEP and CSP within sea ice core sections of the sampling sites

| Station	Core section	TEP Microscopy Number 10^8 L^{-1}	Area 10^3 µm^2 L^{-1}	Photometry µg Xeq.L^{-1}	TEP-C µg L^{-1}	% TEP-C of POC	CSP Microscopy Number 10^8 L^{-1}	Area 10^3 µm^2 L^{-1}	Photometry CSP µg BSAeq.L^{-1}
1	Bottom	21,5	230	160 ± 5	120 ± 4	22	0,7	401	364 ± 0
	Top	0,2	18	166 ± 7	125 ± 6	23	1,3	489	458 ± 3
2	Bottom	59,4	529	207 ± 23	155 ± 17	10	0,9	348	803 ± 27
	Top	1,4	147	118 ± 23	89 ± 17	12	1,4	392	393 ± 19
3	Bottom	1,1	305	140 ± 15	105 ± 11	20	1,1	205	388 ± 3
	Top	13,5	317	150 ± 9	112 ± 6	21	0,7	338	367 ± 28
6	Bottom	19,2	279	149 ± 13	112 ± 10	18	0,5	310	388 ± 10
	Top	1,2	158	159 ± 4	119 ± 3	17	0,7	525	378 ± 38
9	Bottom	2,2	386	144 ± 7	108 ± 5	17	1,0	518	489 ± 48
	Top	1,0	195	144 ± 14	108 ± 10	23	0,7	236	447 ± 65
10	Bottom	2,5	695	155 ± 7	116 ± 5	21	1,0	224	553 ± 74
	Top	1,0	129	132 ± 23	99 ± 17	16	0,3	376	347 ± 18
7	Bottom	0,3	142	137 ± 0	103 ± 0	24	0,1	118	362 ± 15
	Top	0,5	213	162 ± 10	121 ± 7	19	0,3	97	471 ± 17
8	Bottom	0,4	54	102 ± 1	77 ± 1	16	0,2	132	360 ± 48
	Top	0,5	82	140 ± 4	105 ± 3	24	0,2	277	391 ± 32
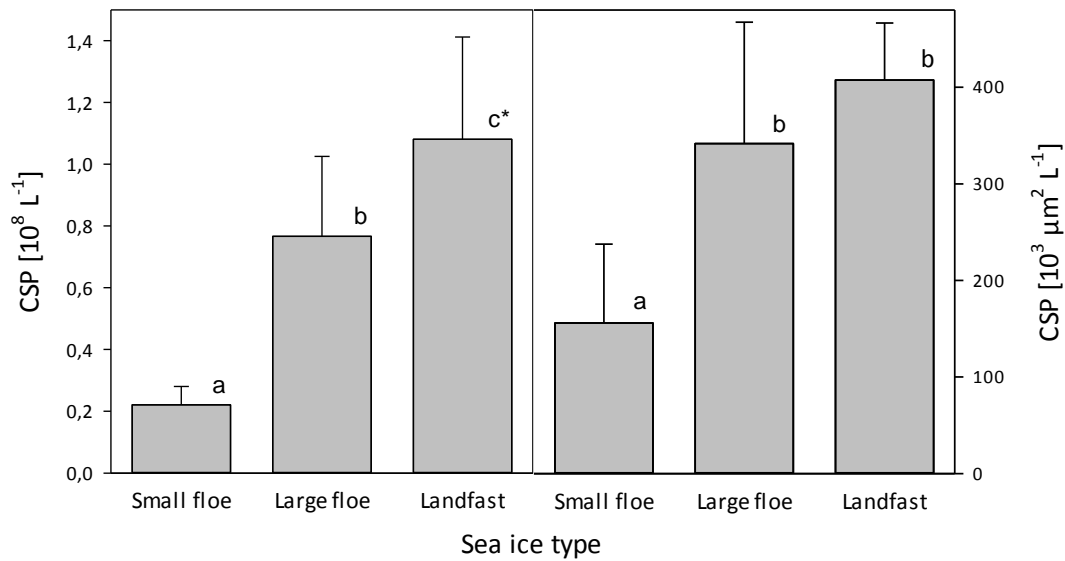
Figure 7. CSP number and area in different sea ice types. Average of stations (small floe and landfast n = 4, large floe n = 8) with standard error. Almost significant differences between all sea ice types for CSP number (one way ANOVA; small versus large p < 0.001, small versus landfast p = 0.007, large versus landfast p = 0.061). CSP area of small ice floes is significantly different from large ice floes (p = 0.024) and landfast ice (p = 0.014).
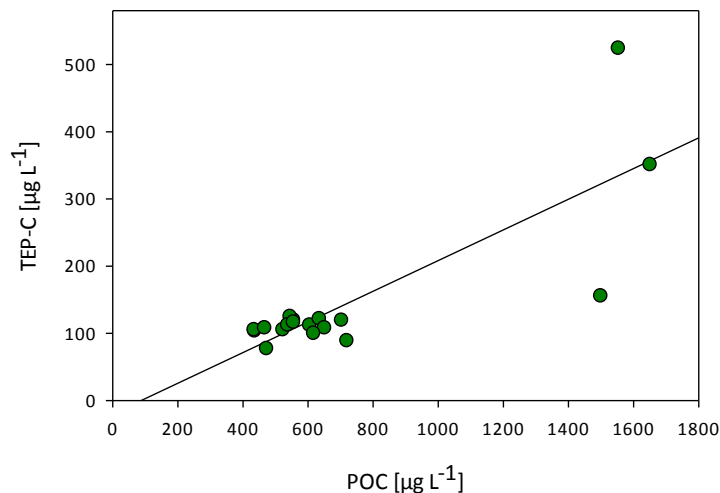
Figure 8. Relationship between photometrically determined TEP-carbon and particulate organic carbon (POC) based on data from all stations. The adjusted r^2 is 0.640, n = 18, p < 0.001.

3.1.4 Correlation of TEP, CSP and Bacteria with Sea Ice Parameters

Relevant sea ice parameters were compared statistically to TEP, CSP and bacterial cell numbers via multiple regression to explore any relationships within sea ice. Results are listed in Table 15. Adjusted r^2 is a measure of the percentage of variation that can be explained by the independent variables that actually affect the dependent variables. Fig. 9 shows linear regressions of the highest correlations of TEP and CSP with sea ice parameters. Neither TEP nor CSP measurements show any significant correlation to ice core temperature, snow coverage or salinity.

Most of the variation within TEP (number, area and concentration) can be explained by chlorophyll *a* (total, bigger and smaller than 10 µm), POC (except for area) and PON (except for area) concentrations, with highest values for TEP number with POC (69.4%), TEP area with total chlorophyll *a* (55.1%) and TEP concentration with chlorophyll *a* bigger than 10 µm (85.3%).

For CSP (number and area) most of the variation can be explained by under-ice water temperature (only correlated to bottom half section), transmission of light through the ice (both being negatively correlated), ice type and ice thickness, with highest values for under-ice water temperature (72.9% for number and 50.6% area).

TEP number and concentration seems to be mainly driven by biotic and abiotic factors (TEP area only by biotic factors), whereas variations in CSP area and number can be explained by physical parameters. However, CSP concentration shows the same pattern as TEP, possessing strongest correlation with POC (66.8%).

Bacterial cell numbers are well correlated with TEP (number, area and concentration) as well as CSP concentration as shown in Fig. 10, with highest value for the correlation with TEP area (83.1%). Furthermore, ice type and under-ice water temperature explain a part of the variation in bacterial cell number by 47.6% and 36.8%, respectively.

Table 15: Linear regressions of TEP, CSP and bacterial measurements with sea ice parameters, biotic and abiotic factors of all stations

Dependent parameter	Ice type Adj r^2	p	Ice thickness Adj r^2	p	UIW temp. Adj r^2	p	Transmission Adj r^2	p	Core section Adj r^2	p
TEP number	0,173	0,061	n.s.		n.s.		n.s.		n.s.	
TEP area	n.s.		0,220	0,038	n.s.		n.s.		0,191	0,051
TEP concentration	n.s.		n.s.		n.s.		n.s.		0,429	0,002
CSP number	0,605	< 0,001	0,293	0,018	**0,729**	0,009	0,345	0,01	n.s.	
CSP area	0,409	0,005	0,232	0,034	**0,506**	0,044	0,409	0,005	n.s.	
CSP concentration	n.s.		n.s.		n.s.		n.s.		n.s.	
Bacteria	0,476	0,002	n.s.		0,368	0,013	0,163	0,068	-	

Dependent parameter	> 10 µm Chl*a* Adj r^2	p	< 10 µm Chl*a* Adj r^2	p	Total Chl*a* Adj r^2	p	PON Adj r^2	p	POC Adj r^2	p	Bacteria Adj r^2	p
TEP number	n.s.		0,661	< 0,001	0,388	0,006	0,670	< 0,001	**0,694**	< 0,001	0,723	0,009
TEP area	0,538	< 0,001	0,458	0,002	**0,551**	< 0,001	n.s.		n.s.		**0,831**	0,003
TEP concentration	**0,853**	< 0,001	0,748	< 0,001	0,827	< 0,001	0,799	< 0,001	0,640	< 0,001	0,742	0,008
CSP number	n.s.		n.s.		n.s.		n.s.		n.s.		n.s.	
CSP area	n.s.		n.s.		n.s.		n.s.		n.s.		n.s.	
CSP concentration	0,307	0,015	0,581	< 0,001	0,467	0,002	0,662	< 0,001	**0,668**	< 0,001	0,810	0,004
Bacteria	n.s.		0,265	0,029	n.s.		n.s.		0,216	0,046	-	

Adjusted r^2 (Adj r^2); grey numbers: almost significant; bold numbers: highest adjusted r^2 value

TEP/CSP number and area n = 16, TEP/CSP concentration n = 18

bacteria n = 8, under-ice water temperature n = 8
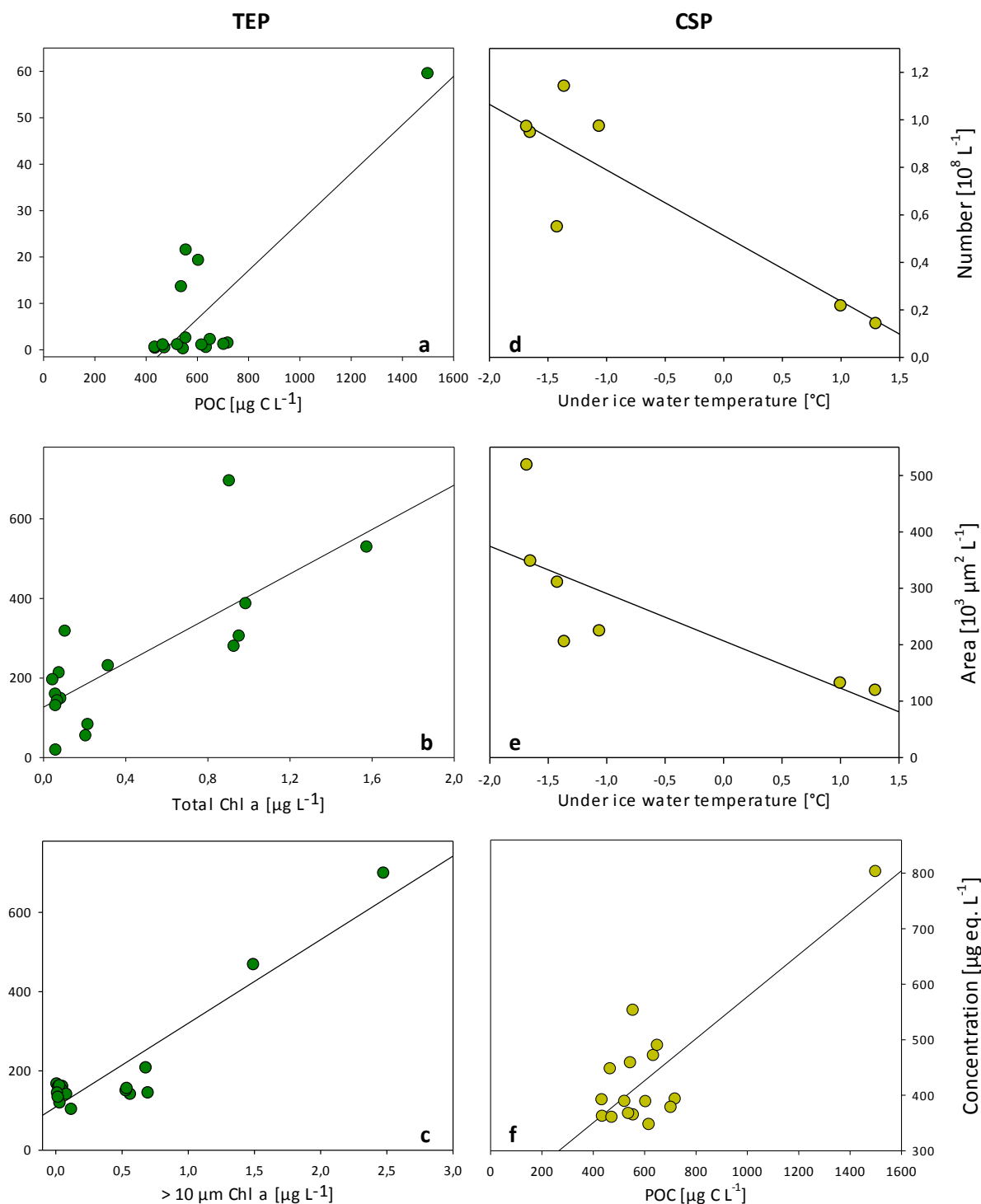
Figure 9. Highest correlation of (a) TEP number with POC (µg C L^{-1}), (b) TEP area with total Chl*a* (µg L^{-1}), (c) TEP (µg Xeq. L^{-1}) with > 10 µm Chl*a* (µg L^{-1}), (d) CSP number with under-ice water temperature (°C), (e) CSP area with under-ice water temperature (°C), and (f) CSP (µg BSAeq. L^{-1}) with POC (µg C L^{-1}). The adjusted r^2 are given in Table 16. Regressions (a) and (f) were dragged by one outlier only. Outlier bottom section of station 2 was not excluded from analysis as explained in section 3.1.2.
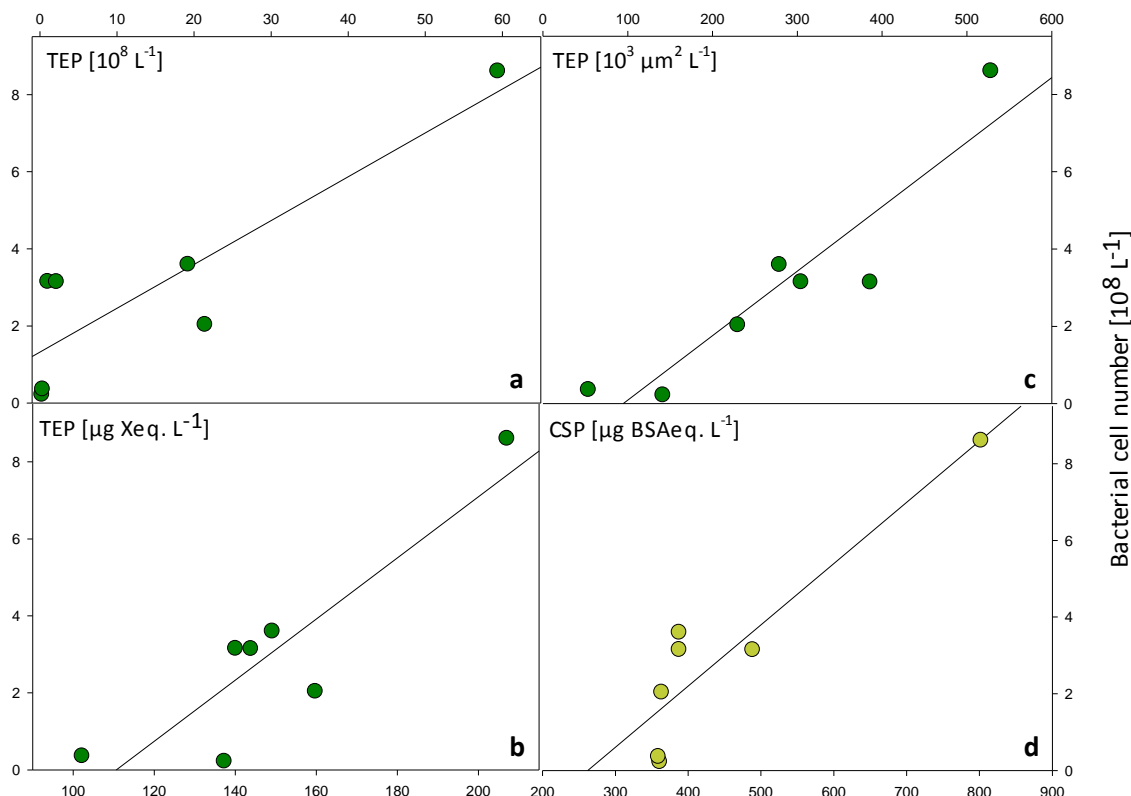
Figure 10. Significant results of the linear regression of bacterial cell number (10^8 L^{-1}) with (a) TEP number, (b) TEP (µg Xeq. L^{-1}), (c) TEP area, and (d) CSP (µg BSAeq. L^{-1}). The adjusted r^2 are given in Table 16.

3.1.5 DGGE Analysis of Sea Ice Stations

Denaturing gradient gel electrophoresis (DGGE) profiles of PCR amplified 16S rRNA gene fragments were obtained from eight sea ice stations in order to compare bacterial diversity and community structure of different sea ice types (Fig. 11). All bands of the same position between lanes were excised twice and sequenced. Table 16 lists the successfully sequenced bands and their closest relatives in the silva database (http://www.arb-silva.de). In general, the number of bands is a measure of community diversity, whereas the intensity of a band might tell something about the abundance. Landfast ice of station 1 and 2 look quite similar, with station 1 showing higher community diversity. Stations of large ice floes seem to be similar in diversity, but band intensity is reduced in station 6. The very small ice floe seems to be more reduced in diversity and intensity of bands than the small ice floe. Landfast ice and

large ice floes are quite similar in diversity and intensity of bands, but differing greatly in the upper section of lanes where mainly chloroplasts and *Flavobacteria* could be detected.

   In addition, melted sea ice samples were fractioned on filters of different pore size. The 2.0 µm fraction, encompassing microbial organisms that are ≥ 2.0 µm, was chosen to exclude most of the free-living bacterial cells as long rods can measure up to 0.65 µm x 4.0 µm (Helmke & Weyland, 1995). The 0.2 µm fraction contains microbial organisms in the size range between 2.0 and 0.2 µm and should mainly comprise free-living bacteria. Basically, banding patterns and intensities of fractionated samples look similar across the different stations, but the diversity and intensity of bands in the lower section of lanes seems to be higher in the "free-living" fraction (< 2.0 µm). Highest bacterial diversity was detected in the "free-living" fraction of station 1 (landfast ice). DGGE profiles in general indicate that there is a high overlap in biodiversity between the particle-attached and free-living fraction of bacteria.

Bacteria of the excised bands belonged most frequently to the γ-proteobacteria, here highest diversity of phylotypes was found with *Glaciecola spp.* as the dominant phylotype. Sequences retrieved from DGGE bands were closely related to members of *Glaciecola spp., Alteromonas spp., Granulosicoccus spp.*, and *Pseudomonas spp.* (γ-proteobacteria), *Polaribacter spp.* (*Flavobacteria*) and the *Roseobacter* clade (α-proteobacteria).
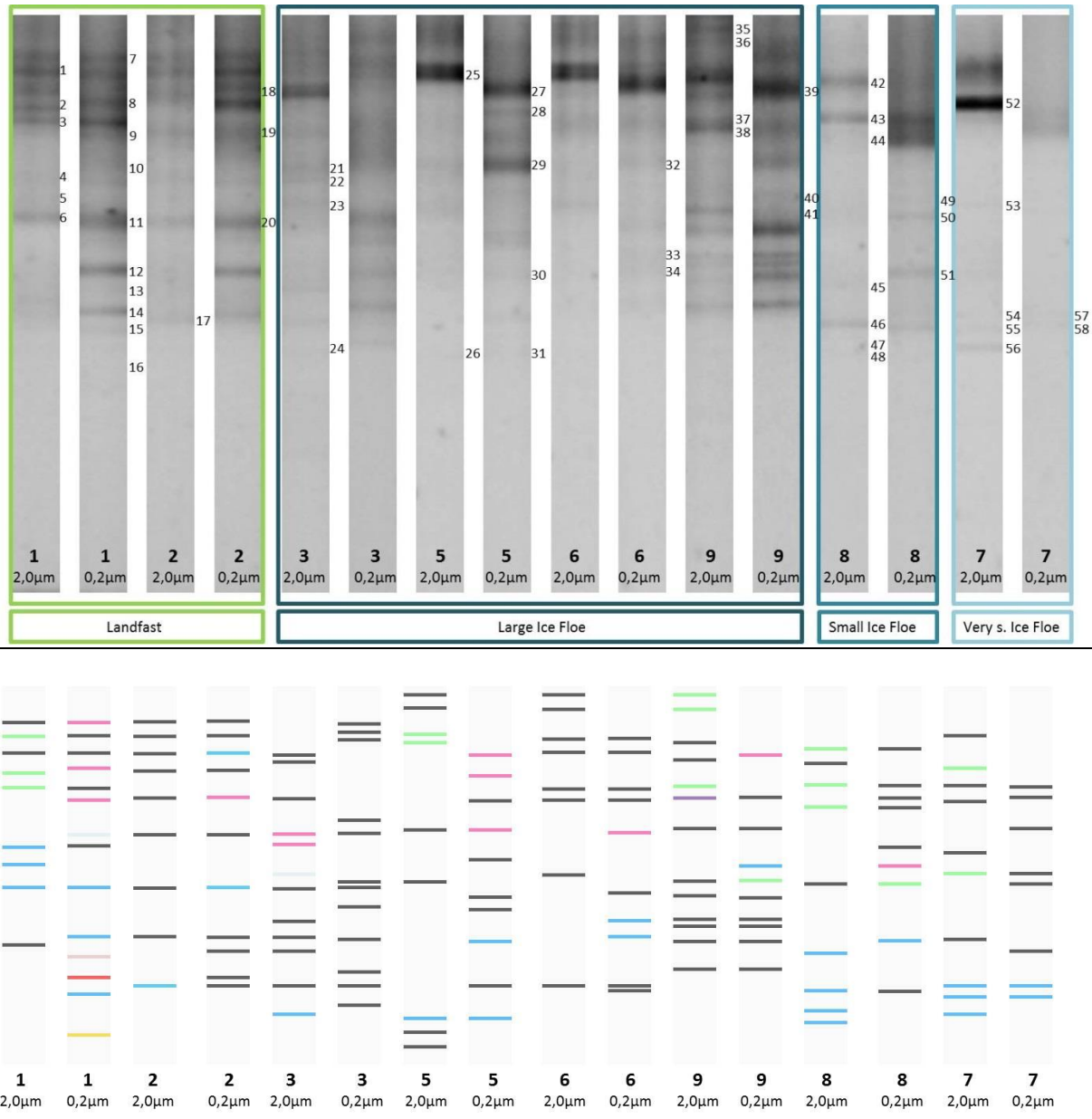
Figure 11. DGGE profiles of 16S rRNA gene fragments of sea ice samples from different ice types and size classes based on different filters. Numbering on the right hand side of the lanes indicates the names of excised DGGE bands listed in Table 16 with their closest relative in the Silva database. The chromogram below shows the phyla that the excised bands belong to.

α-proteobacteria
β-proteobacteria
γ-proteobacteria
Flavobacteria
Acidobacteria
Sphingobacteria
Planctomycetes
Chloroplast

Table 16: Sequence similarity of excised DGGE bands that appear in Fig. 11 and 14 based on SINA sequence alignment

Band	Closest relative ArbSilva database	Accession No.	% Identity	Alignment length	Phylogenetic group	Genus	Remarks
1	uncultured bacterium	JF272031	84,72	553	Cyanobacteria	Chloroplast	Natural marine biofilms
2	uncultured bacterium	AB696371	94,17	531	Cyanobacteria	Chloroplast	Loess Plateau, soil, China
3	Navicula phyllepta	FJ002222	95,07	526	Bacillariophyceae	Navicula	
4	Arctic sea ice bacterium ARK10218	AF468399	74,81	523	γ-Proteobacteria	Glaciecola	Arctic sea ice
5	uncultured Antarctic sea ice bacterium	AY165570	80,22	538	γ-Proteobacteria	Glaciecola	Antarctic pack ice, Lasarev Sea
6	Arctic sea ice bacterium ARK10218	AF468399	99,03	513	γ-Proteobacteria	Glaciecola	Arctic sea ice
7	uncultured Antarctic sea ice bacterium	AY165580	92,36	458	Flavobacteria	Polaribacter	Antarctic pack ice, Lasarev Sea
8	uncultured bacterium	AB232535	93,23	460	Flavobacteria	Flavobacterium	Hydrothermal vent, gill of Alvinocaris longirostris
9	uncultured marine bacterium	GU235511	94,74	494	Flavobacteria	Polaribacter	Antarctic sea water, 5m depth
10	uncultured bacterium	AB476256	83,92	510	Sphingobacteriia	NS11-12 marine group	Ventral setae of Shinkaia crosnieri
11	uncultured bacterium	GQ259243	96,63	533	γ-Proteobacteria	BD7-8 marine group	Surface water, Arctic ocean
12	uncultured bacterium	DQ015788	96,64	534	γ-Proteobacteria	BD7-8 marine group	Lake water, Antarctica
13	uncultured bacterium	DQ015789	93,06	517	Planctomycetes	SM1A02	Lake water, Antarctica
14	uncultured bacterium	GQ259242	95,85	529	α-Proteobacteria	Roseobacter clade	Surface water, Arctic ocean
15	uncultured bacterium	GQ259243	93,48	505	γ-Proteobacteria	BD7-8 marine group	Surface water, Arctic ocean
16	Betaproteobacteria bacterium MOLA814	AYMW01000003	80,57	517	β-Proteobacteria	BAL58 marine group	Seawater, Canada
17	uncultured bacterium	AF468287	94,28	507	γ-Proteobacteria	Alteromonas	Arctic pack ice, northern Fram Strait
18	uncultured proteobacterium	DQ330805	60,63	502	γ-Proteobacteria	Halochromatium	hypersaline microbial mat, Mexico
19	Polaribacter irgensii	AY167317	92,54	496	Flavobacteria	Polaribacter	Antarctic pack ice, Weddell Sea
20	uncultured bacterium	DQ015788	95,9	535	γ-Proteobacteria	BD7-8 marine group	Lake water, Antarctica
21	uncultured Antarctic sea ice bacterium	AY165564	90,53	433	Flavobacteria	Polaribacter	Antarctic pack ice, Lasarev Sea
22	Olleya sp. 204Z-30	GU584182	75,14	510	Flavobacteria	Olleya	Water sample, Antarctica
23	uncultured Bacteroidetes bacterium	DQ269087	68,74	512	Sphingobacteriia	Lewinella	Surface of marine macro-alga, Delisea pulchra
24	uncultured marine bacterium	GU234740	86,34	547	γ-Proteobacteria	Granulosicoccus	Antarctic sea water, 5m depth
25	Nitzschia closterium	FJ002221	98,77	488	Bacillariophyceae	Nitschia	
26	Granulosicoccus antarcticus	EF495228	85,21	544	γ-Proteobacteria	Granulosicoccus	Seawater, Maxwell Bay, Antarctica
27	uncultured bacterium	AB232535	94,86	506	Flavobacteria	Flavobacterium	Hydrothermal vent, gill of Alvinocaris longirostris
28	Polaribacter franzmannii	AY167319	86,08	501	Flavobacteria	Polaribacter	Antarctic pack ice, Weddell Sea
29	Polaribacter sp. SW019	AF493675	96,87	511	Flavobacteria	Polaribacter	Coastal seawater, UK
30	uncultured bacterium	DQ015788	92,15	520	γ-Proteobacteria	BD7-8 marine group	Lake water, Antarctica
31	uncultured bacterium	AB694360	82,05	509	γ-Proteobacteria	Alteromonas	Deep-sea sediment
32	uncultured Antarctic sea ice bacterium	AY165564	90,14	511	Flavobacteria	Polaribacter	Antarctic pack ice, Lasarev Sea
33	polar sea bacterium R9879	AJ295716	93,75	538	γ-Proteobacteria	Glaciecola	Polar seas
34	Arctic sea ice bacterium ARK10218	AF468399	95,84	527	γ-Proteobacteria	Glaciecola	Arctic sea ice
35	Nitzschia closterium	FJ002221	94,46	503	Bacillariophyceae	Nitschia	
36	Nitzschia closterium	FJ002221	95,03	501	Bacillariophyceae	Nitschia	
37	uncultured cyanobacterium	JF344518	94,74	493	Cyanobacteria	Chloroplast	Hydrocarbon polluted marine sediments, Spain
38	uncultured Acidobacteria bacterium	JF344519	94,51	491	Acidobacteria	Subgroup 22	Hydrocarbon polluted marine sediments, Spain
39	uncultured bacterium	AB232535	95,4	500	Flavobacteria	Flavobacterium	Hydrothermal vent, gill of Alvinocaris longirostris
40	uncultured bacterium	AF468296	93,65	518	γ-Proteobacteria	Glaciecola	Arctic pack ice, northern Fram Strait
41	uncultured bacterium	HQ916629	76,19	499	Cyanobacteria	Chloroplast	Lei-Gong-Huo mud volcano, China
42	Bacillaria paxillifer	AJ536452	92,41	472	Cyanobacteria	Chloroplast	

Band	Closest relative ArbSilva database	Accession No.	% Identity	Alignment length	Phylogenetic group	Genus	Remarks
43	uncultured phototrophic eukaryote	FJ946517	93,96	493		Chloroplast	Arctic snow, Svalbard
44	uncultured bacterium	EF574700	76,4	407	Cyanobacteria		Coco's Island
45	Pseudomonas sp. DVS6dIIb	AY864639	86,06	553	γ-Proteobacteria	Pseudomonas	Dry Valley, Antarctica
46	uncultured bacterium	AM932545	91,76	518	γ-Proteobacteria	Pseudomonas	Mouse cecum
47	Pseudomonas stutzeri DSM 4166	CP002622	84,62	527	γ-Proteobacteria	Pseudomonas	Rhizosphere-associated bacterium
48	Pseudomonas sp. 5-2	EU307935	77,61	443	γ-Proteobacteria	Pseudomonas	Soil sample from sewage treatment plant
49	uncultured deep-sea bacterium	AM997541	61,13	515	Flavobacteria	Owenweeksia	Deep-sea bacterium, South-Atlantic Ocean
50	uncultured bacterium	EU919841	84,24	502	Cyanobacteria	Chloroplast	Ocean water, Kongsfjorden, Svalbard
51	uncultured bacterium	DQ015788	91,75	518	γ-Proteobacteria	BD7-8 marine group	Lake water, Antarctica
52	uncultured phototrophic eukaryote	FJ946517	98,63	510			Artic snow, Svalbard
53	uncultured bacterium	EU919841	80,91	516	Cyanobacteria	Chloroplast	Ocean water, Kongsfjord, Svalbard
54	Pseudomonas sp. Da2	AY570696	93,81	533	γ-Proteobacteria	Pseudomonas	Low-temperature biodegraded Canadian oil reservoir
55	uncultured bacterium	AB745418	93,05	544	γ-Proteobacteria	Pseudomonas	Hot Spring, Indonesia
56	Pseudomonas stutzeri	AB680286	94,25	539	γ-Proteobacteria	Pseudomonas	
57	uncultured bacterium	AF468287	87,74	529	γ-Proteobacteria	Alteromonas	Arctic pack ice, northern Fram Strait
58	uncultured bacterium	AF468334	76,85	524	γ-Proteobacteria	Pseudomonas	Melt pond, Arctic sea ice floe
59	uncultured Polaribacter sp.	AF354621	84,02	510	Flavobacteria	Polaribacter	Bacterioplankton assemblages from the Arctic Ocean
60	uncultured bacterium	AF468296	94,59	534	γ-Proteobacteria	Glaciecola	Arctic pack ice, northern Fram Strait
61	uncultured bacterium	AF468295	91,95	509	γ-Proteobacteria	Colwellia	Arctic pack ice, northern Fram Strait
62	uncultured bacterium	AF468296	83,27	511	γ-Proteobacteria	Glaciecola	Arctic pack ice, northern Fram Strait
63	Polaribacter irgensii	AY771779	97,01	502	Flavobacteria	Polaribacter	Arctic bacteria
64	Polaribacter irgensii	AY771779	98,07	517	Flavobacteria	Polaribacter	Arctic bacteria
65	Polaribacter sp. SW019	AF493675	98,4	498	Flavobacteria	Polaribacter	Coastal seawater, UK
66	uncultured Antarctic sea ice bacterium	AY165570	91,59	540	γ-Proteobacteria	Glaciecola	Antarctic pack ice, Lasarev Sea
67	uncultured bacterium	AF468296	85,36	541	γ-Proteobacteria	Glaciecola	Arctic pack ice, northern Fram Strait
68	uncultured bacterium	AF468268	94,94	514	γ-Proteobacteria	Glaciecola	Arctic pack ice, northern Fram Strait
69	uncultured Antarctic sea ice bacterium	AY165564	95,69	510	Flavobacteria	Polaribacter	Antarctic pack ice, Lasarev Sea
70	uncultured bacterium	AF468296	90,84	511	γ-Proteobacteria	Glaciecola	Arctic pack ice, northern Fram Strait
71	uncultured bacterium	AF468296	94,64	521	γ-Proteobacteria	Glaciecola	Arctic pack ice, northern Fram Strait
72	uncultured bacterium	AF468268	97,46	511	γ-Proteobacteria	Glaciecola	Arctic pack ice, northern Fram Strait
73	uncultured bacterium	AF468268	98,26	518	γ-Proteobacteria	Glaciecola	Arctic pack ice, northern Fram Strait
74	Arctic sea ice bacterium ARK10218	AF468399	96,56	522	γ-Proteobacteria	Glaciecola	Arctic sea ice
75	uncultured Antarctic sea ice bacterium	AY165570	97,61	501	γ-Proteobacteria	Glaciecola	Antarctic pack ice, Lasarev Sea
76	uncultured bacterium	AF468268	97,41	501	γ-Proteobacteria	Glaciecola	Arctic pack ice, northern Fram Strait
77	uncultured phototrophic eukaryot	AF454328	70,49	463			Alkaline, hypersaline Mono Lake, California
78	uncultured Cytophaga sp.	AB015261	78,03	519	Flavobacteria	Flavobacterium	Cold-seep area of the Japan Trench
79	uncultured bacterium	AF468296	95,32	512	γ-Proteobacteria	Glaciecola	Arctic pack ice, northern Fram Strait
80	Pseudomonas sp. J62	AJ864855	87,13	505	γ-Proteobacteria	Pseudomonas	Lake water, Swiss
81	uncultured eukaryote	HQ230139	94,16	513			Snow, Canada
82	uncultured cyanobacterium	JF344518	90,89	515	Cyanobacteria	Chloroplast	Hydrocarbon polluted marine sediments, Spain
83	uncultured Antarctic sea ice bacterium	AY165570	97,11	518	γ-Proteobacteria	Glaciecola	Antarctic pack ice, Lasarev Sea
84	uncultured Antarctic sea ice bacterium	AY165564	90,27	509	Flavobacteria	Polaribacter	Antarctic pack ice, Lasarev Sea

3.2 Experiments

The experiments were conducted to study if the presence of pEPS influences the bacterial community composition. Therefore, melted sea ice samples were treated differently (see section 2.2). Treatment "precursor" samples should only contain dissolved organic matter (potential particle precursors), whereas the "bubbled" treatment, which was air ventilated throughout the whole experiment, should contain precursors as well as pEPS. The control is the undiluted natural sea ice inoculum of the respective experiment.

Experiment 1 was conducted with landfast ice, experiment 2 and 3 with sea ice from large floes. Since there was no significant difference detected for any of the parameters measured between landfast ice and large sea ice floes, the three experiments were handled as replicates for further analysis.

3.2.1 TEP, CSP Concentration and Bacterial Abundance

Bacterial cell numbers increased tremendously from day zero to day four by 464% ($\pm_{24}^{115}$) and 640% ($\pm_{86}^{209}$) in the "precursor" treatment and control, respectively, but stayed constant for the "bubbled" treatment (increase of 0% $\pm_{11}^{34}$; Fig. 12). Thus, bacterial cell growth seems to be strongly repressed by air ventilation. Significantly highest bacterial cell numbers were detected in controls after four days of incubation (Table 17).

TEP and CSP concentrations of different treatments within an experiment show similar patterns over time. Concentrations of TEP were highest in experiment 1, but over all there is no significant difference between experiments, treatments or days (three-way ANOVA). TEP concentrations correlate positively with bacterial cell numbers, explaining 48% (p < 0.001) of variation in bacterial abundance (Fig. 13). Concentration of CSP in the controls was similar between experiments and days. Treatments "bubbled" and "precursor" yielded negative values for CSP concentration. This might be due to comparably low sample volumes of 25 mL (150 mL for stations) and possible contaminated MilliQ water (onboard MilliQ filtration device did not run properly) that was used for blanks. Therefore, it can only be stated that there is no significant difference between treatments and days within experiment 1. Although the photometric determination of TEP and CSP seems to be highly susceptible to high standard

deviations and blanks, resulting in negative concentrations for CSP, TEP and CSP concentrations can be compared between treatments within the same experiment and day.

TEP and CSP concentrations were usually highest in the undiluted control and similar in the "precursor" and "bubbled" treatment. This indicates that the incubation of flasks on shaking platforms (to keep solids in solution) resulted in shear stress that was strong enough to form pEPS from dissolved precursors. Since pEPS were generated in all treatments the initial concept of the experiment failed. Therefore, for the following analysis, the focus was put on the controls as they simulate what might happen to the bacterial community composition after sea ice had melted.

Table 17: Average values ± SD of TEP, CSP and bacterial cell number of subsamples taken after zero, two and four days of incubation

| Exp.	Day	Treatment	Melted ice and inoculum from	Photometric TEP µg XG eq.L^{-1}	CSP µg BSA eq.L^{-1}	Bacterial cell number 10^8 L^{-1}
1	0	Precursor	Landfast	1166 ± 209	149 ± 32	
		Bubbled		1627 ± 101	154 ± 104	
		Control		2680 ± 310	140 ± 51	
	2	Precursor		530 ± 91	267 ± 44	1,16
		Bubbled		591 ± 67	281 ± 46	0,38
		Control		1109 ± 95	280 ± 112	10,90 ± 2,39
	4	Precursor		586 ± 0	218 ± 7	3,78
		Bubbled		586 ± 52	241 ± 30	0,50
		Control		1387 ± 17	325 ± 32	21,76 ± 4,99
2	0	Precursor	Large floe	589 ± 17	-57 ± 12	0,60
		Bubbled		476 ± 81	-1 ± 23	0,50
		Control		698 ± 24	213 ± 37	4,06 ± 1,11
	2	Precursor		531 ± 26	-6 ± 28	0,96
		Bubbled		501 ± 187	-277 ± 72	0,38
		Control		655 ± 60	187 ± 28	2,89
	4	Precursor		528 ± 34	158 ± 41	1,97
		Bubbled		601 ± 17	205 ± 23	0,36
		Control		595 ± 94	329 ± 74	16,77 ± 3,86
3	0	Precursor	Large floe	200 ± 17	-514 ± 14	0,22
		Bubbled		194 ± 43	-529 ± 30	0,24
		Control		468 ± 140	-367 ± 65	2,40 ± 0,77
	2	Precursor		226 ± 118	-770 ± 35	0,53
		Bubbled		294 ± 140	-821 ± 16	0,27
		Control		222 ± 17	-648 ± 101	2,01
	4	Precursor		688 ± 71	-64 ± 25	1,18
		Bubbled		765 ± 164	-23 ± 34	0,25
		Control		785 ± 115	295 ± 20	7,19 ± 2,41
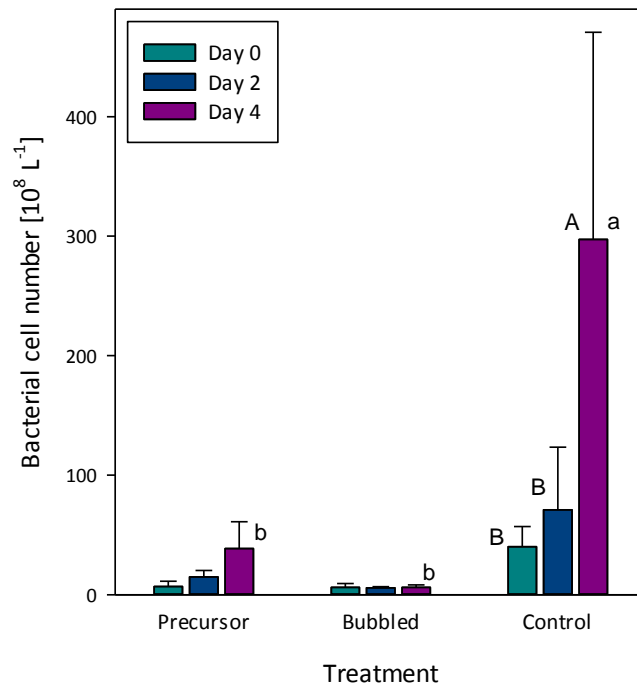
Figure 12. Cell numbers of the free-living bacterial fraction of differently treated melted sea ice over the course of the experiment. Values represent average values of all experiments with standard errors. Bacterial cell numbers are significantly higher in the control treatment at day four compared to the other treatments, and to days zero and two of the same treatment (paired t-test, p < 0.001 and 0.002, respectively, n = 3).
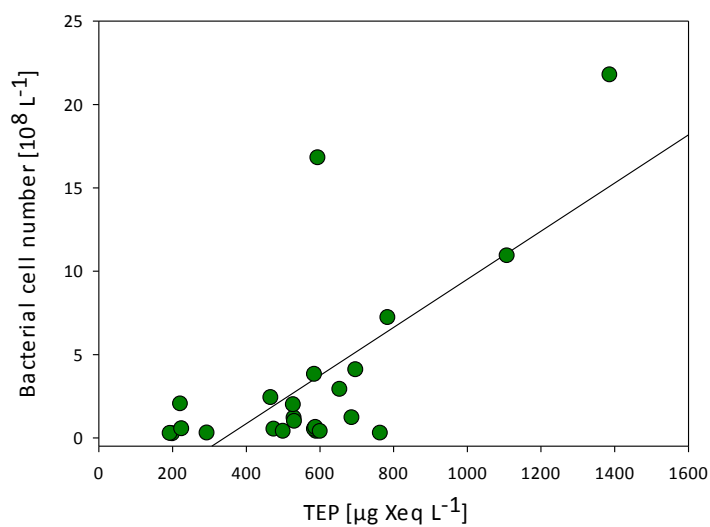

Figure 13. Significant correlation between TEP concentration (µg Xeq. L^{-1}) and bacterial cell number (10^8 L^{-1}). The adjusted r^2 is 0.48, n = 24, p < 0.001.

3.2.2 DGGE Analysis of Experiments

DGGE profiles of PCR amplified 16S rRNA gene fragments were obtained from the three experiments after zero and four days of incubation. Each respective sea ice station served as a natural bacterial sea ice inoculum, such that we could identify changes in bacterial diversity and community structure between days and treatments (Fig. 11). Subsamples of the experiment were filtered onto 0.2 µm PC-filters. Flask 1, 2 and 3 are equivalent to treatment "precursor", "bubbled" and control, respectively. All bands of the same position between lanes were excised twice and sequenced. Table 16 lists the successfully sequenced bands and their closest relatives in the silva database.

Banding patterns after zero days of incubation are similar to the respective ice stations for all treatments, with less intense bands for treatments "precursor" and "bubbled" (10 mL inoculum were added to 100 mL filtered and autoclaved sea ice water). This indicates that no bacterial growth took place during preincubation of the two treatments.

There was significant overlap in banding patterns between the different treatments and the inoculum after four days of incubation, with minor reductions in community diversity and clear reductions in abundance in the bubbled treatment. This is well in accordance with observed stagnant bacterial cell numbers over the course of the experiment in air ventilated flasks, pointing out that air bubbling affected all strains present. The high overlap in banding patterns indicates that the different treatments do not seem to affect bacterial community composition. Furthermore, there seems to be no apparent shift in bacterial sea ice community within four days after melting. Only two bands of experiment 1 (marked with arrows; Fig. 14) decreased in intensity over the course of the experiment. Both are affiliated to the marine group BD7-8 and were extracted from Antarctic lake water. In experiment 2 the bacterial diversity seems to be elevated in the "precursor" treatment after four days of incubation.
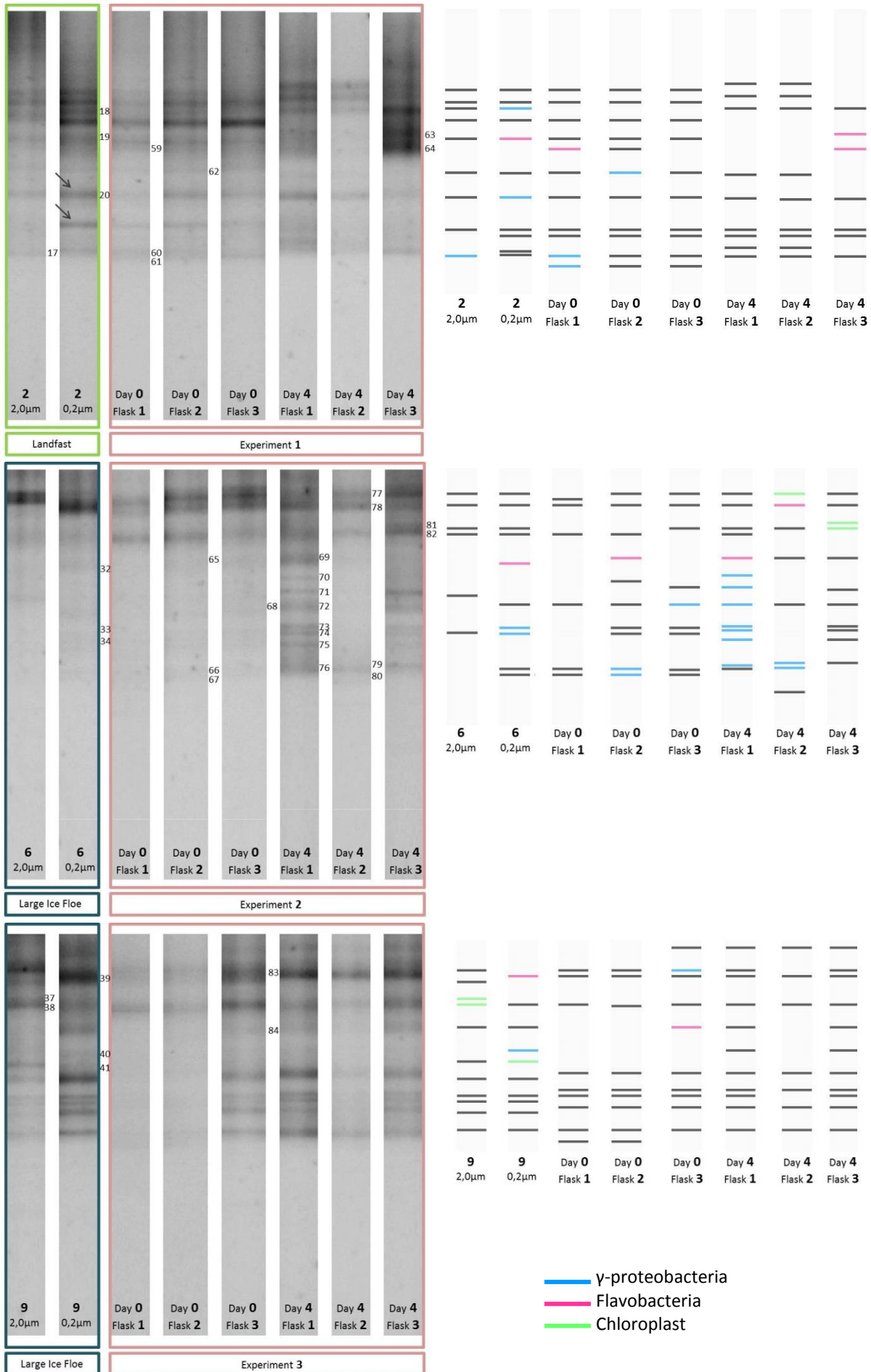
Figure 14. DGGE profiles of 16S rRNA gene fragments of sea ice samples from the experiments after zero and four days of incubation and their respective natural bacterial sea ice inoculum separated in two size classes (< 2 and > 2 μm). Flask 1, 2 and 3 are equivalent to treatment "precursor", "bubbled" and control, respectively. Numbering on the right hand side of the lanes indicates the names of excised DGGE bands listed in Table 16 with their closest relative in the Silva database. Chromograms on the right hand side show the phyla that the excised bands belong to.

3.2.3 Community Composition

We used catalyzed reporter deposition fluorescence in-situ hybridization (CARD-FISH) to microscopically examine community structure and relative abundances of bacterial groups. By combining CARD-FISH methods with the particle specific staining techniques, DAPI-stained and probe-labeled bacterial cells could be directly enumerated on either TEP or CSP. Percent distributions of free living bacteria from the control treatment after zero (day two for experiment 1) and four days of incubation as well as TEP and CSP attached bacteria that hybridized with domain to species-specific probes are listed in Table 18. Phylogenetic groups detected by DGGE were also detectable with FISH in all cases.

Most of the bacteria visualized with DAPI staining (~99%) were detectable with the EUB338 probe specific for bacteria. The background signal of samples observed with the probe NON338 was negligible (0 to 0.2%). For all substrates most of the DAPI-stained cells (89, 77, 95, and 78% of free-living cells at day zero, day four, TEP and CSP attached bacteria, respectively; Fig. 15) could be assigned with probes targeting the larger phylogenetic groups within the domain *Bacteria*.

For all substrates, highest percentage of bacterial cells (50, 44, 37, and 40%, respectively) was detected with the *Bacteroidetes* specific probe CF319a. The γ-proteobacteria and the β-proteobacteria accounted for 21, 11, 25, and 15% and 8, 14, 16, and 10% of the total DAPI-stained cells, respectively. α-Proteobacteria (in this study detected with probe ROS537 specific for the *Roseobacter* clade) were also detected, making up 9, 8, 18, and 14% of the total DAPI-stained cells. Planctomycetes were not detectable neither with FISH nor DGGE.

Table 18: Average percentages of DAPI stained cells for all horseradish-peroxidase (HRP)-labeled probes used in this study; Probe EUB338 targets bacteria, NON338 as negative control, ROS537 targets *Roseobacter clade*, BET42a - β-proteobacteria, GAM42a - ɣ-proteobacteria, ALT413 - *Alteromonas-Colwellia*, PSA184 - *Pseudoalteromonas-Colwellia*, GLAC227 − *Glaciecola spp.*, MB-IC022a - *Marinobacter spp.*, SF825 - *Shewanella frigidimarina*, CF319 - *Bacteroidetes*, POL740 - *Polaribacter spp.*, PLA46 - *Planctomycetes*

| Exp.	Day	Substrate	EUB	NON	ROS	BET	GAM	ALT	PSA	GLAC	MB	SF	CF	POL	PLA
1	2	Free	99,3	0,0	3,9	13,5	29,5	2,8	21,8	27,9	< 1	< 1	49,4	16,2	< 1
	4	Free	97,8	0,0	2,9	22,2	15,6	9,0	26,5	24,5	< 1	< 1	42,0	41,2	< 1
	4	TEP	99,3	0,0	9,8	14,8	56,2	6,8	22,1	47,3	< 1	< 1	34,9	12,9	< 1
	4	CSP			4,3	14,0	26,9	5,7	30,1	41,8	< 1	< 1	40,7	26,0	< 1
2	0	Free	99,6	0,0	7,8	5,8	19,4	0,0	3,0	5,7	< 1	< 1	58,6	17,4	< 1
	4	Free	99,4	0,0	10,9	8,0	7,1	0,3	9,4	10,7	< 1	< 1	47,2	33,1	< 1
	4	TEP	99,8	0,0	26,5	6,9	10,9		11,4	25,3	< 1	< 1	43,2	21,7	< 1
	4	CSP			16,7	10,4	14,1		30,5	27,9	< 1	< 1	37,8	20,4	< 1
3	0	Free	98,4	0,0	15,2	6,6	15,5	0,7	4,7	3,6	< 1	< 1	40,5	14,0	< 1
	4	Free	99,0	0,2	8,7	12,7	9,7	0,7	8,7	23,4	< 1	2,4	42,1	35,5	< 1
	4	TEP			34,2	16,9	19,9		15,6	20,3	< 1	< 1	49,5	16,9	< 1
	4	CSP			37,9	14,2	13,3		14,4	21,1	< 1	< 1	40,5	21,2	< 1
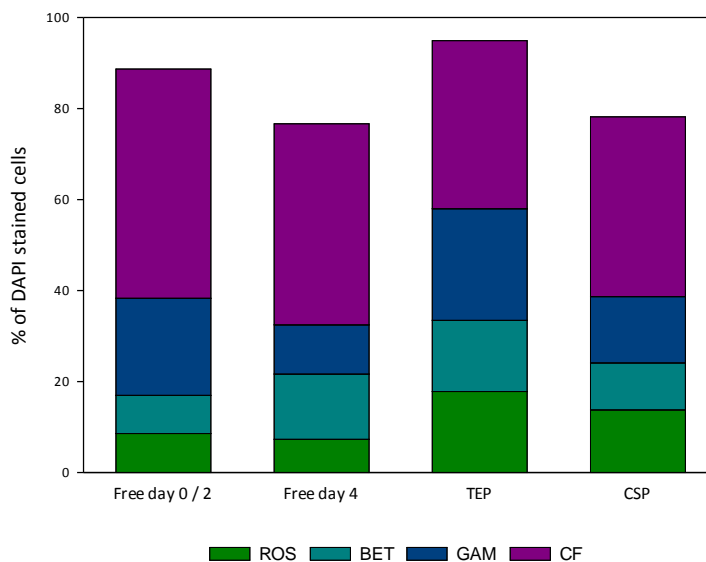
Figure 15. Percentage of DAPI stained bacteria detected by FISH of main phylogenetic groups using probes ROS537 for the *Roseobacter clade* (α-proteobacteria), BET42a for β-proteobacteria, GAM42a for ɣ-proteobacteria, and CF319a for the *Cytophaga-Flavobacteria* of the *Bacteroidetes* group.

A closer look at the community composition was taken using probes more specific for sea ice bacteria. ALT1413, PSA184, GLAC227, MB-ICO22a and SF825 belong to ɣ-proteobacteria and POL740 belongs to the bacteroidetes group. Most of the ɣ-proteobacteria could be assigned with probe GLAC227 targeting *Glaciecola* (Table 19). Abundances of probes SF825 targeting *Shewanella frigidimarina* (except for experiment 3, free living fraction after 4 days) and MB-ICO22a targeting *Marinobacter spp.* (both ɣ-proteobacteria) were below the detection limit of FISH and were also not present in sequences obtained from DGGE gels.

Application of two partially overlapping probes specific for the *Alteromonas-Colwellia* (ALT1413) and *Pseudoalteromonas-Colwellia* (PSA184) groups within the *Colwellia* assemblage resulted in quite different values. Probes ALT1413 and PSA184 hybridized with ~1 and ~10% of DAPI-stained cells in the free living fraction after zero days of incubation. This is in contrast to sequenced DGGE bands, here, 3 bands could be assigned to *Alteromonas* but none could be assigned to *Pseudoalteromonas* or *Colwellia*.

ALT1413 and PSA184 match with 42 and 34% of *Glaciecola* sequencens. GLAC227 shares 39 sequences (out of 41) with PSA184 but only two with ALT1413. In some cases, relative abundances of GLAC227 were higher than for PSA184 although GLAC227 targets no major outgroups and is almost entirely covered by PSA184. Higher percentages of DAPI-stained cells for GLAC227 cannot be explained by the two *Glaciecola* sequences that match with GLAC227 but not with PSA184, since they were not extracted from polar habitats. But it might be explained by taking one possible mismatch into account, then, GLAC227 targets a *Flavobacterium* that was extracted from Antarctic sea ice.

It is quite likely that the general probe GAM42a underestimates the total contribution of ɣ-proteobacteria to the sea ice community as it does not match with any *Colwellia* sequence targeted with ALT1413 or PSA184. Furthermore, only one *Glaciecola* sequence is targeted with both, probe GAM42a and GLAC227. Thus, in some cases, relative abundances of GLAC227 and/or PSA184 were higher than GAM42a.

A great proportion of *Bacteroidetes* could be assigned to *Polaribacter*, targeted with probe POL740. This is well in accordance with DGGE results; here, *Polaribacter* is the second most common genus.

Table 19: Percentage of DAPI stained cells by species-specific probes which group into the γ-proteobacteria

Probe	Probe target group	Experiment 1			Experiment 2			Experiment 3		
		free	TEP	CSP	free	TEP	CSP	free	TEP	CSP
GAM42a	γ-subgroup of Proteobacteria	15,6	56,2	26,9	7,1	10,9	14,1	9,7	19,9	13,3
Alt1413	*Alteromonas / Colwellia*	9,0	6,8	5,7	0,3	< 1	< 1	< 1	< 1	< 1
PSA184	*Pseudoalteromonas/ Colwellia*	26,5	22,1	30,1	9,4	11,4	30,5	8,7	15,6	14,4
GLAC227	*Glaciecola*	24,5	47,3	41,8	10,7	25,3	27,9	23,4	20,3	21,1
MB-IC022a	*Marinobacter* sp. strain IC022	< 1	< 1	< 1	< 1	< 1	< 1	< 1	< 1	< 1
SF825	*Shewanella frigidimarina*	< 1	< 1	< 1	< 1	< 1	< 1	2,4	< 1	< 1

3.2.3.1 Free-living Bacterial Fraction

Bacteroidetes, detected with probe CF319a dominate the non-attached living bacterial sea ice community after zero and four days of incubation, with ~50 and ~44% of DAPI-stained cells, respectively (Table 20). During the course of the experiment, relative abundances of β-proteobacteria*, Pseudoalteromonas-Colwellia, Alteromonas-Colwellia, Glaciecola spp.* and *Polaribacter spp.* increase, whereas γ-proteobacteria and *Bacteroidetes* decrease. The contribution of the *Roseobacter* clade to the community does not change during four days of incubation. Significant changes in relative abundances over time are shown in Fig. 16. Percentage of DAPI-stained cells that hybridized with POL740 more than doubled, making up 32% of *Bacteroidetes* after zero and 83% after four days of incubation.

Table 20: Mean percentages of DAPI stained cells of various bacterial groups and comparison between the free-living bacterial fraction after zero days (two days for experiment 1) and four days of incubation

| | Free-living | | | | Paired t-test | |
| | Day 0 / 2 | | Day 4 | | two tailed | one tailed |
Probe	Mean	SEM	Mean	SEM	p	p
ROS	8,7 ±	1,6	7,5 ±	2,4	n.s.	n.s.
BET	8,4 ±	1,6	14,3 ±	2,3	n.s.	0,048
GAM	21,3 ±	1,6	10,8 ±	2,4	0,049	0,025
PSA	10,3 ±	1,5	17,6 ±	2,0	0,019	0,010
ALT	1,1 ±	1,5	3,4 ±	1,9	n.s.	n.s.
GLAC	13,2 ±	1,6	19,4 ±	2,0	n.s.	n.s.
CF	50,4 ±	1,5	44,2 ±	2,0	n.s.	n.s.
POL	15,9 ±	1,6	36,8 ±	2,1	0,017	0,008

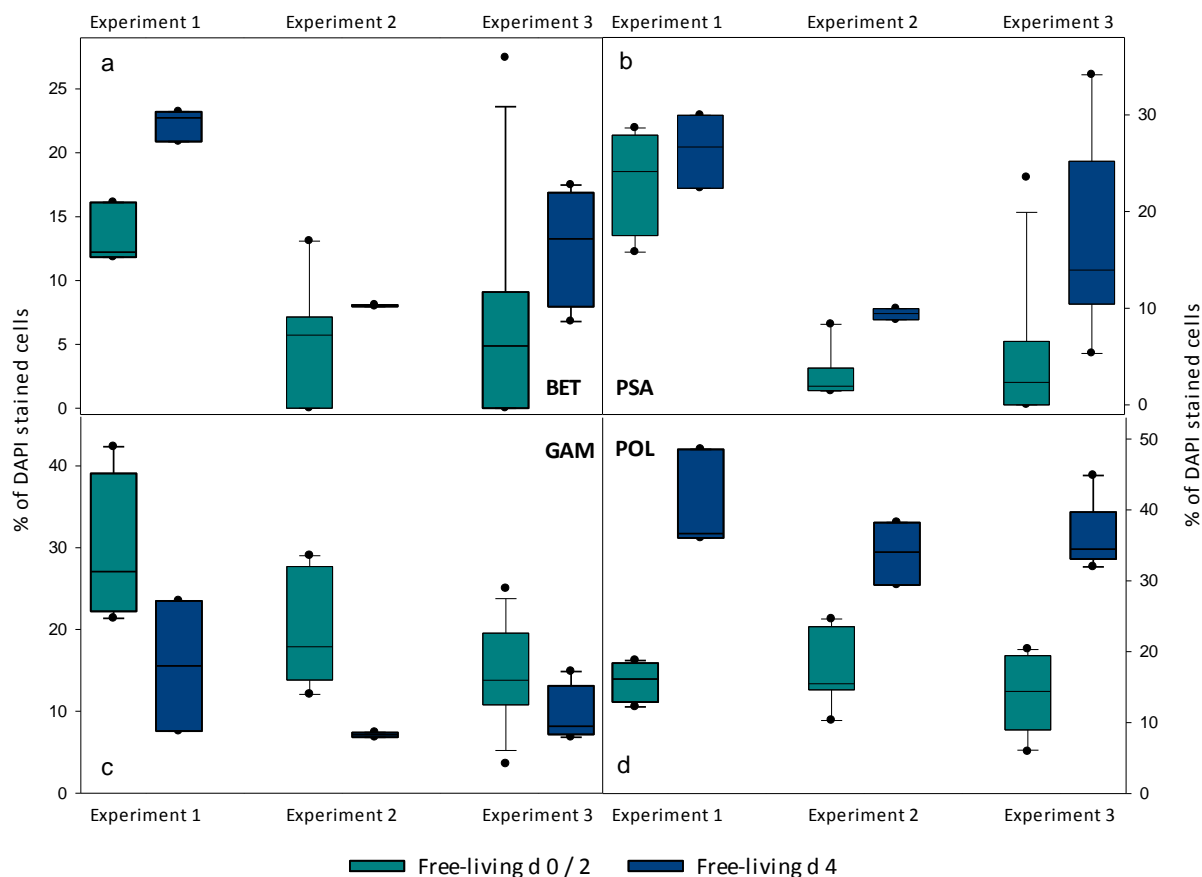Mean values ± SEM were calculated from data of all experiments.

n.s., not significant

Figure 16. Percentages of (a) β-proteobacteria, (b)γ-proteobacteria, (c) *Pseudoalteromonas-Colwellia*, and (d) *Polaribacter* in the free-living bacterial fraction of melted sea ice over the course of the experiment (green after 0 days (2 days for experiment 1) and 4 days of incubation, blue).Boxes show 50% quartiles, whiskers 10 and 90 percentiles, and dots 5 and 95 percentiles. Full central line shows median.

3.2.3.2 Particle Attached Bacterial Fraction

Bacteroidetes dominate both, the free-living fraction and the bacterial community attached to TEP and CSP, with ~37 and ~40% (Table 21). *Roseobacter* clade, β-, γ-proteobacteria and *Alteromonas-Colwellia* seem to prefer carbon-rich TEP. Protein containing CSP were preferred by *Pseudoalteromonas-Colwellia* and *Polaribacter spp.*. *Galciecola spp.* and *Bacteroidetes* did not show a preference for one of the particle types. Microscopic analysis of TEP and CSP did not reveal differences in colonization densities between the two particle types.

Although, bacteria that belong to the Bacteroidetes group are well known for their attached life styles, relative abundances of CF319a and POL740 were reduced on both particle

types. The reduction in relative abundance of *Polaribacter* compared to the free-living fraction after four days of incubation (Fig. 17) is siginificant for CSP (p = 0.002) and almost significant for TEP (p = 0.058).

Table 21: Mean percentages of DAPI stained cells of various bacterial groups and comparison between the free-living, TEP and CSP attached living bacterial fraction after four days of incubation

	Free		TEP		CSP		Paired t-test two-tailed Free vs. TEP	Free vs. CSP
Probe	Mean	SEM	Mean	SEM	Mean	SEM	p	p
ROS	7,9 ±	6,8	18,0 ±	2,8	13,9 ±	2,8	n.s.	n.s.
BET	14,9 ±	7,2	15,6 ±	2,7	10,3 ±	2,7	n.s.	n.s.
GAM	10,5 ±	7,2	24,5 ±	3,0	14,6 ±	2,8	n.s.	n.s.
PSA	17,4 ±	6,2	18,9 ±	2,8	24,3 ±	2,7	n.s.	n.s.
ALT	9,1 ±	12,4	13,8 ±	4,6	5,2 ±	4,6	n.s.	n.s.
GLAC	19,0 ±	6,5	33,7 ±	2,8	35,6 ±	2,7	n.s.	n.s.
CF	43,8 ±	6,0	36,9 ±	3,1	39,5 ±	2,8	n.s.	n.s.
POL	36,6 ±	6,5	17,7 ±	2,7	26,4 ±	2,7	0,058	0,002

Mean values ± SEM were calculated from data of all experiments. n.s., not significant
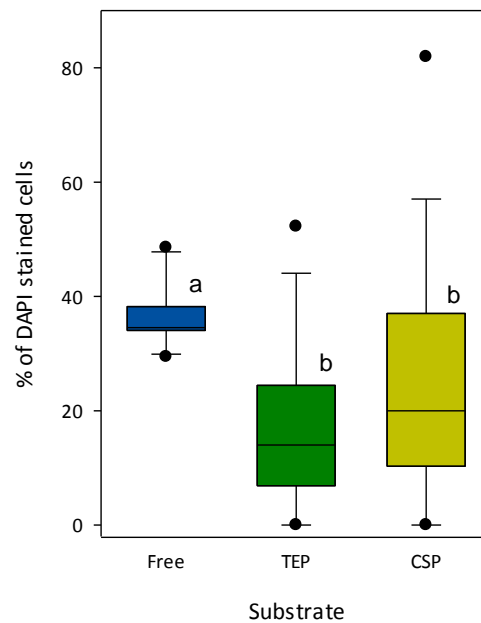
Figure 17. Percentages of free-living (blue), TEP (green) and CSP (yellow) attached living *Polaribacter* within melted sea ice after four days of incubation. Contribution of *Polaribacter* to the free-living fraction is significantly greater than to CSP and almost significant to TEP (paired t-test, p = 0.002 and 0.058, respectively; n = 3).Boxes show 50% quartiles, whiskers 10 and 90 percentiles, and dots 5 and 95 percentiles. Full central line shows median.

Over all, the *Roseobacter* clade, γ-proteobacteria, *Pseudoalteromonas-Colwellia* and *Glaciecola spp.* are likely to prefer particles as habitat, whereas *Bacteroidetes* and *Polaribacter spp.* seem to be better adapted to a free-living lifestyle (*Table 22*). The relative abundance of bacteria that hybridize with POL740 is significantly reduced on pEPS (p = 0.026, Fig. 18). β-Proebacteria do not indicate a preference for one of the studied habitats.

Table 22: Mean percentages of DAPI stained cells of various bacterial groups and comparison between the free-living and particulate EPS (pEPS) attached living bacterial fraction after four days of incubation.

	Free		Particle attached		Paired t-test two tailed
Probe	Mean	SEM	Mean	SEM	p
ROS	7,9 ±	6,9	15,9 ±	2,0	n.s.
BET	14,9 ±	7,2	13,0 ±	1,9	n.s.
GAM	10,5 ±	7,2	19,2 ±	2,1	n.s.
PSA	17,4 ±	6,3	21,6 ±	1,9	n.s.
GLAC	19,0 ±	6,5	34,7 ±	2,0	n.s.
CF	43,8 ±	6,0	38,3 ±	2,1	n.s.
POL	36,6 ±	6,5	22,1 ±	1,9	0,026

Mean values ± SEM were calculated from data of all experiments.
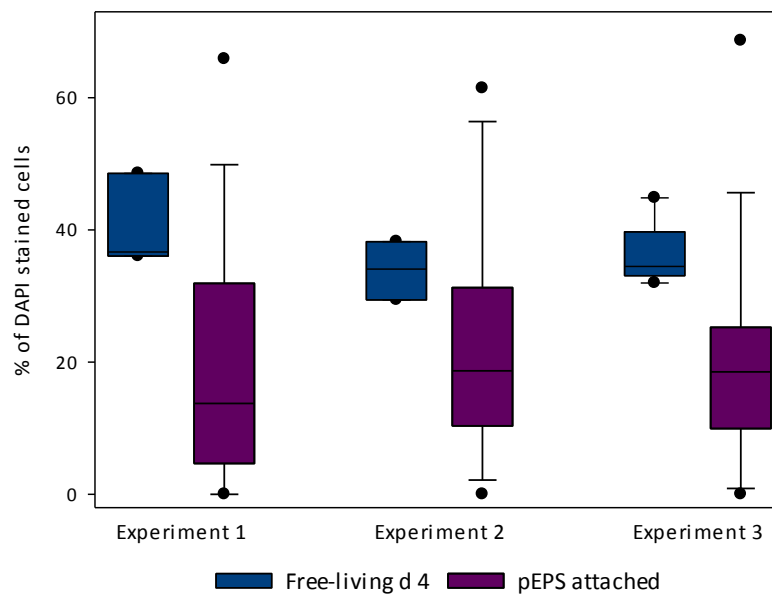
n.s., not significant

Figure 18. Percentages of free-living (blue) and particulate EPS (pEPS) attached (purple) living *Polaribacter* within melted sea ice after four days of incubation. Contribution of *Polaribacter* to the free-living fraction is significantly greater than to the pEPS attached fraction (paired t-test, p = 0.026; n = 3). Boxes show 50% quartiles, whiskers 10 and 90 percentiles, and dots 5 and 95 percentiles. Full central line shows median.

3.3 Gallery

Collection of aggregates (Fig. 19 and 20), undefined particles (Fig. 21) and sea ice microalgae (Fig. 22) that were either stained with Alcian Blue (AB) to detect polysaccharide containing TEP or Coomassie Brilliant Blue G (CBBG) to detect protein containing CSP. Total bacterial cells and other DNA containing material was stained with DAPI and visualized under UV-light excitation. HRP-labeled bacteria-specific probes, ranging in specificity from genus to species level, were used to determine their relative contribution to the total bacterial community and were visualized under green-light excitation. Under the microscope TEP and CSP aggregates could not be distinguished from each other, they do not seem to differ in size nor structure. Sea ice microalgae that stain positive with AB were usually only surrounded by the stain, whereas microalgae that stain positive with CBBG in most cases seemed to be completely covered by the stain. This is the only apparent difference between TEP and CSP that could be recognized. TEP are well known to be sticky, resulting in big aggregates containing detritus and microorganism. It is very likely that CSP are sticky too. In this study, CSP aggregates tended to contain even more microorganisms than TEP.
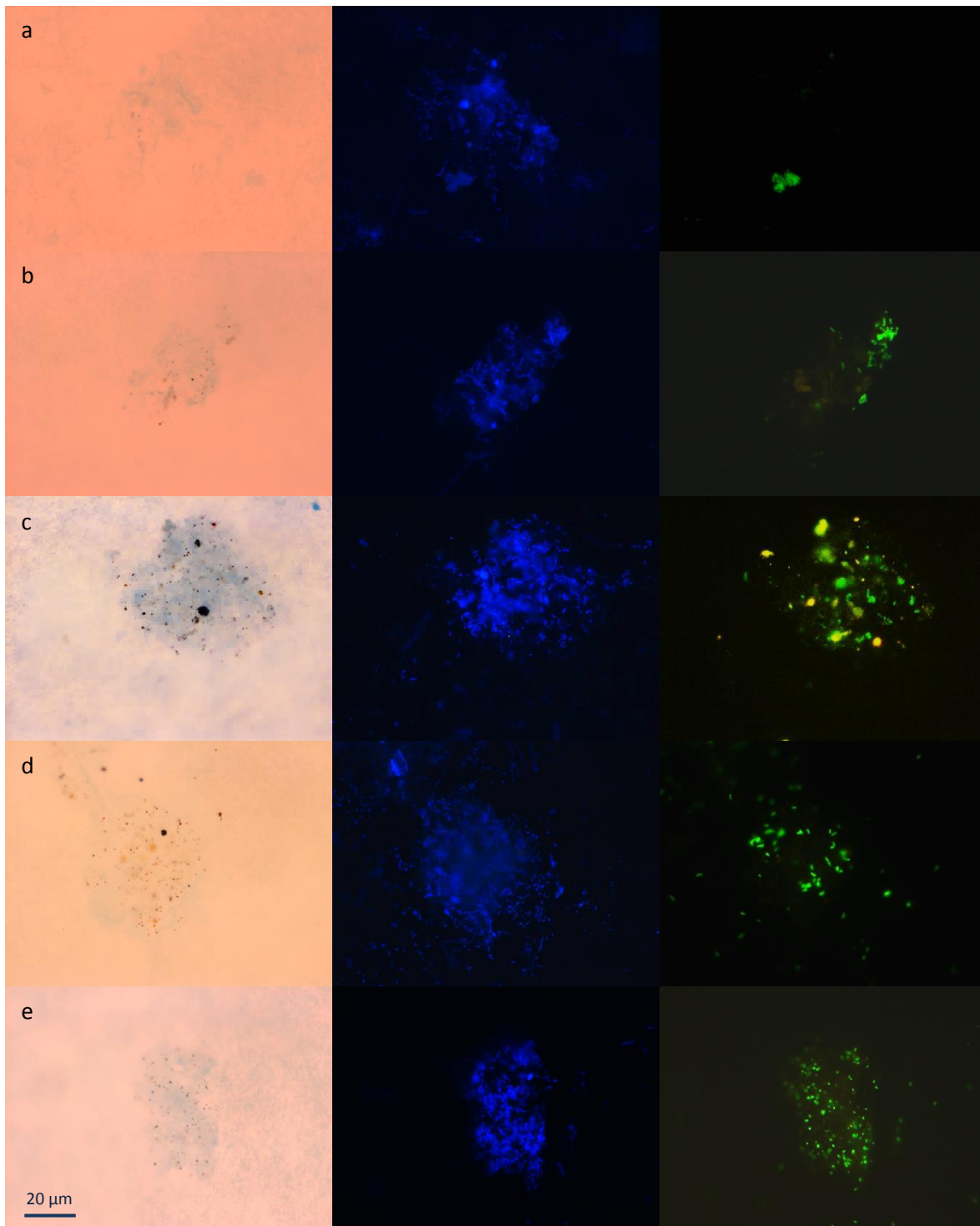
Figure 19. TEP and CSP aggregates of the experiment after four days of incubation. (a) Alcian Blue stained, probe ROS537 (*Roseobacter* clade); (b) AB stained, probe BET42a (β-proteobacteria); (c) Coomassie Brilliant Blue stained, probe GAM42a (γ-proteobacteria); (d) AB stained, probe GLAC227 (*Glaciecola*) and (e) CBBG stained, probe POL740 (*Polaribacter*). Pictures were taken under brightfield, UV- and green light excitation (from left to right).
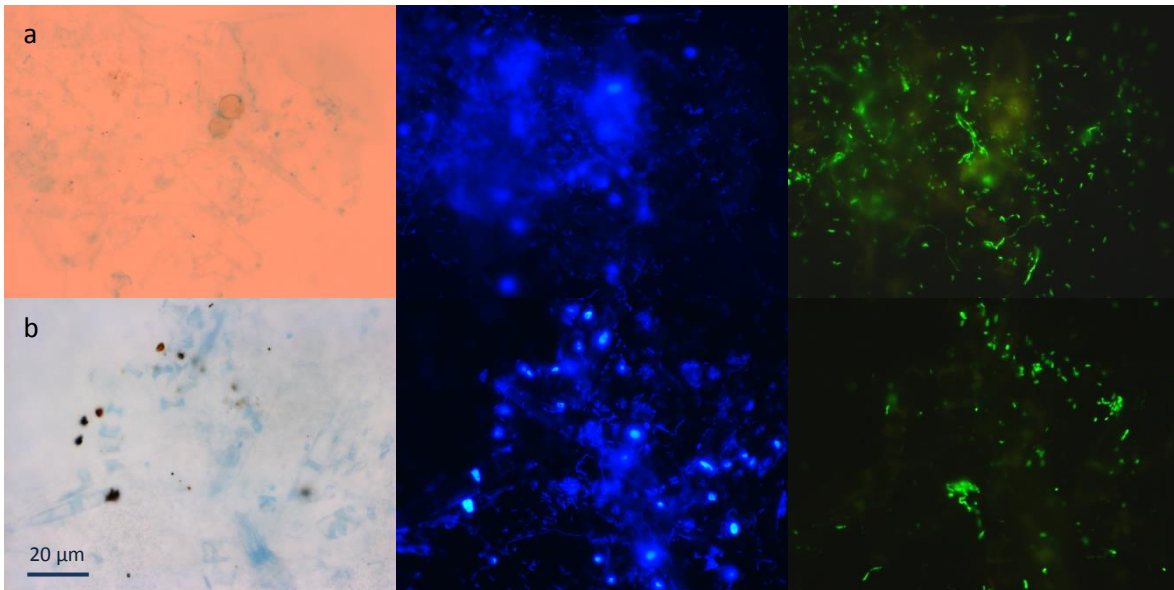
Figure 20. Densely colonized giant aggregates. (a) Alcian Blue stained, probe CF319a (Bacteroidetes); (b) Coomassie Brilliant Blue stained, probe BET42a (β-Proteobacteria). Pictures were taken under brightfield, UV- and green light excitation (from left to right).
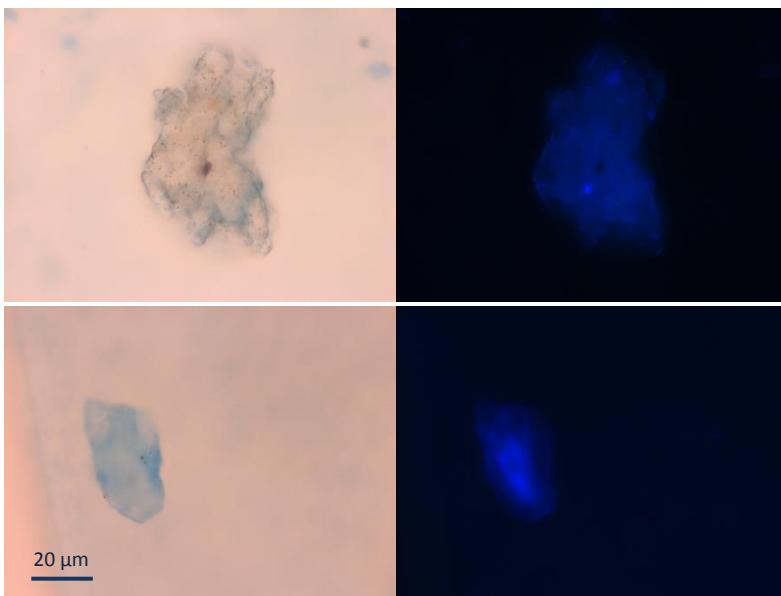

Figure 21. Particles of unknown origin. Both stained with Coomassie Brilliant Blue. Pictures were taken under brightfield and UV-light excitation (from left to right).
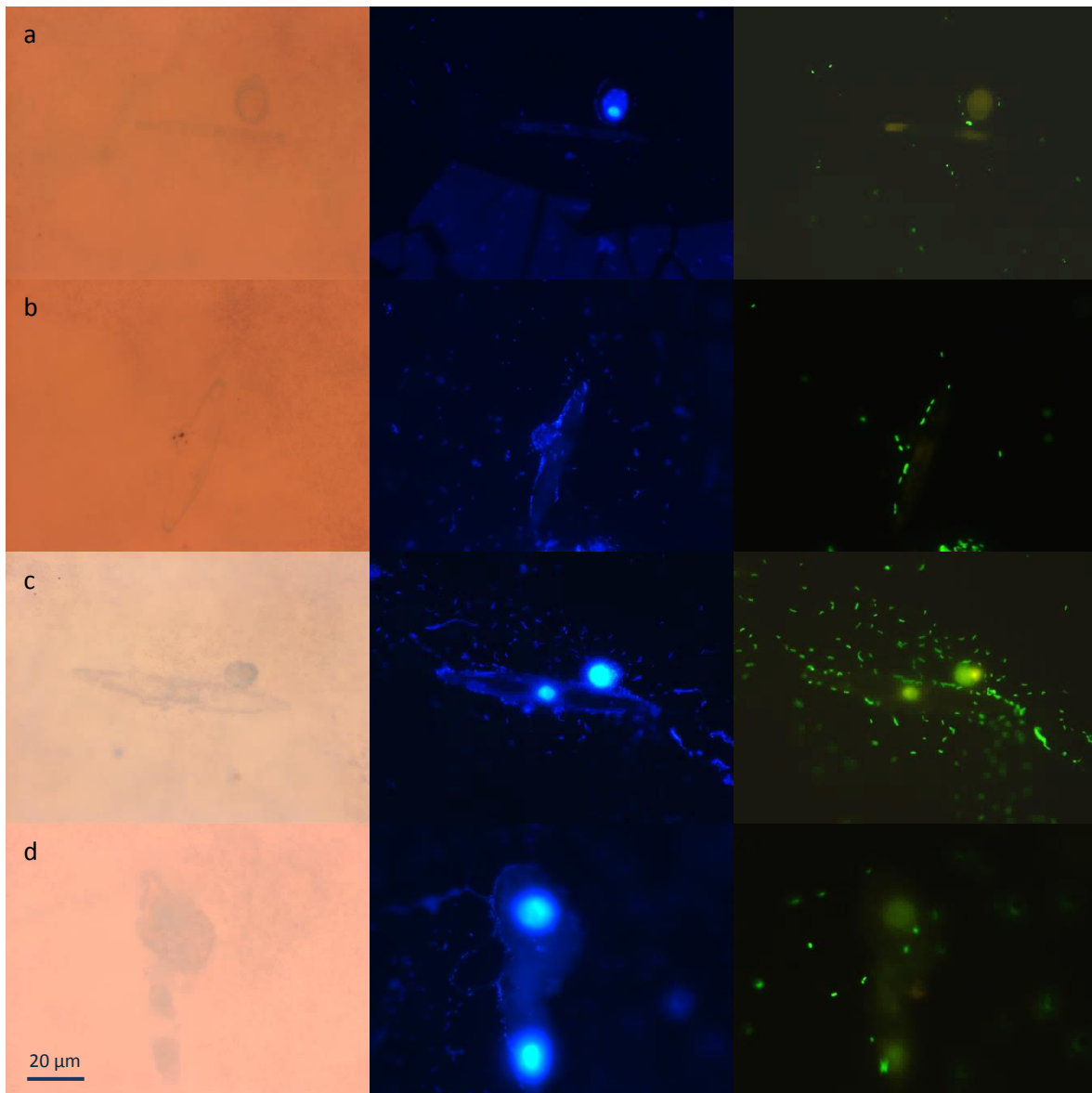
Figure 22. Sea ice microalgae surrounded by either TEP or CSP. (a) Alcian Blue stained, probe POL740 (*Polaribacter*), microalgae with comparably thick TEP coating; (b) AB stained, probe PSA184 (*Pseudoalteromonas-Colwellia*); (c) Coomassie Brilliant Blue stained, probe POL740; (d) CBBG stained, probe PSA184. Except for (a), microalgae seem to be attacked by dinoflagellates. Pictures were taken under brightfield, UV- and green light excitation (from left to right).

IV Discussion

Particulate extracellular polymeric substances (pEPS) abundant in sea ice can alter the microbial ecology of sea ice through alteration of sea ice microstructure, improvement of ice habitability, as well as increasing the potential for increased primary production (Krembs et al., 2011). As hot spots of microbial activity, pEPS are also known to be densely colonized by bacteria within sea ice (Mock & Thomas, 2005). However, it has not been determined whether particle associated bacteria in sea ice differ from those living freely. Moreover, bacterial groups are likely to show a preference for different chemical fractions of pEPS, either transparent exopolymeric particles (TEP) identified with negatively charged carbohydrate end groups and stained with Alcian Blue (AB), or Coomassie stainable particles (CSP) stained with Coomassie Brilliant Blue G (CBBG), attaching preferentially to protein moieties. Here we made measurements of TEP and CSP particles in a transect across the Fram Strait, investigating environmental correlates of these particle types in sea ice. We then executed a detailed analysis of TEP- and CSP-associated bacteria and compared these to the free-living fraction.

4.1 Particulate EPS

4.1.1 Methodological Considerations

We executed a number of different types of TEP and CSP analyses, including microscopic analysis of particles, and phototometric (colorimetric) analysis of extracted stain bound to particles which were collected on filters. We have documented several drawbacks to the photometric method. Both TEP and CSP are heteropolymeric particles of diverse origin and composition, and their chemical composition might change with their age. Hence, the amount of dye that binds to specific monomers within the gel particle will depend on the particle´s

origin and composition (Cisternas-Novoa et al., 2014). Moreover, the monomeric composition of marine gels varies widely among substances released by diatoms, depending on species and physiological stage (Myklestad, 1977). This heterogeneity limits the application of TEP and CSP staining techniques, since gel particle measurements are always semi-quantitative, and relative to a standard.

Another problem is that the spectrophotometric method does not differentiate between gel material attached to phytoplankton cells and free particles. Thus, TEP may be overestimated if organisms with stainable coatings are abundant, as per definition TEP should not contain cell coatings (Passow, 2002a).

Because different standards for the determination of TEP and CSP are used, it does not allow true quantitative comparison of the two types of gel particles. TEP and CSP concentrations measured spectrophotometrically sometimes yielded very high variations between replicates and high blank values (here likely an artefact of impure distilled water on board, since the MilliQ device did not run properly), thus results seem to be overall less reliable than the microscopic method.

However, the spectrophotometric method allows a comparison of TEP and CSP concentrations in relative terms, in that temporal and spatial variations can be compared (Cisternas-Novoa et al., 2014), so it is worthwhile to further test the applicability of CSP photometry in different environments.

The more labour-intensive microscopic analysis of gel particles allows the determination of the number and size of particles. Due to the flattening of particles during filtration and the calculation of the area which assumes a smooth particle surface, the actual surface area of gels is likely to be underestimated (Long & Azam, 1996). Furthermore, the threshold adjustment in ImageJ is prone to individual error. If not processed by the same person, number and size of gels cannot be directly compared. These values should therefore be interpreted with caution.

Despite not being directly comparable, several studies reported that the results are consistent between the microscopic and photometric approaches (Passow & Alldredge, 1995; Engel, 2000; Berman & Viner-Mozzini, 2001). In our study, this was true for TEP measurements across all ice types. Regardless of the method, TEP abundance seems to be statistically

correlated with the same parameters. However, depending on the method, CSP measurements showed quite different patterns, especially for large ice floes and landfast ice: In contrast to microscopic results, the photometric determination of CSP follows the pattern of TEP measurements and is statistically correlated with the same parameters.

Generally, the choice of method depends on the focus of the study. If the goal is to determine changes in surface area, shape or the extent of bacterial colonization of gel particles, the microscopic method might be the better choice. But if the goal is to study how TEP and CSP are related to each other and other parameters in different environments or at different times (by different people), the spectrophotometry will be the method of choice.

4.1.2 Characterization of Different Sea Ice Types

The Fram Strait is an area where Atlantic (warm) and Arctic (cold) water masses exchange (Beszczynska-Möller et al., 2012; Fig. 1), which allows the sampling of sea ice exposed to different environmental conditions. Landfast ice is formed in nearshore areas, whereas ice floes (pack ice) had formed (e.g., on the Siberian shelves) and transported over the pole through the Fram Strait via the Transpolar Drift (Polyak et al., 2010). Despite their different origin, biological parameters of landfast ice and large ice floes were similar in many respects in our study, showing the strong correlation with the underlying water, whereas Atlantic-water-influenced small ice floes seem to be significantly different from both landfast ice and large ice floes, across a number of parameters.

Landfast ice is surrounded by cold Arctic waters. It is characterized by the lowest under-ice water- and ice-core temperature, and highest salinity, TEP and CSP values, but similar total chlorophyll *a* concentrations as large ice floes. This is consistent with the notion that sea ice algae exude higher amounts of TEP and CSP precursors at colder temperatures and higher salinity as a cryoprotectant (Krembs et al., 2002; Collins et al., 2007). Furthermore, despite representing the harshest conditions, landfast ice seems to be the most suitable habitat for bacteria, with highest values of TEP and CSP that serve as a potential food source and microhabitats protecting cells. Due to its close proximity to land, landfast ice probably also has

a higher terrestrial input of carbon, indicated by the lowest ratio of TEP-carbon to particulate organic carbon (POC) across all ice types.

The large ice floes we sampled were mainly located in a transition zone between the cold Arctic and warm Atlantic water masses (Beszczynska-Möller et al., 2012). Station 9 is the northernmost station located at the eastern margin of Fram Strait, where warm Atlantic waters are flowing into the Arctic (Fig. 4). However, it has the lowest under-ice water temperature of all stations, which strongly implies that warm Atlantic waters already subducted under Arctic water masses in that region.

Small ice floes were floating on warm Atlantic waters with temperatures above 1 °C. Small ice floes are characterized by highest transmission of light through the ice and significantly reduced bacterial cell number and CSP. In contrast to landfast ice and large ice floes, small ice floes did not have any melt ponds, and had considerably lower concentrations of particulate organic matter (POM; see Table 13 and 14) in the bottom half of ice cores, suggesting that melting from the bottom possibly exceeds melting processes at the top when floating on warm Atlantic waters.

4.1.3 Abundance and Distribution of TEP and CSP within Sea Ice

Our work measured TEP and CSP simultaneously in Arctic sea ice for the first time. We found TEP and CSP values to be highest in landfast ice and lowest in small ice floes.

Generally it can be stated that pEPS, particularly TEP, occur in all horizons of sea ice (Krembs et al., 2002; Underwood et al., 2010). TEP within landfast ice and large ice floes was primarily located in the bottom half of the ice core, whereas CSP seemed to have a more even distribution within the ice. The study by Lemarchand et al. (2006) in a lake system presented results similar to our observations. Krembs et al. (2011) also detected more TEP near the growing ice front (where sea ice microorganisms (SIMCO) are most abundant), by applying the phenol/sulfuric acid assay based on sugar-monomer content. Compared to TEP, CSP in our study had a more uniform distribution within the ice. However, in small ice floes, both particle types were more abundant in the top half section of ice cores.

Our TEP areas (0.02 - 0.70 mm^2 L^{-1}) and TEP concentrations (102 - 207 µg Xeq. L^{-1}) were on the low end of those measured in other studies, whose maximum values were 2 - 3 orders of magnitude higher (Krembs & Engel, 2001; Riedel et al., 2006).

In fact, TEP and chlorophyll *a* concentrations observed in this study are quite similar to the pre-bloom conditions observed by Riedel et al. (2006) in March, and TEP:chlorophyll *a* ratio observed by Riedel et al. (2006) under low snow cover in June is similar to our results, 211 and 201, respectively. TEP and chlorophyll *a* concentrations observed in this study were therefore unseasonably low, possibly characteristic for sea ice of later season with almost no remaining sea ice algae.

TEP-carbon (estimated from TEP concentration) contributed on average 20% to the total POC. This is well in line with results obtained by other scientists in Arctic (Riedel et al., 2006; Krembs et al., 2002; Meiners et al., 2003) and Antarctic sea ice (Meiners et al., 2004) with average values ranging from 14 to 32%. This confirms that TEP may contribute significantly to polar ocean carbon cycles, not only within the ice, but after springtime release of organic matter into the water column and subsequent export to deeper regions (Krembs et al., 2001). Riedel et al. (2006) further recognized an increased contribution of TEP-carbon to total POC of up to 72% during melt period. As our sampling was conducted during June, we therefore might have expected a higher contribution of TEP-carbon to POC than we actually observed.

The carbon content of TEP can only be seen as an approximation, since the formula was developed on the basis of lab experiments with different diatom species, which can differ significantly (Engel & Passow, 2001). TEP form a continuum between the particulate and the dissolved organic matter (DOM) and because some significant fraction of TEP is not retained on GF/F-filters (0.6 µm pore size), TEP (0.4 µm pore size) are only partially included in POC measurements, thus, our TEP-carbon contribution to POC is likely to be overestimated.

To the best of my knowledge, this is the first study that investigated CSP area, number and concentration in sea ice. CSP number of Arctic early summer sea ice ranged between 2 and 14x10^7 particles L^{-1} and a total area of 0.1 to 0.5 mm^2 L^{-1}. Results are similar to CSP numbers found in surface waters of Scripps Pier (west coast of USA; Long & Azam, 1996), yet, CSP area

of sea ice is three-orders of magnitude lower, indicating a comparably small size of the CSP pool in Arctic sea ice.

4.1.4 Possible Drivers of TEP and CSP Concentration

In general, we observed TEP values to be statistically correlated with chlorophyll *a*, POC and PON concentrations. In general, TEP positively correlates with chlorophyll *a* not only in sea ice (Krembs & Engel, 2001; Riedel et al., 2006, 2008) but also limnic environments (Lemarchand et al., 2006) and diatom blooms (Waite et al., 1997; Passow, 2002b). However, Krembs et al. (2002) did not find a correlation between TEP and chlorophyll *a* and macronutrients in Arctic winter sea ice. After long residence times, TEP and chlorophyll *a* can become decoupled, particularly post-bloom or after melting of sea ice (Passow, 2002b; Riedel et al., 2006).

In the present study, TEP values were positively correlated with biotic and abiotic factors that are generally seen as a measure for the productivity and the nutritional status of the environment. The strong correlation between TEP and chlorophyll *a* further supports the observation of other scientists (Krembs & Engel, 2001; Meiners et al., 2003, 2008; Krembs et al., 2001) that ice algae are the main producers of TEP.

Furthermore, as observed in this study, TEP strongly correlates with bacterial abundance in Arctic summer and winter sea ice (Krembs & Engel, 2001; Krembs et al., 2002) and lakes (Lemarchand et al., 2006). However, the interactions are likely to be complex. Bacteria might degrade or modify TEP. While they are able to produce TEP, their contribution to total TEP within sea ice is believed to be insignificant (Schuster & Herndl, 1995; Krembs et al., 2001). Another possible indirect relationship could be that both TEP and bacteria depend on the organic substances released by phytoplankton for formation and nutrition, respectively. In contrast, Junge et al. (2004) could not find a correlation between TEP and bacteria in springtime Arctic se ice, arguing that the relationship between both might be the cryoprotective role of TEP during winter.

We observed CSP to be much less obviously dependent on the productivity of the system. CSP number and area seem to be mainly affected by under-ice water temperature, the type of ice, and the transmission of light through the ice. However, CSP concentration seems to be driven

by the same parameters as TEP. It is important to note that, as indicated above, the photometric determination of CSP concentration appears to be less reliable than the microscopic particle determination method. We therefore excluded photometric CSP concentrations in the following discussion.

While Berman and Viner-Mozzini (2001) found a positive relationship between chlorophyll *a* and CSP in Lake Kinneret, our data and data by Lemarchand et al. (2006) did not show such a correlation.

We observed CSP values in Arctic early summer sea ice to be mainly correlated with physical parameters, particularly low temperatures and light, which might in turn have negative effects on the survival of SIMCO due to changing sea ice conditions. Increased mechanical stress due to decreasing temperatures or lowered transmission of light could lead to cell lysis, death, or the release of anti-freeze proteins by diatoms (Raymond et al., 1994; Bayer-Giraldi et al., 2010). All of these responses to changing sea ice conditions possibly increase CSP abundance (Long & Azam, 1996).

4.1.5 Dominant Particle Type

Parallel studies of TEP and CSP are scarce and contradictory. CSP have been found either to be more abundant in marine systems (Long & Azam, 1996), or similar in abundance in the lab (Grossart et al., 1999), or less abundant during a diatom bloom (Prieto et al., 2002). Since different standards were used to determine concentrations of TEP and CSP, concentrations cannot be compared, only particle number and area can be directly compared.

This is the first study that investigated TEP and CSP of sea ice in parallel samples. Results suggest that TEP number and area possibly dominate in the more productive bottom half of Arctic sea ice, whereas in the top half TEP appears to dominate in number and CSP dominates in total particle area.

This suggests that, since TEP significantly correlates with chlorophyll *a* concentrations, sea ice with high levels of primary production is likely to be dominated by TEP particles, especially at the sea ice-water interface. CSP might dominate at the air-ice interface, where SIMCO are exposed to most severe and less stable conditions, possibly leading to increased cell death or

the need to protect them against freezing. It is also likely that CSP dominates in newly formed ice. Microorganisms which are not adapted to life in sea ice might become encased during the formation of sea ice and die due to decreasing temperatures or increasing salinity, releasing proteins that possibly form CSP. Further we might speculate that CSP are released during sea ice formation as cryoprotectent (anti-freeze proteins have been shown to occur in sea ice; Bayer-Giraldi et al., 2010).

4.1.6 Are TEP and CSP Distinct Particles?

TEP and CSP characteristics overlap in many respects, and so far it is not known to what extent CSP and TEP represent different chemical subunits (proteins and polysaccharides, respectively) of the same gel particle (Engel, 2009). In line with observations by Long and Azam (1996), we observed TEP and CSP to be similar in both size range and particle shape. Furthermore, both particle types seem to be equally colonized by bacteria.

The only apparent difference we could observe is the staining behavior of sea ice algal membranes or coatings. Under the microscope, sea ice algae that stain positive with AB (for TEP) appeared to be only framed by the stain, whereas microalgae that stain positive with CBBG (for CSP) in most cases seem to be completely covered by the stain.

Due to their chemical composition TEP are sticky, thus it is very likely that TEP also coagulate with proteinaceous CSP, forming aggregates. However, we observed TEP and CSP to have statistically different distribution patterns and abundances within the ice. Moreover, TEP and CSP values seem to be statistically driven by different parameters. Thus, while TEP and CSP may overlap, the majority of particles appear to be discrete. However, it is possible that some particles stain for both, polysaccharide and protein, with an increased probability with age of the particle or turbulent conditions.

4.2 Bacteria

4.2.1 Congruence of DGGE and FISH

It is well known that several potential biases may affect denaturing gradient gel electrophoresis (DGGE) analysis of PCR amplicons. Although DGGE does not provide a complete or quantitative picture of the bacterial community composition, it can be seen as a simplified, low cost fingerprint of the community. Moreover, since DGGE is based on the analysis of 16S rRNA genes, the microbial diversity may be underestimated due to the conserved nature of this gene (Fuhrman et al., 1998; Ward & Campbell, 1998).

However, in sea ice environments, results obtained with DGGE generally overlap with data obtained with FISH. The results highlight the exceptional nature of sea ice bacterial communities, which are likely to have highly active members despite extreme conditions in sea ice. There is a strong agreement between the cultivatable fraction and the PCR-detected fraction (Brown & Bowman, 2001; Brinkmeyer et al., 2003), that can reach 62% (Junge et al., 2002). This is in contrast to other marine environments, where the culturability is assumed to be less than 0.01% (Amann et al., 1995).

In line with other studies (Brinkmeyer et al., 2003; Junge et al., 2004; Pedrotti et al., 2009), we observed a high FISH detection yield of the horseradish-peroxidase (HRP)-labeled probe EUB338, which is specific for the domain *Bacteria,* with 99% of DAPI-stained cells. Since the threshold signal of FISH depends on the cellular rRNA content, FISH detection yields can be interpreted as a sensitive measure of active cells in the community (Karner & Fuhrman, 1997). The observed high proportion of probe-detectable cells indicates that almost all bacterial cells within early summer Arctic sea ice were active at the time of sampling.

For marine environments, bacterial activity assessed by FISH is usually lower than 99%, possibly due to different substrate quantity and quality. High concentrations of DOM in Arctic (and possibly Antarctic) sea ice (Thomas et al., 1998; Herborg et al., 2001), exceeding surface seawater concentrations, might explain this phenomenon. Furthermore, sea ice DOM appears to be very labile, providing an easily utilizable substrate for bacteria (Amon et al., 2001).

Thus, although we observed relatively low chlorophyll *a*, POC and PON concentrations, the sea ice we sampled can still be described as a highly productive environment compared to the water column.

4.2.2 Bacterial Sea Ice Community and Abundance

Our observed bacterial cell numbers (0.2 to 8.6×10^5 mL^{-1} for the very small ice floe and landfast ice, respectively) were in the same range as reported by other scientists. Brinkmeyer et al. (2003) found bacterial cell numbers to range from 0.98 to 14.9×10^5 mL^{-1} in Arctic summer sea ice, and Krembs et al. (2002) reported a bacterial abundance of 12×10^5 cells mL^{-1} in the lower section of Arctic sea ice in May.

Our study suggested that the bacterial abundance was primarily affected by the ice type, under-ice water temperature and the abundance of sea ice algae (with multiple interactions with TEP). Highest concentrations of bacterial cells were observed in landfast ice, characterized by lowest under-ice water temperature (-1.65 °C) and highest chlorophyll *a* concentration (1.6 µg L^{-1}). A statistical correlation between bacterial abundance and TEP abundance has been reported previously by Mari and Kiørboe (1996).

In general, the most abundant phylogenetic groups identified with DGGE and FISH agree well with results obtained by other scientists. Sea ice samples from landfast ice and large ice floes were dominated by *Bacteroidetes*, γ-, α-, and β-proteobacteria contributing on average 50, 21, 9, and 8% to the total bacterial community. Studies by Brown and Bowman (2001), Petri and Imhoff (2001), Brinkmeyer et al. (2003), and Groudieva et al. (2004) further identified high- and low-*G+C Gram positives*, the *Bacillus-Clostridium* group and *Actinomycetales* to live within sea ice. In Arctic summer sea ice γ-proteobacteria (Brinkmeyer et al., 2003) or α-proteobacteria (Han et al., 2014) were observed to dominate in terms of number. However, in our study during early summer *Bacteroidetes* were most abundant although their contribution to the community is assumed to increase with decreasing temperatures (Junge et al., 2004).

In line with our results, highest diversity was detected within the γ-subclass of *Proteobacteria* (Brinkmeyer et al., 2003; Groudieva et al., 2004). With both methods, we identified *Glaciecola spp.* to be the dominant phylotype, whereas Brinkmeyer et al. (2003) observed *Marinobacter spp*. to be most abundant. In contrast to their results, we could not detect *Marinobacter spp*. with any of the applied methods.

The most striking difference to the study of Brinkmeyer et al. (2003) is that we observed *Polaribacter spp*. to be the dominant phylotype within the *Bacteroidetes* group, whereas the

former study detected only 1% of cells to belong to *Polaribacter spp.*. It is worthwhile to mention that Brinkmeyer et al. (2003) used another probe (PB223) to detect *Polaribacter*. PB223 shares 90 sequences (out of 101) with POL740, five of those only targeted by PB740 were extracted from polar habitats. However, in Antarctic sea ice samples using the probe PB223, *Polaribacter spp.* dominated the *Bacteroidetes* fraction (Brinkmeyer et al., 2003), as observed in our study.

On the genus level, *Polaribacter spp.* and *Glaciecola spp.* were identified to dominate in early summer sea ice of the Arctic. The general dominance of γ-proteobacteria and *Bacteroidetes* within sea ice could be explained by their ability to degrade a broad spectrum of substrates (Thomas & Dieckman, 2003).

Although differences in banding patterns and band intensities could be observed for the different stations/ice types, the resolution of DGGE was not great enough to clearly identify statistically relevant differences in the bacterial community composition, suggesting no major differentiation of the bacterial community across the different water masses observed. Nevertheless, it is noteworthy that some close relatives to the 16S rRNA sequences obtained from sea ice have been isolated from meltponds (band 58, sequenced from very small ice floe) indicating apparent melting processes at the air-ice interface, from deep sea hydrothermal vents, from sediments that might have been recruited during ice formation via attachment to anchor ice (Thomas & Dieckmann, 2003), and from Arctic and Antarctic surface waters that might have become incorporated via enclosure of water during ice formation, adherence of cells to ice crystals moving through the water column (Gleitz & Thomas, 1993) or active colonization (Thomas & Dieckmann, 2003). The terrestrial influence on the Arctic sea ice community was further confirmed by a number of closest relatives reported from soil and lake waters. These results represent possible mechanisms by which bacteria might become encased in the ice.

4.2.3 Experiments

Experimental treatments were used to simulate natural melting processes beneath the ice in small scale lab experiments, thus providing insight into how melting processes affect the bacterial sea ice community. As the ice melts, bacteria, along with pEPS, sea ice algae,

particulate and dissolved matter, are released into the under-ice water. In the under-ice water, sea ice bacteria are exposed to increased temperatures, lower salinity, currents/turbulence and lower concentrations of dissolved and particulate nutrients. We note that the effect of the natural under-ice water bacterial community, which is known to differ from the sea ice community (Helmke & Weyland, 1995; Bowman et al., 1997; Collins et al., 2007), was neglected in our experiment.

4.2.3.1 Free-living Bacterial Community

After melting, bacterial abundance increased by 640% within four days (suggesting a growth rate of ~1.6 d^{-1}, or a turnover time of 0.625 d). The free-living bacterial groups *Bacteroidetes* and ɣ-proteobacteria/*Glaciecola spp*. dominated in the just melted samples (day 0 resembles the community composition in sea ice) and after four days of incubation.

FISH analysis revealed a significant increase in the contribution to the bacterial community of β-proteobacteria, *Pseudoalteromonas-Colwellia* and *Polaribacter spp*. and a significant decrease of ɣ-proteobacteria after melting. The contribution of *Polaribacter spp*. to the *Bacteroidetes* group increased from 32% directly after melting to 83% at the end of the experiment (a replacement time of ~8 days). DGGE results were consistent with FISH, underscoring the likely reduction in the contribution of ɣ-proteobacteria to the bacterial community in the melted treatment.

However, differences in the bacterial community composition could also be an artefact caused by incubation. In bottle experiments, organic matter might become absorbed and concentrated onto the surface, increasing adhesion of bacteria to solid surfaces, where nutrients are more available (Morita, 1997). For seawater, Zobell (1943) observed that the number of bacteria on surfaces was dramatically higher than in the surrounding medium. The so called "bottle effect" leads to a high increase in cell numbers (Zobell & Anderson, 1936), potentially favoring bacteria with the ability to attach to surfaces. The greater the surface area in relation to the volume of water, the more rapidly growth of bacteria takes place (Morita, 1997). Hence, for future experiments, the bottle effect could be reduced by decreasing the surface:volume ratio.

None of the tested bacterial groups were displaced over the 4 d period of the experiment. Since bacteria were exposed to significantly different environments (sea ice and "under-ice water"), we might have expected greater changes in the bacterial community composition than we actually observed. The apparent resilience of the bacterial community could be explained by the ability of sea ice bacteria to acclimate rapidly to changing physicochemical conditions within sea ice brines. Even small temperature changes greatly influence the structure as well as the chemical and physical properties of the ice (Mock & Thomas, 2005). The capability of responding to rapid changes in their environment is of major importance to survive in the ice and might also enable sea ice bacteria to thrive in the water column after sea ice had melted.

4.2.3.2 Particulate EPS Attached Bacterial Community

Several studies have revealed phylogenetic differences between organic aggregates and the surrounding water in marine environments (DeLong et al., 1993; Knoll et al., 2001), suggesting that the bacterial community attached to TEP and CSP differs from that of free-living cells. However, in sea ice, most bacterial strains were observed to contribute to both the free-living and the particle-attached fraction (Brown & Bowman, 2001; Junge et al., 2002), possibly due to high concentrations of highly bioavailable DOM compared to surface waters (Amon et al., 2001).

"DGGE fingerprints" of the free-living and the particle-attached bacterial fraction (separated by different pore sizes) of sea ice stations overlap strongly. Although the free-living bacterial fraction appears to be more diverse, there were no bacterial groups or strains that solely occurred in only one of the fractions. This might be due to the selected pore sizes that could have allowed small particles to remain in the free-living fraction.

Our FISH data confirm that there are differences between the free-living and the particle-attached fraction, but every particle-attached group was also present in the free-living fraction.

High throughput sequencing by Bižić-Ionescu et al. (2014) revealed a significant overlap of particle-attached and free-living bacteria in marine systems, highlighting a largely underestimated connectivity between the two fractions. They suggested that a significant

number of taxa might hop on and off particles, for example due to changes in nutrient supply or grazer pressure (Riemann et al., 2000). *Bacteroidetes* have previously been observed to represent a significant part of both particle-attached and free-living bacterial communities in nutrient-rich environments (Fandino et al., 2005). Moreover, the presence of same strains in the free-living and particle-attached fraction is not surprising, as particle specialists need to have a free-living phase to disperse between particles (Bižić-Ionescu et al., 2014). This is certainly consistent with the patterns seen in our study.

In line with most studies (Simon et al., 1999; Bidle & Azam, 2001), we observed Bacteroidetes and γ-proteobacteria (*Glaciecola spp*.) to dominate the particle-attached fraction in marine systems. Some other studies additionally identified *Planctomycetes* to be important members (DeLong et al., 1993; Bižić-Ionescu et al., 2014). Riemann et al. (2000) and Bižić-Ionescu et al. (2014) further identified α-proteobacteria to be abundant on particles. In contrast, limnic particles (TEP and CSP) seem to be dominated by *Bacteroidetes* and β-proteobacteria, which have been shown to possess higher enzymatic activities than free-living bacteria (Lemarchand et al., 2006). However, we could not observe a difference in the bacterial activity between the free-living and particle attached fraction by FISH detection yields, indicating that the nutrient supply in the "melted sea ice" was still comparably high.

The dominance of the *Bacteroidetes* group may be explained by their rapid colonization of particulate matter combined with high growth rates as well as high hydrolytic activities (Riemann et al., 2000). Although the diversity of *Bacteroidetes* is large, the ability to degrade polymeric substances seems to be a common feature (Cottrell & Kirchman, 2000; Bauer et al., 2006), allowing them to use these substances as carbon and energy source, revealing their major role in the marine carbon cycle (Bauer et al., 2006). γ-Proteobacteria can also degrade a broad spectrum of substances (Thomas & Dieckman, 2003) and the *Colwellia* assemblage is known for its strong association with surfaces (DeLong et al., 1993), which might have led to the recruitment of these bacteria into sea ice. Even though *Glaciecola spp*. apparently utilize only a limited number of substrates as carbon and energy source, mostly organic acids (Bowman et al., 1998), we observed them to be one of the major groups attached to pEPS.

Within sea ice, pEPS may represent a crucial habitat for the survival of bacterial cells, protecting them from extreme physicochemical conditions and freezing temperatures. When the ice melts, bacteria are released to the under-ice water, where they are exposed to more stable physicochemical conditions on the one hand but decreased nutrient supply on the other hand. Thus, the major role of pEPS for bacteria might switch from protecting cells against harsh conditions, to pEPS providing the major source of nutrients. Particles are a concentrated source of organic compounds compared to the surrounding water, possibly promoting growth of bacteria that are particle specialists (DeLong et al., 1993; Lemarchand et al., 2006). Bižić-Ionescu et al. (2014) found γ-proteobacteria, *Bacteroidetes* and *Planctomycetes* to be enriched and α-proteobacteria to be reduced in the particle-attached fraction. In a lake system, Lemarchand et al. (2006) recognized a similar pattern. *Bacteroidetes* were enriched, whereas α-proteobacteria were found to be reduced, on particles (TEP and CSP). In contrast, we observed an enrichment of α-proteobacteria (*Roseobacter* clade) and γ-proteobacteria on pEPS and a significantly reduced relative abundance of *Polaribacter spp.* (*Bacteroidetes*) compared to the free-living fraction.

The enrichment of the *Roseobacter* clade may be explained by their strong association with surfaces, which has been reported from marine waters (Dang & Lovell, 2000). *Bacteroidetes* have been observed to be dominant on various types of particles (DeLong et al., 1993; Simon et al., 1999; Bidle & Azam, 2001; Lemarchand et al., 2006). 84% of the free-living *Bacteroidetes* were affiliated to *Polaribacter spp.*, but only 58% of *Bacteroidetes* were identified as *Polaribacter spp.* on pEPS. This indicates that *Bacteroidetes*, except for *Polaribacter spp.*, are potentially also enriched on pEPS.

In spite of their ability to degrade polymers (Gonzalez et al., 2008), we observed *Polaribacter spp.* to be significantly reduced on particles. Factors such as nutrient supply, and the presence of grazers and viruses (Riemann et al., 2000) may explain their reduced relative contribution to the bacterial community. Since pEPS are highly nutritious, in-situ they might attract grazers, hence increasing feeding pressure on the attached bacterial community. Moreover, as aggregates, pEPS, especially TEP are known to sink (Alldredge et al., 1993), sequestering the attached bacterial community from the surface to deep waters. In deep waters, bacteria

would be exposed to a number of physical changes including increasing pressure. As a consequence, it might be beneficial for bacteria to detach from pEPS after the ice had melted.

Gas vacuoles are a common feature among sea ice bacteria (Gosink et al., 1993). They reduce the cell density as compared with the cytoplasm, providing buoyancy (Walsby, 1972) and act as organelles of motility, regulating the vertical movement of cells via their synthesis and degradation (Staley, 1980). Within sea ice, bacteria are not known specifically to synthesize gas vacuoles, but the vacuoles might be of major importance in allowing bacteria to become incorporated into the ice (Gosink et al., 1997).

Polaribacter irgensii and *Polaribacter franzmannii* were identified to be the closest relatives to common sequences obtained by DGGE. Both are known to produce gas vacuoles (Gosink et al., 1998). During melting, bacteria are exposed to severe changes in salinity and temperature, which might induce the synthesis of gas vacuoles by *Polaribacter spp*., resulting in their detachment from particles, but preventing sedimentation. Gas vacuoles could enable free-living *Polaribacter spp*. to stay close to the melting ice front or the surface after the ice had melted, were they encounter comparably high nutrient concentrations. Moreover, gas vacuoles increase the probability for a rapid resettlement of newly formed sea ice by *Polaribacter spp*.. So far, *Polaribacter spp*. is the only common bacterial genus detected in summer and winter sea ice (Collins et al., 2010). Thus, we hypothesize that *Polaribacter spp*. seems to be exceptionally well adapted to changing environmental conditions with seasons.

4.2.3.3 Bacterial Colonization of TEP versus CSP

Carrias et al. (2002) defined the bacterial colonization of pelagic detrital particles as a function of the nature of the particle and the productivity of the system, suggesting potential differences in the composition of bacteria attached to different types of particles. pEPS can be rendered accessible to bacterial permeases through polymer hydrolyses by exoenzymes. Enzyme profiles of isolates indicated specialization among marine heterotrophic bacteria for different polymeric substances (Martinez et al., 1996). The composition of the bacterial community attached to TEP and CSP thus depends not only on the increased substrate concentration found in the gel but also on the matching of polymer composition and the type and level of bacterial exoenzymes being expressed (Verdugo et al., 2004).

Although FISH data revealed no significant differences in the bacterial community composition of the two particle types, we observed a preference of γ-proteobacteria and *Alteromonas-Colwellia* for TEP. *Polaribacter spp*. seems to prefer CSP over TEP, whereas no preference could be detected for the *Bacteroidetes* group.

Bacteroidetes are, as mentioned above, highly adapted to degrade a broad range of polymeric substances, thus, it is likely that this group does not show a specialization for one of the particle types. Both *Polaribacter* strains were reported to be able to utilize yeast extract and casamino acids, next to weak hydrolysis of starch (Gosink et al., 1998). *Polaribacter franzmannii* was further observed to hydrolyze gelatin, β-galactosidase and aesculin. *Polaribacter spp*. seem to be able to degrade a number of proteins, hence, the observed preference of *Polaribacter spp*. for protein-containing CSP is feasible.

We observed both particle types to be densely colonized, not showing a general preference by bacteria for either TEP or CSP. But, since we did not count the number of attached bacterial cells in relation to the particle size, this observation cannot be verified by numbers.

Berman and Viner-Mozzini (2001) found CSP to be more colonized, whereas Lemarchand et al. (2006) observed higher numbers of bacterial cells associated with TEP. Studies by Mattfeldt (2011) and Cisternas-Novoa et al. (2014) revealed low concentrations of CSP in deeper layers. Since proteins are a valuable carbon and nitrogen source for marine bacteria, CSP may be more labile than TEP, suggesting high consumption rates by bacteria, whereas TEP appeared to remain longer in the water column (Cisternas-Novoa et al., 2014).

4.3 Conclusion

In general, we observed low concentrations of TEP and chlorophyll *a* across an Arctic transect, which are not typical for the spring to late summer season studied. In this sea ice, highest concentrations of TEP were located at the ice-water interface, whereas CSP was homogeneously distributed, suggesting different roles of these pEPS in sea ice. Both particle types show reduced concentrations in the bottom section of small ice floes, suggesting that melting at the ice-water interface exceeds melting at the air-ice interface of sea ice floating on warm Atlantic waters. TEP concentrations were mainly correlated with chlorophyll *a* concentrations. In contrast, CSP concentrations appear to be mainly driven by physical parameters that may in turn affect the survivability of sea ice microorganisms (SIMCO). TEP seem to dominate in the bottom section of sea ice, whereas CSP dominate in terms of particle area in the top section, where SIMCO are exposed to most severe conditions and where it might get incorporated during ice formation. With 20%, TEP-carbon makes up a significant portion of the total sea ice POC, indicating that TEP may contribute significantly to polar ocean carbon cycles.

In early summer sea ice of the Arctic almost all bacterial cells were active. Based on the results obtained by FISH and DGGE, we conclude that sea ice bacteria are able to acclimate rapidly to changing physicochemical conditions. The composition of particulate EPS associated bacteria is different from that of free-living bacteria, but may overlap in many respects. *Polaribacter spp.* is the only genus that was observed to be significantly reduced on particles compared to the free-living fraction after the ice had melted. Identified *Polaribacter* strains are known to synthesize gas vacuoles, which enables them to move in the water column, possibly to avoid sedimentation and to stay in close vicinity of newly forming ice, indicating a high degree of adaptation to the seasonal sea ice cycle. We further observed preferences of some bacterial groups for either TEP or CSP, yet, no significant differences were detected in the bacterial community composition of the two particle types.

Acknowledgements

References

Ackley, S.F. & Sullivan, C.W. (1994) Physical controls on the development and characteristics of Antarctic sea ice biological communities – a review and synthesis. *Deep-Sea Res* **41**: 1583-1604.

Alldredge, A.L., Passow, U., Logan, B.E. (1993) The abundance and significance of a class of large, transparent organic particles in the ocean. *Deep-Sea Res I* **40**: 1131–1140.

Aluwihare, L. I. & Repeta, D. J. (1999) A comparison of the chemical characteristics of oceanic DOM and extracellular DOM produced by marine algae. *Mar Ecol Prog Ser* **186**: 105–117.

Amann, R. I., Binder, B. J., Olson, R. J., Chisholm, S. W., Devereux, R., Stahl, D. A. (1990) Combination of 16S rRNA-targeted oligonucleotide probes with flow cytometry for analyzing mixed microbial populations. *Appl Environ Microbiol* **56**: 1919-1925.

Amann, R.I., Ludwig, W., Schleifer, K.H. (1995) Phylogenetic identification and in situ detection of individual microbial cell without cultivation. *Microbiol Rev* **59**: 143–169.

Amon, R.M.W., Fitznar, H.-P., Benner, R. (2001) Linkages among the bioreactivity, chemical composition, and diagenetic state of marine dissolved organic matter. *Limnol Oceanogr* **46**: 287–297.

Arnous, M.-B., Courcol, N., Carria, J.-F. (2010) The significance of transparent exopolymeric particles in the vertical distribution of bacteria and heterotrophic nanoflagellates in Lake Pavin. *Aquat Sci* **72**: 245-253.

Azetsu-Scott, K. & Passow, U. (2004) Ascending marine particles: significance of transparent exopolymer particles (TEP) in the upper ocean. *Limnol Oceanogr* **49**: 741–748.

Baines, S.B. & Pace, M.L. (1991) The production of dissolved organic matter by phytoplankton and its importance to bacteria: patterns across marine and freshwater systems. *Limnol Oceanogr* **36**: 1078–1090.

Bauer, M.M. et al. (2006) Whole genome analysis of the marine *Bacteroidetes 'Gramella forsetii'* reveals adaptations to degradation of polymeric organic matter. *Environ Microbiol* **8**: 2201–2213.

Bayer-Giraldi, M., Uhlig, C., John, U., Mock, T., Valentin, K. (2010) Antifreeze proteins in polar sea ice diatoms: diversity and gene expression in the genus *Fragilariopsis*. *Environ Microbial* **12**: 1041-1052.

Berman, T. & Viner-Mozzini, Y. (2001) Abundance and characteristics of polysaccharide and proteinaceous particles in Lake Kinneret. *Aquat Microb Ecol* **24**: 255–264.

References

Bernardet, J.-F., Segers, P., Vancanneyt, M., Berthe, F., Kersters, K., Vandamme, P. (1996) Cutting a Gordian knot: emended classification and description of the genus *Flavobacterium*, emended description of the family *Flavobacteriaceae*, and proposal *of Flavobacterium hydatis* nom. nov. (basonym, *Cytophaga aquatilis* Strohl and Tait 1978). *Int J Syst Bacteriol* **46**: 128-148.

Beszczynska-Möller, A., Fahrbach, E., Schauer, U., and Hansen, E. (2012) Variability in Atlantic water temperature and transport at the entrance to the Arctic Ocean, 1997–2010. - *ICES J Mar Sci*.

Bidle, K.D. & Azam, F. (2001) Bacterial control of silicon regeneration from diatom detritus: significance of bacterial ectohydrolases and species identity. *Limnol Oceanogr* **46**: 1606-1623.

Bižić-Ionescu, M., Zeder, M., Ionescu, D., Orlić, S., Fuchs, B. M., Grossart, H.-P., Amann, R. (2014) Comparison of bacterial communities on limnic versus coastal marine particles reveals profound differences in colonization. *Environ Microbiol* doi: 10.1111/1462-2920.12466.

Bowman, J. P., McCammon, S. A., Brown, M. V., Nichols, D. S., McMeekin, T. A. (1997) Diversity and association of psychrophilic bacteria in Antarctic sea ice. *Appl Environ Microbiol* **63**: 3068–3078.

Bowman, J.P., McCammon, S.A., Brown, J.L., McMeekin, T.A. (1998) *Glaciecola punicea gen. nov., sp. nov*. and *Glaciecola pallidula gen. nov., sp. nov*. : psychrophilic bacteria from Antarctic sea-ice habitats. *Int J Syst Bacteriol* **48**: 1213-1222.

Brinkmeyer, R., Knittel, K., Juergens, J., Weyland, H., Amann, R., Helmke, E. (2003) Diversity and structure of bacterial communities in Arctic versus Antarctic sea ice: a comparison. *Appl Environ Microbiol* **69**: 6610-6619.

Brown, M.V. & Bowman, J.P. (2001) A molecular phylogenetic survey of sea-ice microbial communities (SIMCO). *FEMS Microbiol Ecol* **35**: 267– 275.

Carrias, J.F., Serre, J.P., Sime-Ngando, T., Amblard, C. (2002) Distribution, size, and bacterial colonization of pico and nano-detrital organic particles (DOP) in two lakes of different trophic status. *Limnol Oceanogr* **47**: 1202–1209.

Chateauvert, C.A., Lesack, L.F.W., Bothwell, M.L. (2012) Abundance and patterns of transparent exopolymer particles (TEP) in Arctic floodplain lakes of the Mackenzie River Delta. *J Geophys Res* **117**: G04013

Chin, W.C., Orellana, M.V., Verdugo, P. (1998) Spontaneous assembly of marine dissolved organic matter into polymer gels. *Nature* **391**: 568–572.

Chresten Lund-Hansen, L., Sorrell, B.K., Markager, S., Hancke, K., Stratmann, T., Rysgaard, S., Ramløv, H. (2015) Effects of sea ice light attenuation and CDOM absorption in the water below - Eurasian sector of central Arctic Ocean (> 88° N). *Pol Res*, accepted for publication.

Cisternas-Novoa, C., Lee, C., Engel, A. (2014) A semi-quantitative spectrophotometric, dye-binding assay for determination of Coomassie Blue stainable particles. *Limnol Oceanogr: Methods* **12**: 604-616.

Collins, R.E., Carpenter, S.D., and Deming, J.W. (2007) Spatial heterogeneity and temporal dynamics of particles, bacteria, and pEPS in Arctic winter sea ice. *J Mar Sys* **74:** 902–917.

Collins, R.E., Rocap, G., Deming, J.W. (2010) Persistence of bacterial and archaeal communities in sea ice through an Arctic winter. *Environ Microbiol* **12**(7): 1828-1841.

Cooksey, K.E. & Wigglesworth-Cooksey, B. (1995) Adhesion of bacteria and diatom to surfaces in the sea: a review. *Aquat Microb Ecol* **9**: 87–96.

Cottrell, M.T. & Kirchman, D.L. (2000) Natural assemblages of marine Proteobacteria and members of the Cytophaga-Flavobacter cluster consuming low- and high-molecular weight dissolved organic matter. *Appl Environ Microbiol* **66**: 1692–1697.

Dang, H. & Lovell, C.R. (2000) Bacterial Primary Colonization and Early Succession on Surfaces in Marine Waters as Determined by Amplified rRNA Gene Restriction Analysis and Sequence Analysis of 16S rRNA Genes. *Appl Environ Microbiol* **66**(2): 467-475.

Decho, A. (1990) Microbial exopolymer secretions in ocean environments: their role(s) in food webs and marine processes. *Oceanogr Mar Biol Annu Rev* **28**: 73–153.

Decho, A.W. & Lopez, G.R. (1993) Exopolymer microenvironments of microbial flora: Multiple and interactive effects on trophic relationships. *Limnol Oceanogr* **38**: 1633–1645.**Decho, A.W. & Moriarty, D.J.W.** (1990) Bacterial exopolymer utilization by a harpactkoid copepod: A methodology and results. *Limnol Oceanogr* **35**: 1039-1049.

Eicken, H. (1992) The role of sea ice in structuring Antarctic ecosystems. *Polar Biol* **12**: 3-13.

Eicken, H., Reimnitz E., Alexandrov, V., Martin, T., Kassens, H., Viehoff, T. (1997) Sea-ice processes in the Laptev Sea and their importance for sediment export. *Contin Shelf Res* **17**: 205-233.

Eicken, H., Deming, J., Krembs, C., Stierle, A., Junge, K., Bock, C., Miller, H. (1999) Morphology and microphysics of sea-ice brine inclusions and their importance for fluid transport and microbial activity. Abstract, *American Geophysical Union Annual Meeting*, December 1999, San Francisco, USA.

Eicken, H., Bocj, C., Wittig, R., Miller, H., Poertner, H.-O. (2000) Nuclear magnetic resonance imaging of sea ice pore fluids: methods and thermal evolution of pore microstructure. *Cold Reg Sci Technol* **31**: 207-225.

Eilers, H., Pernthaler, J., Glöckner, F., Aman, R. (2000) Culturability and in situ abundance of pelagic bacteria from the North Sea. *Appl Environ Microbiol* **66**: 3044-3051.

Eilers, H., Pernthaler, J., Peplies, J., Glockne,r F.O., Gerdts, G., Amann, R. (2001) Isolation of novel pelagic bacteria from the German bight and their seasonal contributions to surface picoplankton. *Appl Environ Microbiol* **67**: 5134-42.

Engel, A. (2000) The role of transparent exopolymer particles (TEP) in the increase in apparent particle stickiness (α) during the decline of a diatom bloom. *J Plankton Res* **22**: 485-497.

Engel, A. & Passow, U. (2001) Carbon and nitrogen content of transparent exopolymer particles (TEP) in relation to their Alcian blue adsorption. *Mar Ecol Prog Ser* **219**: 1–10.

Engel, A. (2009) Determination of Marine Gel Particles. In Wurl O. (Ed.), Practical Guidelines for the Analysis of Seawater, p125-142, *CRC Press Taylor & Francis Group*, Boca Raton, Florida.

References

Evans, C.A. & O'Reily, J.E. (1987) A handbook for the measurement of chlorophyll a in netplankton and nanoplankton. *Biomass Handb* **9**: 1–14.

Fandino, L.B., Riemann, L., Steward, G.F., Azam, F. (2005) Population dynamics of *Cytophaga-Flavobacteria* during marine phytoplankton blooms analyzed by real-time quantitative PCR. *Aquat Microb Ecol* **40**: 251–25.

Feller, G. & Gerday, C. (2003) Psychrophilic enzymes: hot topics in cold adaptation. *Nat Rev Microbiol* **1**: 200-208.

Fuhrman, J.A. & Campbell, L. (1998) Microbial microdiversity. *Nature* **393**: 410–411.

Gerdes, B., Brinkmeyer, R., Dieckmann, G.S., Helmke, E. (2005) Influence of crude oil on changes of bacterial communities in Arctic sea-ice. *FEMS Microb Ecol* **53**: 129-139.

Gerdes, R. & Schauer, U. (1997) Large-scale circulation and water mass distribution in the Arctic Ocean from model results and observations. *J Geophys Res* **102**(C4): 8467-8484.

Gleitz, M. & Thomas, D.N. (1993) Variation in phytoplankton standing stock, chemical composition and physiology during sea-ice formation in the southeastern Weddell Sea. *J Exp Mar Biol Ecol* **173**: 211–230.

Gloersen, P., Campbell, W.J., Cavalieri, D.J., Comiso, J.C., Zwally, H.J. (1992) Arctic and Antarctic sea ice, 1978 1987: Satellite passive Microwave Observations and Analysis. *NASA Special Publication* **511**: 289 pp. National Aeronautics and Space Administration, Washington, D.C.

Gonzalez, J.M., Fernandez-Gomez, B., Fernandez-Guerra, A., Gomez-Consarnau, L., Sanchez, O., Coll-Llado, M. (2008) Genome analysis of the proteorhodopsin- containing marine bacterium *Polaribacter sp*. MED152 (*Flavobacteria*). *Proc Natl Acad Sci USA* **105**: 8724–8729.

Gosink, J.J., Irgens, R.L., Staley, J.T. (1993) Vertical distribution of bacteria from arctic sea ice. *FEMS Microbiol Ecol* **102**: 85–90.

Gosink, J.J., Herwig, R.P., Staley, J.T. (1997) *Octadecabacter arcticus gen. nov., sp. nov*., and *O. antarcticus sp. nov.*, nonpigmented, psychrophilic gas vacuolated bacteria from polar sea ice and water. *Syst Appl Microbiol* **20**: 356–365.

Gosink, J.J., Woese, C.R., Staley, J.T. (1998) *Polaribacter gen. nov*., with three new species, *P. irgensii sp. nov., P. franzmannii sp.nov*. and *P. filamentus sp. nov*., gas vacuolated polar marine bacteria of the *Cyophaga-Flavobacterium-Bacteroides* group and reclassification of ' *Flectobacillus glomeratus* as *Polaribacter glomeratus comb. nov.. Int J Syst Bacteriol* **48**: 223-235.

Gosselin, M., Levasseur, M., Wheeler, P.A., Horner, R.A., Booth, B.C. (1997) New measurements of phytoplankton and ice algal production in the Arctic Ocean. *Deep-Sea Res II* **44**: 1623–1644.

Gradinger, R. & Ikävalko, J. (1998) Organism incorporation into newly forming Arctic sea ice in the Greenland Sea. *J Plankton Res* **20**: 871-886.

Gradinger, R. (1999) Integrated abundance and biomass of sympagic meiofauna in Arctic and Antarctic pack ice. *Polar Biol* **22**: 169–177.

Grossart, H.-P. (1999) Interactions between marine bacteria and axenic diatoms (*Cylindrotheca fusiformis, Nitzschia laevis* and *Thalassiosira weissflogii*) incubated under various conditions in the lab. *Aquat Microb Ecol* **19**: 1–11.

Groudieva, T., Kambourova, M., Yusef, H., Royter, M., Grote, R., Trinks, H., Antranikian, G. (2004) Diversity and cold-active hydrolytic enzymes of culturable bacteria associated with Arctic sea ice, Spitzbergen. *Extremophiles* **8**: 475-488.

Han, D., Kang, I., Ha, H.K., Kim, H.C., Kim, O.-S., Lee, B.Y., Cho, J.-C., Hur, H.-G., Lee, Y.K. (2014) Bacterial Communities of Surface Mixed Layers in the Pacific Sector of the Western Arctic Ocean during Sea-Ice Melting. *PLoS ONE* **9**(1): e86887.

Helmke, E. & Weyland, H. (1995) Bacteria in sea ice and underlying water of the eastern Weddell Sea in midwinter. *Mar Ecol Prog Ser* **117**: 269–287.

Herborg, L.M., Thomas, D.N., Kennedy, H., Haas, C., Dieckmann, G.S. (2001) Dissolved carbohydrates in Antarctic sea ice. *Antarct Sci* **13**: 119–125.

Horner, R.A., Ackley, S.F., Dieckmann, G.S., Gulliksen, B., Hoshiai, T., Legendre, L., Melnikov, I.A., Reeburgh, W.S., Spindler, M., Sullivan, C.W. (1992) Ecology of sea ice biota. 1. Habitat, terminology, and methodology. *Polar Biol* **12**: 417–427.

Junge, K., Krembs, C., Deming, J. W., Stierle, A., Eicken, H. (2001) A microscopic approach to investigate bacteria under in-situ conditions in sea-ice samples. *Ann Glaciol* **33**: 304–310.

Junge, K., Imhoff, J. F., Staley, J. T., Deming. J. W. (2002) Phylogenetic diversity of numerically important bacteria in Arctic sea ice. *Microb Ecol* **43**: 315–328.

Junge, K., Eicken, H., Deming, J.W. (2004) Bacterial activity at -2 to -20 °C in Arctic Wintertime sea ice. *Appl Environ Microbiol* **70**: 550–557.

Karner, M.B. & Fuhrman, J.A. (1997) Determination of active marine bacterioplankton: a comparison of universal 16S rRNA probes, autoradiography, and nucleoid staining. *Appl Environ Microbiol* **63**: 1208–1213.

Kattner, G., Thomas, D.N., Haas, C., Kennedy, H.A., Dieckmann, G.S. (2004) Surface ice and gap layers in Antarctic sea ice: highly productive habitats. *Mar Ecol Prog Ser* **277:** 1–12.

Knoll, S., Zwisler, W., Simon, M. (2001) Bacterial colonization of early stages of limnetic diatom microaggregates. *Aquat Microb Ecol* **25**: 141–150.

Kottmeier, S.T., Grossi, S.M., Sullivan, C.W. (1987) Sea ice microbial communities. VIII. Bacterial production in annual sea ice of McMurdo Sound, Antarctica. *Mar Ecol Prog Ser* **35**: 175-86.

Krembs, C. & Engel, A., (2001) Abundance and variability of microorganisms and transparent exopolymer particles across the ice–water interface of melting first-year sea ice in the Laptev Sea (Arctic). *Mar Biol* **138**: 173-185.

References

Krembs, C., Eicken, H., Junge, K., Deming, J. W. (2002) High concentrations of exopolymeric substances in wintertime sea ice: implications for the polar ocean carbon cycle and cryoprotection of diatoms. *Deep-Sea Res I* **9**: 2163–2181.

Krembs, C. & Deming, J.W. (2008) The role of exopolymers in microbial adaptation to sea ice. In *Psychrophiles: From Biodiversity to Biotechnology.* Margesin, R., Schinner, F., Marx, J.C., and Gerday, C. (eds). *Springer*, New York, 247–264.

Krembs, C., Eicken, H., **Deming. J. W.** (2011) Exopolymer alteration of physical properties of sea ice and implications for ice habitability and biogeochemistry in a warmer Arctic. *PNAS* **108**: 3653-3658.

Legendre, L., Ackley, S.F., Dieckmann, G.S., Gulliksen, B. (1992) Ecology of sea ice biota. 2. Global significance. *Polar Biol* **12**: 429–444.

Lemarchand C., Jardillier, L., Carrias, J.F., Richardot, M., Debroas, D., Sime-Ngando, T., Amblard, C. (2006) Community composition and activity of prokaryotes associated to detrital particles in two contrasting lake ecosystems. *FEMS Microbial Ecol* **57**: 442-451.

Logan, B. E., Passow, U., Alldredge, A. L., Grossart, H.-P., Simon, M. (1995) Rapid formation and sedimentation of large aggregates is predictable from coagulation rates (half-lives) of transparent exopolymer particles (TEP). *Deep-Sea Research II* **42**: 203–214.

Long, R.A. & Azam, F. (1996) Abundant protein-containing particles in the sea. *Aquat Microb Ecol* **10**: 213-221.

Malmstrom, R.R., Straza, T.R.A., Cottrell, M.T., Kirchman, D.L. (2007) Diversity, abundance, and biomass production of bacterial groups in the western Arctic Ocean. *Aquat Microb Ecol* **47**: 45-55.

Mancuso Nichols, C.A., Guezennec, J., Bowman, J.P. (2005) Bacterial exopolysaccharides from extreme marine environments with special consideration of the southern ocean, sea ice and deep-sea hydrothermal vents: a review. *Mar Biotechnol* **7**: 253–271.

Manz, W., Amann, R., Ludwig, W., Wagner, M., Schleifer, K.-H. (1992) Phylogenetic oligodeoxynucleotide probes for the major subclasses of *Proteobacteria*: problems and solutions. *Syst Appl Microbiol* **15**: 593 - 600.

Manz, W., Amann, R., Ludwig, W., Vancanneyt, M., Schleifer, K.-H. (1996) Application of a suite of 16S rRNA-specific oligonucleotide probes designed to investigate bacteria of the phylum *cytophaga-flavobacter-bacteroides* in the natural environment. *Microbiol* **142**: 1097-1106.

Mari, X. & Kiørboe, T. (1996) Abundance, size distribution and bacterial colonization of transparent exopolymer particles (TEP) in the Kattegat. *J Plankton Res* **18**: 969–986.

Mari, X. (1999) Carbon content and C:N ratio of transparent exopolymer particles (TEP) produced by bubbling of exudates of diatoms. *Mar Ecol Prog Ser* **33**: 59–71.

Mariotti, A. (1983) Atmospheric nitrogen is a reliable standard for natural 15N abundance measurements. *Nature* **303**: 685-687.

Martinez, J., Smith, D.C., Steward, G.F., Azam, F. (1996) Variability in ectohydrolytic enzyme activities of pelagic marine bacteria and its significance for substrate processing in the sea. *Aquat Microb Ecol* **10**: 223–230.

Mattfeldt, T. (2011) Abundance, size frequency distribution and carbon content of transparent exopolymer particles (TEP) and Coomassie stained particles (CSP) in the Greenland Sea. Diploma thesis.

Maykut, G.A. (1986) The surface heat and mass balance. *NATO ASI Ser B* **9-164**: 395–463.

Meiners, K., Gradinger, R., Fehling, J., Civitarese, G., Spindler, M. (2003) Vertical distribution of exopolymer particles in sea ice of the Fram Strait (Arctic) during autumn. *Mar Ecol Prog Ser* **248**: 1–13.

Meiners, K., Brinkmeyer, R., Granskog, M.A., Lindfors, A. (2004) Abundance, size distribution and bacterial colonization of exopolymer particles in Antarctic sea ice (Bellingshausen Sea). *Aquat Microb Ecol* **35**: 283–296.

Meiners, K., Krembs, C., Gradinger, R. (2008) Exopolymer particles: microbial hotspots of enhanced bacterial activity in Arctic fast ice (Chukchi Sea). *Aquat Microb Ecol* **52**: 195-207.

Meredith, M., Heywood, K., Dennis, P., Goldson, L., White, R., Fahrbach, E., Schauer, U., Osterhus. S. (2001) Freshwater fluxes through the western Fram Strait. *Geophys Res Let* **28**(8): 1615-1618.

Michel, C., Nielsen, T.G., Nozais, C., Gosselin, M. (2002) Significance of sedimentation and grazing by ice micro- and meiofauna for carbon cycling in annual sea ice (northern Baffin Bay). *Aquat Microb Ecol* **30**: 57–68.

Mock, T. & Thomas, D.N. (2005) Recent advances in sea-ice microbiology. *Environ Microbiol* **7** (5): 605–619.

Mopper, K., Zhou, J., Ramana, K.S., Passow, U., Dam, H.G., Drapeau, D.T. (1995) The role of surface-active carbohydrates in the flocculation of a diatom bloom in a mesocosm. *Deep-Sea Res II* **42**: 47–73.

Morita, R.Y. (1997) Bacteria in Oligotrophic Environments. Starvation-Survival Lifestyle, 529 pp. *Chapman and Hall*, New York.

Muyzer, G., de Waal, E.C., Uitterlinden, A.G. (1993) Profiling of complex microbial populations by denaturing gradient gel electrophoresis analysis of polymerase chain reaction-amplified genes coding for 16S rRNA. *Appl Environ Microbiol* **59**: 695-700.

Muyzer, G., Brinkhoff, T., Nübel, U., Santegoeds, C., Schäfer, H., Wawer, C. (1997) In: Molecular Microbial Ecology Manual (Akkerman, S.B., Van Elsas, J.D. and De Bruijn, F.J., Eds.), Vol. 3.4.4. *Kluwer Academic Publisher*, Dordrecht, Netherlands.

Myklestad, S.M. (1977) Production of carbohydrates by marine planktonic diatoms. II Influence of the N/P ratio in the growth medium on the assimilation ratio, growth rate and production of cellular and extracellular carbohydrates by *Chaetoceros affinis var Willei* (Gran) Hustedt and *Skeletonema costatum* (Grev) Cleve. *J Exp Mar Biol Ecol* **29**: 161–179.

Myklestad, S.M., Holm-Hansen, O., Varum, K.M., Volcani, B.E. (1989) Rate of release of extracellular amino acids and carbohydrates from the marine diatom *Chaetoceros affinis*. *J Plankton Res* **11**: 763–773.

Myklestad, S.M. (1995) Release of extracellular products by phytoplankton with special emphasis on polysaccharides. *Sci Total Environ* **165**: 155–164.

References

Neef, A., Amann, R., Schlesner, H., Schleifer, K.-H. (1998) Monitoring a widespread bacterial group: in situ detection of *planctomycetes* with 16S rRNA-targeted probes. *Microbiol* **144**: 3257-3266.

Palmisano, A.C. & Garrison, D.L. (1993) Microorganisms in Antarctic sea ice. In: Antarctic microbiology (Friedmann, E.I., Ed.), *Wiley-Liss*, New York, 167-218.

Passow, U., Alldredge, A.L., Logan, B.E. (1994) The role of paniculate carbohydrate exudates in the flocculation of diatom blooms. *Deep-Sea Res I* **41**: 335-357.

Passow, U. & Alldredge, A. L. (1995) A dye-binding assay for the spectrophotometric measurement of transparent exopolymer particles (TEP). *Limnol Oceanogr* **40**: 1326–1335.

Passow, U. (2000) Formation of transparent exopolymer particles, TEP, from dissolved precursor material. *Mar Ecol Prog Ser* **192**: 1–11.

Passow, U. (2002a) Transparent exopolymer particles (TEP) in aquatic environments. *Prog Oceanogr* **55**: 287-333.

Passow, U. (2002b) Production of transparent exopolymer particles (TEP) by phyto- and bacterioplankton. *Mar Ecol Prog Ser* **236**: 1–12.

Pedrotti, M.L., Beauvais, S., Kerros, M.-E., Iversen, K., Peters, F. (2009) Bacterial colonization of transparent exopolymeric particles in mesocosms under different turbulence intensities and nutrient conditions. *Aquat Microb Ecol* **55**: 301-312.

Percival, E., Rahman, M.A., Weigel, H. (1980) Chemistry of the polysaccharide of the diatom *Coscinodiscus nobilis*. *Phytochem* **19**: 809–811.

Pernthaler, A., Pernthaler, J., Amann, R. (2004) Sensitive multi-color fluorescence in situ hybridization for the identification of environmental microorganisms, p. 711-726. In G. Kowalchuk, G., de Bruijn, F.J., Head, I.M., Akkermans, A.D.L., van Elsas, J.D. (ed.), Molecular Microbial Ecology Manual, 2nd 3.11 ed. *Kluwer Academic Publishers*, Dordrecht, Boston, London.

Petri, R. & Imhoff, J.F. (2001) Genetic analysis of sea ice bacterial communities of western Baltic Sea using an improved double gradient method. *Polar Biol* **24**: 252–257.

Polyak, L., Alley, R.B., Andrews, J.T., Brigham-Grette, J., Cronin, T.M., Darby, D.A., Dyke, A.S., Fitzpatrick, J.J., Funder, S., Holland, M., Jennings, A.E., Miller, G.H., O'Regan, M., Savelle, J., Serreze, M., St. John, K., White, J.W.C., Wolff, E. (2010) History of sea ice in the Arctic. *Quat Sci Rev* **29**: 1679–1715.

Prieto, L., Ruiz, J., Echevarrı́a, F., Garcı́a, C.M., Ga´lvez, J.A., Bartual, A., Corzo, A., Macı́as, D. (2002) Scales and processes in the aggregation of diatom blooms: high time resolution and wide size range records in a mesocosm study. *Deep-Sea Res I* **49**: 1233-1253.

Pruesse, E., Peplies, J., Glöckner, F.O. (2012) SINA: accurate high-throughput multiple sequence alignment of ribosomal RNA genes. *Bioinformatics* **28**: 1823-1829.

Radi´c, T., Degobbis, D., Fuks, D., Radi´c, J., Djakovac, T. (2005) Seasonal cycle of transparent exopolymer particles, formation in the northern Adriatic during years with (2000) and without (1999) mucilage events. *Fresen Environ Bull* **14**: 224–230.

Raymond, J.A., Sullivan, C.W., DeVries, A.L. (1994). Release of an ice-active substance by Antarctic sea ice diatoms. *Pol Biol* **14**(1): 71-75.

Redfield, A.C., Ketchum, B.M., Richards, F.A. (1963) The influence of organism on the composition of sea water. Hill, M.N. (ed) The Sea. *Wiley*, New York, p 26–77.

Reichenbach, H. & Dworkin, M. (1992) The myxobacteria. In The Prokaryotes, 2nd edn. Balows, A., Trüper, H.G., Dworkin, M., Harder, W., and Schleifer, K.H. (eds). *Springer*, New York, 3416–3487.

Riedel, A., Michel, C., Gosselin, M. (2006) Seasonal study of sea ice exopolymeric substances on the Mackenzie shelf: implications for transport of sea-ice bacteria and algae. *Aquat Microb Ecol* **45**: 195–206.

Riedel, A., Michel, C., Gosselin, M., LeBlanc, B. (2008) Winter-spring dynamics in sea-ice carbon cycling in the coastal Arctic Ocean. *J Mar Syst* **74**: 918-932.

Riemann, L., Steward, G.F., Azam, F. (2000) Dynamics of bacterial community composition and activity during a mesocosm diatom bloom. *Appl Environ Microbiol* **66**: 578–587.

Santchi, P.H., Banois, E., Wilkinson, K.J., Zhang, J., Buffle, J. (1998) Fibrillar polysaccharides in marine macromolecular organic matter as imaged by atomic force microscopy and transmission electron microscopy. *Limnol Oceanogr* **43**: 896–908.

Schmitz, W.J. (1995) On the interbasin-scale thermohaline circulation. *Rev of Geophys* **33**(2): 151-173.

Schuster, S. & Herndl, G. J. (1995) Formation and significance of transparent exopolymeric particles in the northern Adriatic Sea. *Mar Ecol Prog Ser* ***124***: 227–236.

Shanks, A.L. & Trent, J.D. (1980) Marine snow: sinking rates and potential role in vertical flux. *Deep-Sea Res I* **27**: 137–143.

Simon, M., Glöckner, F., Amann, R. (1999) Different community structure and temperature optima of heterotrophic picoplankton in various regions of the Southern Ocean. *Aquat Microb Ecol* **18**: 275-284.

Spindler, M. (1990) A coparison of Arctic and Antarctic sea ice and the effects of different properties on sea ice biota. In: Beil, U., Thiede, J. (eds) Geophysical history of polar oceans: Arctic versus Antarctic. *Kluwer Academic Publishers*, Amsterdam, 173-186.

Staley, J.T. (1980) The gas vacuole: an early organelle of prokaryotic motility. *Origins Life* **10**: 111–116.

Sullivan C.W. & Palmisano A.C. (1984) Sea ice microbial communities: distribution, abundance, and diversity of Ice bacteria in McMurdo Sound, Antarctica, in 1980. *Appl Environ Microbiol* **47**: 788-795.

Thomas, D.N., Lara, R.J., Haas, C., Schnack-Schiel, S.B. and others (1998) Biological soup within decaying summer sea ice in the Amundsen Sea, Antarctica. In: Lizotte M, Arrigo K (eds) Antarctic sea ice: biological processes, interactions, and variability. *Antarct Res Ser* **73**: 161–171.

Thomas, D. N. & Dieckmann, G.S. (2002) Antarctic sea ice-a habitat for extremophiles. *Science* **295**: 641–644.

Thomas, D.N. & Dieckmann, G.S. (2003) Sea Ice: An Introduction to its Physics, Chemistry, Biology and Geology, *Blackwell Science*, Oxford.

Unanue, M., Ayo, B., Azu´a, I., Barcina, I., Iriberri, J. (1992) Temporal variability of attached and free-living bacteria in coastal waters. *Microb Ecol* **23**: 27–39.

Underwood, G.J.C., Paterson, D.M., Parkes, R.J. (1995) The measurement of microbial carbohydrate exopolymers from intertidal sediments. *Limnol Oceanogr* **40**: 1243–1253.

Underwood, G.J.C., Fietz, S., Papadimitriou, S., Thomas, D.N., Dieckmann, G.S. (2010) Distribution and composition of dissolved extracellular polymeric substances (EPS) in Antarctic sea ice. *Mar Ecol Prog Ser* **404**: 1-19.

Verdugo, P., Allredge, A.L., Azam, F., Kirchman, D.L., Passow, U., Santschi, P.H. (2004) The oceanic gel phase: a bridge in the DOM-POM continuum. *Mar Chem* **92**: 67–85.

Verdugo, P. (2012) Marine microgels. *Ann Rev Mar Sci* **4**: 9.1-9.25.

Wadhams, P. (2000) Ice in the Ocean. *Gordon and Breach Science Publishers*, Amsterdam

Waite, A.M., Olson, R.J., Dam, H.G., Passow, U. (1995). Sugar-containing compounds on the cell surfaces of marine diatoms measured using concanavalin A and flow cytometry. *J Phycol* **31**: 925–933.

Waite, A.M., Gallager, S., Dam, H.G. (1997) New measurements of phytoplankton aggregation in a flocculator using videography and image analysis. *Mar Ecol Prog Ser* **155**: 77-88.

Wallner, G., Amann, R., Beisker, W. (1993) Optimizing fluorescent in situ hybridization with rRNA-targeted oligonucleotide probes for flow cytometric identification of microorganisms. *Cytometry* **14**: 136-143.

Walsby, A.E. (1972) Structure and function of gas vacuoles. *Bacteriol Rev* **36**: 1–32.

Ward, D.M., Ferris, M.J., Nold, S.C., Bateson, M.M. (1998) A natural view of microbial biodiversity within hot spring Cyanobacterial mat communities. *Microbiol Mol Biol Rev* **62**: 1353–1370.

Weeks, W.F. & Ackley, S.F. (1986) The growth, structure and properties of sea ice. In: Untersteiner, N. (Ed.), The Geophysics of Sea Ice. *Martinus Nijhoff Publishers*, Dordrecht, 9-164.

Wells, M.L. & Goldberg, E.D. (1991) Occurrence of small colloids in sea water. *Nature* **353**: 342-344.

Wetherbee, R., Lind, J.L., Burke, J., Quatrano, R.S. (1998) Minireview: The first kiss: Establishment and control of initial adhesion by raphid diatoms. *J Phycol* **34**: 9–15.

Wurl, O., L. Miller, S. Vagle (2011) Production and fate of transparent exopolymer particles in the ocean. *J Geophys Res* **116**: C00H13.

Zhang, J. & Zhang, X. (2001) Heat and freshwater budgets and pathways in the arctic mediterranean in a coupled ocean/sea-ice model. *J Oceanogr* **57**(2): 207-234.

Zobell, C.E. & Anderson, D.Q. (1936) Observations on the multiplication of bacteria in different volumes of stored sea water and the influence of oxygen tension and solid surfaces. *Biol Bull* **71**: 324-342.

Zobell, C.E. (1943) The effect of solid surfaces on bacterial activity. *J Bacteriol* **46**: 39-56.